A Novel Osteochondral Composite Consisting of a Self-Assembling Peptide Hydrogel and 3D Printed Polycaprolactone Scaffold: Potential for Articular Cartilage Repair
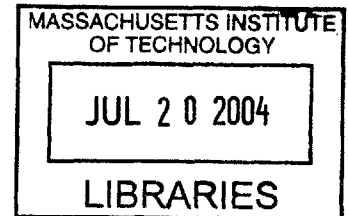
by

Sanaz Saatchi

B.S. Bioengineering
University of California, Berkeley (2002)

Submitted to the Department of Mechanical Engineering in Partial Fulfillment of the
Requirements for the Degree of

Master of Science in Mechanical Engineering
at the
Massachusetts Institute of Technology

June 2004

The author hereby grants to MIT permission to reproduce
and to distribute publicly paper and electronic
copies of this thesis document in whole or in part.

Signature of Author _____
Department of Mechanical Engineering
May 7, 2004

Certified by:_____
Alan J. Grodzinsky
Professor of Biological, Electrical and Mechanical Engineering, MIT
Director of Center for Biomedical Engineering
Thesis Supervisor

Accepted by:_____
Ain A. Sonin
Professor of Mechanical Engineering, MIT
Chairman, Department Committee on Graduate Student

BARKER

A Novel Osteochondral Composite Consisting of a Self-Assembling Peptide Hydrogel and 3D Printed Polycaprolactone Scaffold: Potential for Articular Cartilage Repair

by

Sanaz Saatchi

Submitted to the Department of Mechanical Engineering on May 7, 2004
in Partial Fulfillment of the Requirements for the
Degree of Master of Science in Mechanical Engineering

ABSTRACT

Degenerative diseases, such as osteoarthritis, and traumatic injuries are both prominent causes of cartilage defects. Due to its avascular nature, adult human cartilage displays limited capacity for regeneration. Current surgical treatments to induce a spontaneous repair response rely on access to the subchondral bone region. These procedures result in fibrocartilage generation, as opposed to hyaline cartilage, that is variable in structure, composition, and durability. Furthermore, the success rates of these surgeries are also variable.

Deficiencies in these cartilage repair methods motivate investigation into a tissue engineering means of repairing or regenerating cartilage. Various composites designed to emulate a cartilage and bone interface are under investigation. The aim of this study was to conceive a means of integrating a chondrocyte-seeded peptide hydrogel with an interconnected porous 3D printed polycaprolactone (PCL) scaffold to create a novel osteochondral construct. The self-assembling peptide hydrogel has been shown to provide an environment that maintains chondrocyte phenotype and viability. Furthermore, the 3D scaffold fosters extracellular matrix production and chondrocyte division. PCL is a bioresorbable and biocompatible polymer scaffold, capable of supporting the attachment of both osteogenic and chondrogenic cells and cell-specific extracellular matrix production, that can be integrated with the peptide hydrogel to constitute an osteochondral construct. A primary advantage of the 3D printing technology is the ability to control the microarchitecture and macroarchitecture of the PCL scaffold in a layer by layer fashion. Integration of the peptide hydrogel into the porous PCL scaffold may be enhanced by creating a gradient of porosity at the interface of the materials, while the lower portion of the PCL scaffold would possess a scaffold microarchitecture optimized for bone ingrowth.

Through the use of an agarose mold, the construction of an osteochondral composite consisting of the chondrocyte-seeded peptide hydrogel and porous PCL scaffold was made possible in an integrated, controlled, and repeatable fashion. PCL was found to act as an inert material with regard to chondrocyte behavior, as chondrocyte morphology, viability, extracellular matrix production, and biosynthesis rates proved to be analogous to those seen in the chondrocyte-seeded peptide hydrogel only systems previously studied. A distinction in the microarchitecture of the PCL scaffold, 70% porosity versus 90% porosity, was not found to markedly impact chondrocyte behavior in the peptide hydrogel. The efficacy of the peptide hydrogel material selection was illustrated by comparison to a chondrocyte-seeded agarose hydrogel and PCL composite, with an agarose hydrogel serving as a more traditional means of studying chondrocyte behavior. Biochemical, mechanical, and histological characterization of the peptide hydrogel and porous PCL construct delineate the potential use of this composite for

osteochondral defect repair. Future studies may involve dynamic compression of the composite to stimulate extracellular matrix synthesis and accumulation, and *in vivo* investigations to demonstrate the clinical impacts of such a construct on cartilage repair.

Thesis Supervisor: Alan J. Grodzinsky
Title: Professor

Acknowledgements

Table of Contents

12

Chapter 1: Introduction

1.1 Cause of Articular Cartilage Damage

Damage to the articular surface of a joint may be limited to the cartilage, or chondral layer, or may extend into the subchondral, or bone region, of the joint. The prominent causes of chondral and osteochondral defects are traumatic injuries and degenerative diseases, such as osteoarthritis and osteochondritis dissecans. Osteoarthritis is the most common form of joint disease and leads to the destruction of the mechanical integrity and biological functionality of the articular cartilage surface. Osteochondritis dissecans is a disorder in which fragments of cartilage and the underlying bone region separate from the articular surface. This degeneration of the articular surface may be caused by trauma to the chondral layer or an ischemia to the subchondral bone region [1,2].

1.2 Repair Capabilities of Articular Cartilage

Both partial-thickness, or chondral, defects and full-thickness, or osteochondral, defects in adult human cartilage are problematic because this tissue displays a limited capacity for repair and regeneration. Repair capabilities are limited by the avascular nature of the tissue, the potential catabolic response of chondrocytes to pathological mediators, and the limited capacity for chondrocyte proliferation [3]. The repair response that ensues in response to a defect is sensitive to the depth of defect penetration. Because chondral defects are confined to the cartilaginous layer of the articular surface and do not penetrate into the subchondral bone region, blood-bone cells, macrophages, and mesenchymal stem cells cannot access the defect to induce a spontaneous repair response. Therefore, the lesion does not heal. Osteochondral defects, however, do penetrate into the subchondral bone marrow space and can therefore be accessed by these cells. The sequence of events that follows leads to the formation of repair tissue that superficially resembles hyaline cartilage, but lacks the corresponding mechanical integrity and is degraded over six to twelve months [4].

1.3 Available Surgical Treatments and their Limitations

Although surgical treatments do exist to treat cartilage lesions, the success rates are variable and the disadvantages are numerous. Both autologous and allogenic treatments are forms of osteochondral grafting, and a collection of surgeries attempt to induce a spontaneous

repair response by accessing the subchondral bone marrow space. Mosaicplasty is a form of autologous osteochondral grafting that involves transplanting tissue from low weight bearing areas to high weight bearing areas. This surgical treatment results in mechanical overload of the transplanted tissue and the risk of damage due to the implantantion process is high. The inherent challenges of allogenic osteochondral grafts are immunological problems and a scarcity of donor material. The next three methods, abrasion arthroscopy, subchondral bone drilling, and microfracture, rely on access to the subchondral bone marrow space to induce a spontaneous repair response. These treatments lead to bleeding from the bone marrow space, blood clot formation, and migration of mesenchymal stem cells to the cartilage defect. However the repair tissue that is generated is fibrous tissue that is variable in structure, composition, and durability [5].
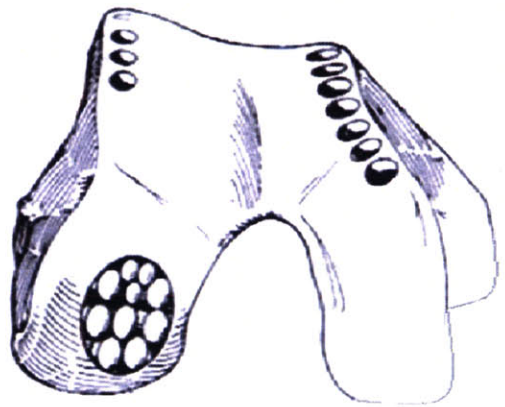
Figure 1.1 Schematic depiction of mosaicplasty: autologous osteochondral grafting of tissue from low weight bearing areas to high weight bearing areas.

1.4 Potential for Tissue Engineering Repair of Articular Cartilage Damage

The limitations of surgical treatments have led investigators to explore the realm of tissue engineering as a means of treatment. The ultimate goal of tissue engineering is to create physiologically functional and mechanically analogous three-dimensional tissues and organs through the use of cells and biomaterials. *In vivo* tissue engineering utilizes non-cell-seeded biomaterials and incites the body's native cell source to regenerate or repair the damaged tissue. *In vitro* tissue engineering entails the use and manipulation of cells and cell-seeded constructs prior to implantation into the *in vivo* environment.

14

1.5 Biomaterials as Scaffolds for Repair

The use of a biomaterial for tissue engineering applications is highly significant because the scaffold material functions as an extracellular matrix (ECM) analogue that provides a three-dimensional space for the development of new tissue with the appropriate structure and function. Although biomaterials may be bypassed and cell suspensions may be directly injected into the *in vivo* environment, scaffolds are an effective means of enhancing the localization and efficiency of the delivery of cells [6]. The impact of scaffolds can be enhanced with the addition of bioactive factors, such as growth factors, that regulate cell function. Furthermore, biomaterials fulfill a mechanical function as well by providing mechanical support against *in vivo* forces [6]. Scaffolds can thereby maintain a defined structure to ensure the proper development of physiologically and mechanically functional tissues.

1.6 Selection of Scaffold Material

The selection of a specific biomaterial is dictated by a variety of factors. The scaffold material must be biocompatible, reproducibly manufactured, easily sterilized, and should possess the appropriate mechanical and physical properties for the site of application. If the material is biodegradable, the degradation products should not produce an inflammatory response and should be capable of being metabolically broken down by the body [6]. The degradation rate of a biodegradable scaffold is also a significant characteristic to take into account. The rate of degradation of the biomaterial should be comparable to the rate of generation of new tissue. This similarity in rates ensures the maintenance of the mechanical support provided by the biomaterial until the regenerated tissue has the appropriate mechanical integrity to maintain itself, thereby avoiding collapse or stress shielding of the new tissue [7]. The microarchitecture, such as the porosity, pore size, and pore structure, is another significant design characteristic to consider. Not only does the microarchitecture affect cell adhesion, viability, extent and dynamics of tissue ingrowth, and formation of the ECM, but it also influences the transport of nutrient supply to the cells and metabolic wastes away from the cells [8]. Therefore, the final selection of a scaffold material should address these issues in order to be effective and successful.

1.7 Motivation for Two-Phase Osteochondral Composite

Although tissue engineering persists as a promising and viable alternative to surgical treatments for the repair of articular cartilage, there are inherent challenges that must be resolved.

15

Obstacles that investigators are attempting to overcome are implantation deformation during delivery of the scaffold into the defect, adhesion of the biomaterial, maintenance of the scaffold's physical structure, and integration at the native cartilage interface. An effective way to address these issues is through the creation of a multi-phase implant design. A two component composite will not only focus on cartilage repair, but will also address subchondral bone repair as well. In such a system, the top region serves as the cartilaginous replacement material and the lower region functions as the bone replacement material. An advantage of using a composite implant is that the bone replacement material provides anchorage and mechanical support for the cartilaginous replacement material [9]. As a vehicle of delivery, the subchondral repair material encourages adhesion of the cartilage substitute and integration with the native tissue [10]. Therefore, a two-phase composite for articular surface repair should include a bone substitute material that mimics native trabecular bone, with regard to microarchitecture and mechanical properties, and can be integrated with a cartilage replacement material.

1.8 Existing Osteochondral Composites: Calcium Phosphate Ceramics

A variety of material combinations have been investigated as potential osteochondral composites. Recent studies have utilized various combinations of calcium phosphate ceramics, calcium carbonates, synthetic polymers, hydrogels, and hyaluronan-derived materials. These studies have integrated progenitor cells, chondrocytes, or both chondrogenic and osteogenic cells into their composites. Calcium phosphates are commonly used because they emulate the microarchitecture, interconnectivity, and environment provided by native trabecular bone. The type of calcium phosphate formed depends on the temperature, presence of water, and pH of the manufacturing process or the environment in which the calcium phosphate will be used [11]. Porous hydroxyapatite (HA), the stable form of calcium phosphate when in contact with aqueous media at body temperature and pH greater than or equal to 4.2, is commonly selected as the bone replacement material because of its high biocompatibility and bioaffinity [12]. It is osteoconductive, thereby promoting bone ingrowth by the surrounding native tissue, and is slowly replaced by the host bone [12]. Hydroxyapatite alone has served as the bone replacement material or has been integrated with collagen type I and beta-tricalcium phosphate (TCP) forming a Collagraft sponge [13, 14]. These studies integrated the bone substitute material with a chondrocyte fibrin-glue cartilaginous substitute and a chondrocyte-seeded polyglycolic acid scaffold (PGA), respectively. However, the results were poor for the HA and fibrin-glue

16

composite, which displayed fibrous tissue formation, osteolysis of the host bone, and disintegration of the fibrin glue. Integration with the native cartilage tissue was also problematic for the latter composite, despite good integration in the bone region. Another composite involving calcium phosphate utilized an injectable calcium phosphate integrated with a hyaluronan sponge [15]. The injectable calcium phosphate not only functioned as a mechanically and structurally analogous material to the mineral component of bone, but it also provided mechanical support and anchorage for the hyaluronan sponge cartilaginous substitute. When combined with marrow-derived progenitor cells, this composite resulted in mostly repair tissue formation and neobone tissue formation. The investigators postulated that the local mechanical environment influenced the differentiation of the progenitor cells into chondrocytes to form a hyaline cartilage-like repair tissue that was well integrated with the surrounding tissue [15].

1.9 Existing Osteochondral Composites: Synthetic Polymers

An assortment of synthetic polymers have been incorporated into both regions of osteochondral composites. These polymers include polyglycolic acid (PGA), poly-L-lactic acid (PLLA), poly-D,L-lactic acid (PDLLA), poly-lactic-co-glycolic acid (PLGA), polyethylene glycol (PEG), and polycaprolactone (PCL). The application of these materials has been in both the chondral and subchondral region of the osteochondral composite. One study created a chondrocyte-seeded composite polymer fleece consisting of PGA and PLLA (90:10) to serve as the cartilaginous substitute portion [9]. The impact of porosity of the bone substitute material on cell suspension penetration and integration of the two regions of the osteochondral construct was studied by comparing calcium carbonate from a natural coralline material to calcite, a synthesized calcium carbonate, when combined with the cell-seeded polymer fleece. Although both composites displayed comparable cell viability, distribution, and ECM production, the calcium carbonate from the natural coralline material allowed for more extensive penetration by the cell suspension and a more stable interaction between the two regions of the composite due to its inherent porosity. Another study involving synthetic polymers depicted the possibility of creating an osteochondral composite seeded with two different cell types. Bovine chondrocytes seeded on a PGA mesh were cultured in chondrogenic medium, independent of bovine periosteal cells seeded on a blend of PLGA/PEG (80:20) cultured in chondrogenic medium with osteogenic medium supplements [16]. After a period of time, the two components of the system were sutured together and cultured in osteogenic medium. This study demonstrated the capability to

create an osteochondral composite co-cultured with two distinct cell sources that retained a well-defined cartilage-bone interface with cell-specific ECM accumulation in each region. Another polymer that has proven to be a viable option for osteochondral application is poly-ε-caprolactone (PCL). Through the co-culture of both chondrogenic and osteogenic cells, PCL has proven to be a potential scaffold material because both types of cells attached to the PCL, proliferated, and produced cartilage and bone specific ECM in their respective regions [17]. This material is biocompatible and has degradation rates that are slower than other synthetic polymers, such as PLA [11].

1.10 Existing Osteochondral Composites: Hydrogels

Another category of materials that has traditionally been used in articular cartilage repair and the study of chondrocyte behavior is the hydrogel. The agarose hydrogel provides a well-characterized cell culture environment which allows for the study of ECM assembly by chondrocytes [18]. Studies have indicated that bovine, rabbit, avian, and human chondrocytes maintain their phenotype when cultured in an agarose gel [19]. The chondrocytic phenotype is characterized by the synthesis of type II collagen, cartilage-specific ECM, and a rounded cell morphology. Because of its capability to preserve the chondrocytic phenotype in cell culture, an agarose hydrogel is an effective means of investigating matrix deposition by chondrocytes and delineating the relationships between mechanical compression, cell-matrix interactions, and the biological and chemical pathways of mechanotransduction [18]. With regard to osteochondral composites, an agarose hydrogel was integrated with devitalized trabecular bone discs to investigate the viability of this composite in terms of the maintenance of chondrocyte viability and biosynthetic activity [20]. This study also investigated the possibility of creating anatomically shaped osteochondral constructs for the replacement of an entire damaged articular joint surface. The chondrocyte-encapsulated agarose was found to infiltrate the trabecular bone scaffold and to maintain viable cells in both the cartilaginous layer and the subchondral bone layer. Cartilage-specific ECM developed in both regions of the osteochondral composite and the trabecular bone was characterized as a potential material that did not adversely affect chondrocytic phenotype, biochemical content, and material properties.

Polyvinyl alcohol (PVA) hydrogel is another hydrogel material that has been incorporated into an osteochondral composite system for articular cartilage repair. PVA hydrogel is a biocompatible rubber-like gel with mechanical properties that have been previously

18

characterized to display its potential as an articular cartilage replacement material [21]. The PVA solution infiltrated the pores of the titanium fiber mesh (TFM) bone substitute material to constitute a composite scaffold. Despite the relatively high porosity of the 60% porous TFM material, there was poor adherence between the two components of the composite due to the high viscosity of the PVA hydrogel. This composite proved to be further problematic as the material strength of the PVA hydrogel was inadequate when tested during animal studies.

1.11 Motivation for Novel Osteochondral Composite: Peptide Hydrogel and 3DP™ PCL

The previous studies elucidate the requirements for an effective and viable osteochondral composite. For a hydrogel cartilaginous layer, this material must maintain chondrocyte phenotype, morphology, and biosynthetic activity. The accumulation of chondrocyte-specific ECM is important to obtain a cartilaginous layer with material properties comparable to that of native articular cartilage. The hydrogel material must be biocompatible and of an appropriate viscosity that allows for infiltration into a porous bone substitute material. Stable adherence to the bone substitute material and integration with the native cartilage tissue are also eminent requirements. Our material selection for this region of an osteochondral composite is a self-assembling peptide hydrogel [22, 23]. The bone substitute material must have the microarchitecture that emulates that of trabecular bone, with the appropriate pore size, porosity, and interconnectivity of void space. This microarchitecture should allow for both hydrogel infiltration and bone ingrowth from the surrounding native tissue. This biocompatible bone substitute material should also be reproducibly manufactured and should not adversely affect chondrocyte phenotype or biosynthetic activity. The mechanical properties and degradation rate of this bone substitute material are also indicative of the efficacy of an osteochondral composite. Our material selection for this region of the osteochondral construct is three-dimensional printed (3DP™) polycaprolactone (PCL) [17, 24-26].

Chapter 2: Self-Assembling Peptide Hydrogel and 3DP™ PCL Osteochondral Composite

2.1 Self-Assembling Peptide Hydrogel

A class of peptide-based biomaterials that have the capability to self-assemble into hydrogels has been under investigation as a molecular-engineered scaffold for tissue engineering. The process of self-assembly can be construed as the spontaneous organization of individual constituents into an ordered structure without any external intervention [27]. The members of this class of materials are denoted as amino acid sequences with alternating hydrophilic and hydrophobic side groups with alternating positive and negative charges. Depending on pH, salt concentration, and time, a variety of peptide polymers have displayed the ability to adopt a β–sheet structure and to aggregate [22, 28, 29]. Some of these polymers include poly-(Val-Lys), poly(Glu-Ala), poly(Tyr-Glu), poly(Lys-Phe), poly(Lys-Leu), and [(Val-Glu-Val-Orn)$_{1-3}$]-Val [28]. Additionally, some amino acid sequences are distinct in that they also possess the ability to form an insoluble macroscopic membrane subsequent to β–sheet structure formation. A few of these sequences include EAK-16 (Glutamic Acid-Alanine-Lysine), RAD-16 (Arginine-Alanine-Aspartic Acid), and KLD-12 (Lysine- Leucine-Aspartic Acid).

2.2 Features of Peptide-Based Biomaterials

A major advantage of the peptide-based biomaterials is the ability to control material properties through the selected design of the individual constituent molecules [30]. Potential characteristics that can be tailored for specific applications based on the molecular sequence of the peptide chain are chemical functionality, mechanical properties, viscoelastic properties, and processibility [30]. Specific motifs, such as RGD (Arginine-Glycine-Aspartic Acid) a ligand for integrin cell adhesion receptors, can be incorporated to promote cell attachment [31]. Furthermore, as a synthetic biomaterial, these materials have minimal risk of introducing biological pathogens or contaminants. The byproducts of the peptide-based biomaterials can be incorporated into newly synthesized biomaterials or metabolized in the host organism [31]. Two peptide sequences, EAKA-4 and RADA-4, have shown positive results in animal studies when testing for immunogenicity [22].

2.3 The Self-Assembly Process

Exposure to an electrolyte solution triggers the self-assembly process as the β-sheet structure takes on the form of interwoven nanofibers [22]. Although each type of bond involved in the self-assembly process is relatively weak, they can collectively form interactions that are stable. These bonds typically include hydrogen bonds, ionic bonds, and hydrophobic and van der Waals interactions [27]. The exact mechanism of how and why exposure to an electrolyte solution triggers the self-assembly process has been investigated and theories have been developed. The exposure to salt is believed to disrupt intramolecular electrostatic interactions, thereby encouraging the peptide to undertake a conformation that enhances intermolecular hydrophobic interactions with adjacent peptides [31]. Intermolecular electrostatic interactions between adjacent peptides may then contribute to the stabilization of the newly formed matrix. Another study corroborates the theory of intermolecular interactions by explaining how the formation of backbone hydrogen bonds and the interment of hydrophobic side chains result in interactions with adjacent β–strands through additional hydrogen bonds and hydrophobic interactions [32]. The interwoven nanofiber network that is then formed after self-assembly consists of nanofibers with a diameter of 10-20nm and pores of about 50-200nm [27].
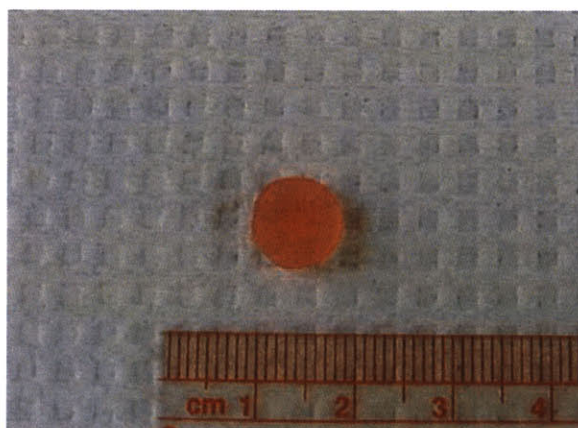
Figure 2.1 9mm chondrocyte-seeded peptide hydrogel plug

2.4 KLD-12 and Chondrocyte Behavior

Recently, KLD-12 (Lysine-Leucine-Aspartic Acid) has been established as a peptide hydrogel scaffold material that maintains chondrocyte phenotype and morphology when cultured

in vitro [22]. With a peptide concentration of 0.5% and a primary chondrocyte cell density of 15 million/mL, Kisiday et al. performed a study that validated the selection of the KLD-12 peptide hydrogel as a favorable choice of material with regard to cell viability, cell division, and development of chondrocyte-specific ECM, rich in proteoglycans and type II collagen [22]. An increase in compressive stiffness as a function of time was validated by the development of a continuous ECM, as depicted by histological analysis. Furthermore, dynamic compression has been well characterized as a means of enhancing synthesis of proteins and proteoglycans in both cartilage explants and chondrocyte-seeded agarose hydrogels [33, 34]. A recent study applied a variety of dynamic loading protocols to conclude that overall proteoglycan accumulation in a chondrocyte-seeded peptide hydrogel increases with applied dynamic compression [35]. This increase in matrix deposition corresponds to an increase in both the equilibrium and dynamic compressive stiffness. Therefore, *in vitro* culture conditions can be tailored to optimize material properties of the peptide hydrogel before application *in vivo*.
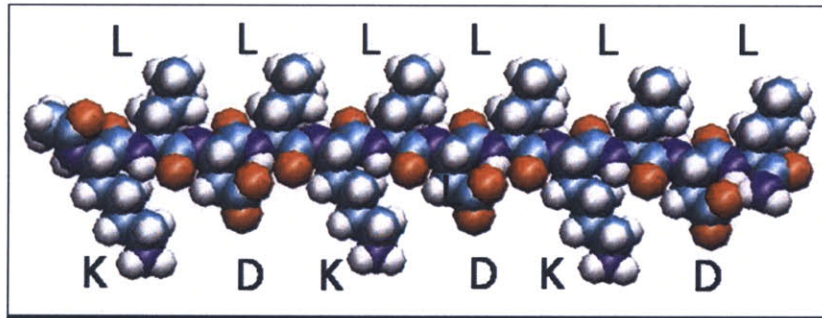
Figure 2.2 Molecular model of the KLD-12 self-assembling peptide sequence [22]. β-sheet formation is promoted by the alternating hydrophobic residues, leucine (L), and hydrophilic residues, lysine (K) and aspartic acid (D). The hydrophobic leucine residues are on the upper side of the β -sheet, while the positively charged lysine and negatively charged aspartic acid residues are on the lower side of the β -sheet.

2.5 Encapsulation of Chondrocytes and Casting Procedure of Peptide Hydrogel

The peptide KLD-12 is custom synthesized (SynPep Corp., Dublin, CA) and lyophilized to a powder. The encapsulation of chondrocytes and casting procedure of the peptide hydrogel has been developed by Kisiday et al [22]. Briefly, KLD-12 powder is dissolved in a 10% sucrose solution at a concentration of 3.6mg/mL. The peptide solution is then sonicated until further use to prevent aggregation. The volume of cell suspension targeted for the desired cell seeding density is centrifuged at 1900 rpm for 8 minutes. Isolated chondrocytes are then resuspended in a 10% sucrose plus 5mM HEPES buffer equal in volume to 10% of the final hydrogel casting

volume. The peptide solution is then added to the cell suspension in volume equal to 90% of the final hydrogel casting volume. The casting solution is then lightly vortexed and injected directly into a stainless steel casting frame, which is then submerged in 1.5X PBS with slight agitation on a stir plate for approximately 45 minutes to invoke self-assembly of the peptide hydrogel. At this point, the casting frame is then removed from the PBS bath, the frame is disassembled, and the peptide hydrogel is then placed into culture medium.

2.6 PCL

Poly-ε-caprolactone (PCL) is a semicrystalline polymer that belongs to the family of α-hydroxy polyesters. PCL possesses inherent material properties, such as an extremely low glass-transition temperature of -60°C, a melting point of 60°C, and a high decomposition temperature of 350°C, that allow for compatibility with a wide range of thermoplastic processing techniques [36]. PCL is both biodegradable and bioresorbable. A biodegradable polymer is one that can be broken down due to macromolecular degradation in vivo; however, these degradation by-products are not necessarily eliminated from the body. Alternatively, bioresorbable polymers produce degradation by-products that are eliminated from the body, either through natural pathways or metabolization, with no residual side effects [24]. Other members of this polyester class of materials include polylactide (PLA), polyglycolide (PGA), and polylactide-co-glycolide (PLGA).
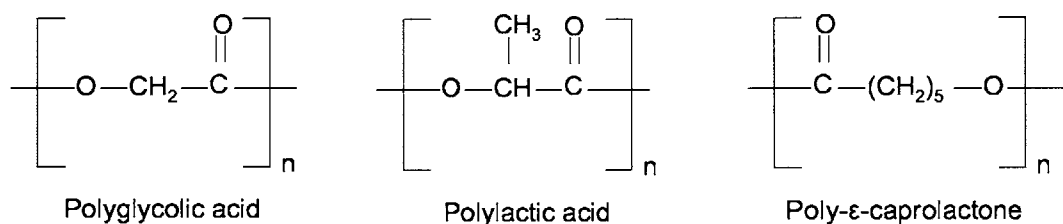
Figure 2.3 Chemical structure of α-hydroxy polyesters: PGA, PLA, PCL

Compared to the other members of this class of materials, PCL displays slower degradation kinetics [37]. If the function of the scaffold material is to maintain the mechanical integrity of the implant until the engineered tissue is remodeled by the host bone tissue, the scaffold should retain its physical properties for at least six months. After this point, the scaffold material will begin to be metabolized by the body over a period of 12-18 months [24]. The degradation rate of polymers is dependent on a variety of factors, such as chemical structure and composition,

24

presence of ionic groups, molecular weight, production and manufacturing procedures, implant design, sterilization method, storage, and implant site [24]. Furthermore, a distinction is drawn between molecular weight loss, which begins a period of time that is unique to the material after placement in an aqueous media, and mass loss, which is not initiated until the molecular chains are reduced to such a size that allows for free diffusion of material mass out of the matrix. As a reference state for the degradation kinetics of PCL, one study indicates that molecular weight loss occurs over a period of 9-12 months and mass loss occurs over 24-36 months for PCL [24]. Mechanical properties of PCL are also variable due to discrepancies in the microarchitecture and structure of the material. Solid PCL (M_w = 44,000) has been shown to have the following material properties: tensile strength of 16MPa, tensile modulus of 400MPa, flexural modulus of 500MPa, elongation at yield of 7.0% and elongation at break at approximately 80% [38]. Because of the ease with which PCL can be processed, its structural stability over a wide range of temperatures, its degradation kinetics, and its biocompatibility and bioresorbability, this material has already received FDA approval for use in a number of drug delivery devices and medical devices, such as staples for wound closures, and is currently under investigation for use as a scaffold material for skin, bone, cartilage, and liver [11, 37, 38].

2.7 Fabrication Processes

A variety of 3D scaffold fabrication technologies are currently utilized within the tissue engineering community. Each technology has its own set of advantages and disadvantages; however, the ability to reproducibly manufacture scaffolds is also an imminent concern. The conventional techniques for scaffold fabrication are solvent casting, particulate leaching, membrane lamination, melt molding, supercritical-fluid technology, emulsion freeze-drying method, thermally-induced phase separation, and rapid prototyping technologies [24]. As seen in the table below, each technology has a unique set of capabilities, limitations, and challenges. The major shortcomings in these technologies, excluding rapid prototyping technologies, are the inability to produce a fully inter-connected porous microarchitecture, variation in pore size, discrepancies in pore wall thickness, and the inability to produce a non-uniform multiple layer design [36].

Fabrication Technology	Processing	Material properties required for processing	Scaffold design and reproducibility	Achievable pore size in μm	Porosity in %	Architecture
Solvent casting in combination with particulate leaching	Casting	Soluble	User, material and technique sensitive	30-300	20.0-50.0	Spherical pores, salt particles remain in matrix
Membrane lamination	Solvent bonding	Soluble	User, material and technique sensitive	30-300	< 85	Irregular pore structure
Melt molding	Molding	Thermoplastic	Machine controlled	50-500	< 80	N/A
Emulsion freeze drying	Casting	Soluble	User, material and technique sensitive	< 200	< 97	High volume of interconnected micropore structure
Thermally induced phase separation	Casting	Soluble	User, material and technique sensitive	< 200	< 97	High volume of interconnected micropore structure
Supercritical-fluid technology	Casting	Amorphous	Material and technique sensitive	< 100	10.0-30.0	High volume of non-interconnected micropore structure
3D printing in and without combination of particle leaching	Solid free form fabrication	Soluble	Machine and computer controlled	45-150	< 60	Fully interconnected macroporosity, layer by layer design and fabrication, incorporation of biological agents into matrix possible
Fused deposition modeling	Solid free form fabrication	Thermoplastic	Machine and computer controlled	>150	< 80	Fully interconnected macroporosity, layer by layer design and fabrication

Figure 2.4 3D scaffold fabrication technologies [24].

2.8 Rapid Prototyping Technology: Three-Dimensional Printing

Rapid prototyping technologies (RP), also known as Solid Free Form fabrication methods (SFF), are unique in their capabilities to fabricate complex 3D structures in a layer by layer manner and through the use of a computer-aided design (CAD) model of the scaffold. 3D printing (3DP™) and fused deposition modeling (FDM) are two distinct forms of RP technologies [24]. 3DP™ is a technology, developed at MIT, originally developed for the fabrication of ceramic and metal objects. The application of this technology to polymer scaffold production is advantageous because of its capability to manufacture scaffolds with a varying

26

multiple layer design, to control microporosity and macroporosity, and to perform surface modifications [25]. As seen in the schematic below, a thin layer of powder is spread by the powder spreader across the surface of the powder bed on top of a piston. An ink-jet printhead then prints a liquid binder based on the CAD design, or specified printing parameters, into the layer of powder, thereby bonding the particles of the polymer together to form a solid. Although 3DP™ does present the advantage of controlling the design of the scaffold via a CAD design, the Theriform™ (Therics, Inc. Princeton, NJ) 3DP™ machine, which will be discussed in further detail in subsequent sections, does not possess this capability. Therefore, the design of the scaffold is controlled through the use of masks and the selected printing parameters. Chloroform is the binder commonly used for manufacturing polymer scaffolds. After the first layer is printed, the piston then lowers the powder bed to a fixed distance and the cycle of powder-spreading and printing is repeated. The process is repeated until a complex 3D scaffold is complete and the scaffold can then be lifted from the powder bed [25].
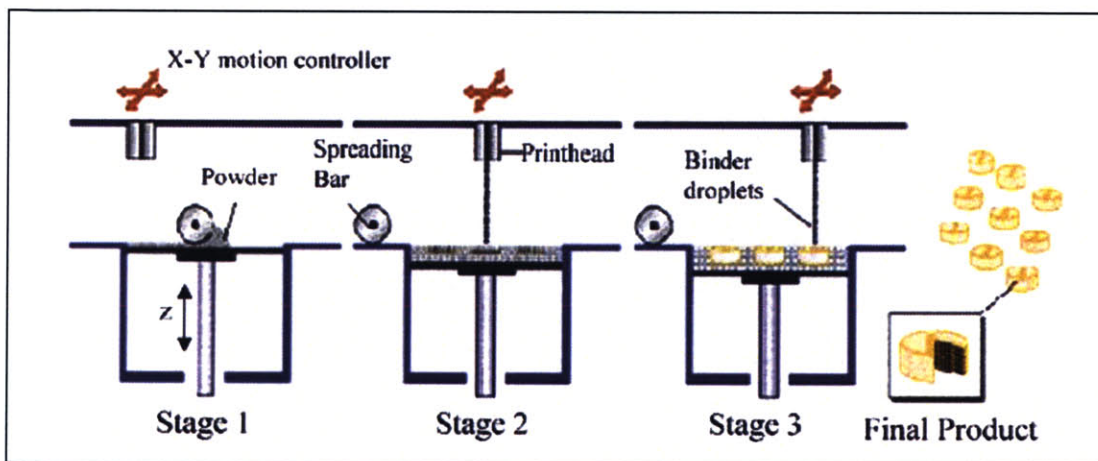
Figure 2.5 The TheriForm™ three-dimensional printing (3DP™) fabrication process. A thin layer of powder, consisting of PCL and NaCl particles, is spread across the powder bed. Chloroform droplets, controlled by the printhead, bind the polymer in a layer by layer fashion [39].

The microarchitecture is controlled through the composition of the powder that is spread across the powder bed. Particles of NaCl and PCL are mixed together in relative proportions to create the desired porosity of the scaffold, as the NaCl particles will later be leached out to create the void space within the scaffolds. The pore size is dictated by the diameter size of the NaCl particles. The macroarchitecture is controlled through the printing parameters, which define the positive feature size, wall thickness, and the negative feature size, channel thickness. After the printing process is complete, scaffolds are placed in water on an orbital shaker to leach out the

NaCl particles. The scaffolds are then frozen at -80°Celsius and lyophilized overnight to remove any residual water. After a 14 hour cycle of sterilization with ethylene oxide, the scaffolds are ready for use. The features of this technology are the ability to manufacture a fully inter-connected porous structure with specified microporosity and macroporosity. Complex internal features, such as channels and a gradient of porosity, can be incorporated into the design of the scaffold. The resolution of the printing process is defined as the line resolution, which is the lateral width of each bound line in a layer. Line resolution is controlled by printhead nozzle diameter, chloroform droplet diameter, print speed, pressure of chloroform deposition, and the polymer being printed. The chloroform droplet diameter is approximately twice the size of the printhead nozzle diameter. The line resolution is then approximately double the chloroform droplet size. Furthermore, this technology possesses the potential to incorporate biological agents, such as cells and growth factors, into the design of the scaffold if non-toxic binders are employed [24].
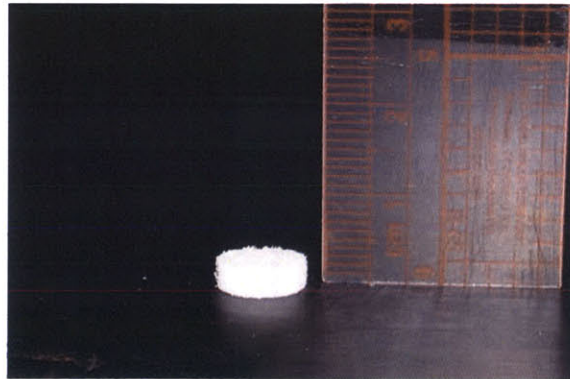
Figure 2.6 Porous PCL scaffold, 9mm diameter x 3mm thick, created via 3DP™ technology.

2.9 Rapid Prototyping: Fused Deposition Modeling Process

A number of studies investigating the efficacy of PCL as a scaffold material in tissue engineering employed fused deposition modeling (FDM) technology to fabricate scaffolds. Similar to 3DP™, FDM uses a CAD model as part of the rapid prototyping technique (RP) to create a scaffold layer by layer. A polymer filament is fed into a temperature-controlled FDM extrusion head. At the end of the extrusion head, the filament is heated to a semi-molten state and deposited onto a platform in a layer by layer fashion. The polymer filament being fed into the extrusion head functions as a piston that drives the semi-molten extrudate onto the platform

as it is pushed down by two rollers in the FDM head [24, 38]. With the completion of each layer, the platform is lowered and the next layer is deposited.
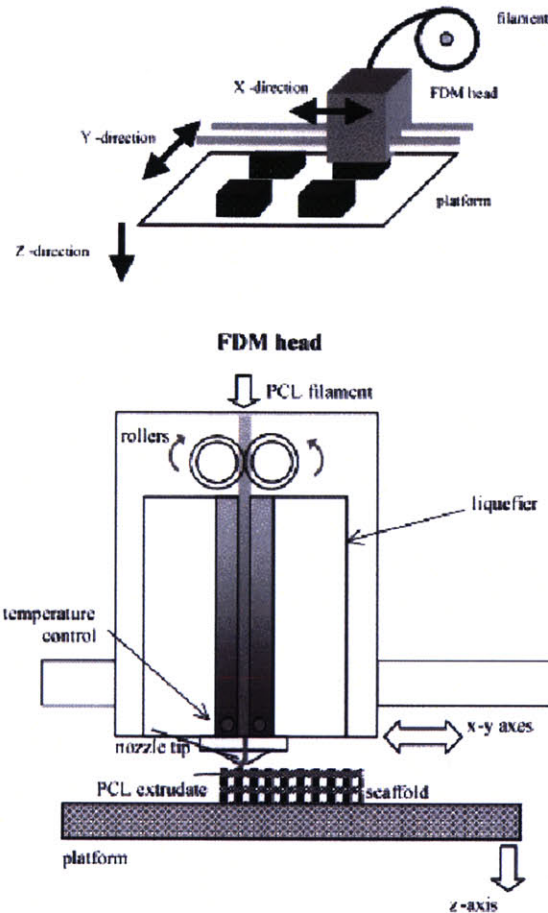
Figure 2.7 The Fused Depostion Modeling (FDM) fabrication process. The FDM head receives PCL in a filament form and deposits the semi-molten polymer onto a platform that is then lowered to allow for the deposition of the subsequent layer [38].

Layers can be manufactured in a particular lay-down pattern by specifying the direction of deposition, or raster angle, for each layer, which is an angle between 0° and 180° with respect to the x-axis [38]. Channels are created within each layer in a regular manner to create a 3D interconnected porous structure with honeycomb-like architecture. An advantage of the FDM process is that it does not require any solvents.

2.10 Current PCL studies using 3DP™ and FDM

Recent studies have delineated the potential of a 3D PCL scaffold fabricated through RP means by investigating cell attachment, ECM accumulation, osteoconductivity, and co-culture of chondrogenic and osteogenic cells. A study performed by Hutmacher et al. revealed the capability of primary human fibroblasts and periosteal cells to proliferate, differentiate, and produce ECM in a 3D fully interconnected porous PCL scaffold fabricated through FDM means [36]. Human fibroblasts were able to develop an interconnected network of cells throughout the scaffold. Additionally, the osteoblast-like cells displayed a 3D phenotype and were able to attach and spread onto the PCL scaffold. This is a significant observation to prove the efficacy of a porous PCL scaffold as a bone substitute material. The attachment and interaction of osteoblast-like cells is essential to the development of new bone tissue and eventual remodeling of tissue within the scaffold. Another study revealed an effective means of enhancing bone ingrowth and osteoconductive properties of an FDM fabricated porous PCL scaffold. By coating the scaffolds with bone marrow, bone ingrowth within the PCL scaffolds was enhanced due to the osteoinductive nature of the bone marrow mesenchymal cells [26]. The 65% porous PCL scaffolds were filled with the formation of cellular tissue and new bone formation at 3 months when implanted into orbital defects, however new bone formation was enhanced from 4.5% to 14.1% with the bone marrow coating [26]. Although some foreign-body giant cells were observed around the PCL implants, there were no indications of an inflammatory reaction. This study reveals an interesting and effective means of enhancing bone ingrowth to ensure the development of new bone tissue within the scaffold. An FDM fabricated porous PCL scaffold was also used to delve into the possibility of co-culturing chondrogenic and osteogenic cells to create an osteochondral composite [17]. The PCL scaffolds in this study were 60-65% porous with pore size in the range of 300 to 580 μm. A marrow stromal cell suspension mixed with fibrin glue was pipetted into the bone compartment of the scaffold. The seeded scaffold was cultured in osteoblastic medium for 18 days before the chodrocyte-fibrin glue suspension was seeded into the cartilage compartment of the scaffold. Both chondrocytes and osteoblasts were found to be attached to the PCL scaffolds and were interconnected at the compartment interface. Cell-specific ECM had developed in each region of the osteochondral composite, with dense and mineralized ECM in the bone substitute region. A mixture of cell types was observed at the interface of the two compartment regions. The novelty of this study lies in the co-culture of two

30

cell types. The finding that PCL is capable of supporting the development of both chondrocyte-specific ECM and osteoblast-specific ECM is critical to the efficacy of PCL as the selected osteochondral scaffold material. This approach of co-culturing two cell types can potentially be integrated with the 3DP process to create a multi-layer design with a porosity gradient to ensure the development of cartilaginous tissue in the top region of the composite and bone tissue in the bottom region of the composite.

2.11 Ultimate Multi-Layer Design

By selecting the 3DP™ technology as the PCL scaffold fabrication process, we have obtained the capability to create a complex scaffold with a varied multi-layer design. This added complexity is ideal for our objective of creating an osteochondral composite. The ultimate design consists of a PCL scaffold (9mm diameter x 3-4mm thickness) with a gradient of porosity to differentiate and optimize the regions of the scaffold. A higher porosity will be invoked in the top region (1-2mm thickness) of the scaffold to enhance the development of a cartilaginous material and integration of the peptide hydrogel into the PCL scaffold. A thin solid PCL region will then be fabricated to serve as a differentiating layer between the cartilage-bone interface and to mimic the natural architecture of the articular joint. The next region (2mm thickness) will have a lower porosity level to allow for the development of bone-like ECM, bone ingrowth, and vascularization. Although different polymers were used, a study by Sherwood et al. illustrates the advantage of creating a unique multi-layer scaffold design for osteochondral repair [39]. The 3DP™ process was utilized to create a scaffold of 90% porosity with pore size between 106-150μm in the top region (2mm thickness) and 55% porosity with pore size between 125-150μm in the bottom region (4.4mm thickness). The 55 % porosity level was chosen as a balance between mechanical properties and a high surface area to optimize bone ingrowth and vascularization. This porosity level is consistent with that of natural trabecular bone, which is in a range of 50-90% porous [39]. This gradient of porosity is the scaffold design characteristic that allowed for the preferential attachment of chondrocytes to the top cartilaginous region, with minimal cell attachment found in the low porosity bone region. Furthermore, after 4 weeks of *in vitro* culture, cartilage-like ECM had developed in the top region of the osteochondral scaffold. Analogously, our ultimate design will incorporate this multi-layer feature to create two distinct, and yet integrated, PCL regions. Our objective was to focus on the interaction of the peptide hydrogel with the top porous region of the overall osteochondral construct. The additional

31

regions, the solid boundary layer and the lower porosity bone region, will be added to the fabrication process at a later date.

Chapter 3: Optimization of Composite Fabrication Process

3.1 Introduction

Although the casting procedure of the KLD-12 peptide into chondrocyte-seeded hydrogel slabs has been developed and optimized by Kisiday et al., there were many challenges to overcome in order to integrate this material with a porous PCL scaffold to form an osteochondral composite [22, 23]. The peptide is normally cast into a stainless steel frame when it is in the molten state and subsequently placed into a PBS bath to initiate self-assembly into a slab-like geometry. The PCL scaffolds are fabricated in a cylindrical core fashion. Therefore, a means of casting the molten peptide onto the cylindrical PCL cores in a controlled and repeatable manner that would result in the integration of the two materials was investigated. An agarose mold in which the peptide could be cast directly onto and into the porous PCL core was conceived to be an effective means of addressing these issues. However, the concentration of agarose utilized to create this mold, as well as the optimal geometry, were significant issues to address because of their potential effects on chondrocyte viability, and diffusion and transport of nutrients to the chondrocytes. Additionally, the traditional casting protocol had to be adapted in terms of the initiation time of the self-assembly process. A delay in the initiation of the gelation process, carried out by submersion into a PBS bath, would allow for the molten cell-encapsulated peptide suspension to seep into the porous PCL scaffold, thereby allowing for the integration of the two materials. However, too long of a delay may lead to a lowered cell viability. The cell seeding density of the peptide hydrogel was another factor to tailor towards the purposes and confines of these studies. Finally, the effects of a PCL scaffold on chondrocyte viability, phenotype, and behavior both in the peptide hydrogel and the PCL scaffold were critical components to study to prove the efficacy of such a composite.

3.2 Methods and Materials

3.2.1 Study 1: Agarose Mold

3.2.1.1 Cell Isolation

Bovine chondrocytes were harvested from the femoral condyles and femoropatellar grooves of 1-2 week old calves within a few hours of slaughter, as previously described [40]. As a brief description, cartilage slices were taken from the femoral condyles and femoropatellar

grooves and manually chopped into fine pieces. The tissue was then transferred to a pronase solution at a concentration of 20U/mL for 2 hours of incubation (Sigma-Aldrich, St. Louis, MO). The pronase-tissue solution was mixed via pipetting every twenty minutes. At the end of this incubation period, the tissue was rinsed twice with 1X PBS and placed into a collagenase solution at a concentration of 200U/mL overnight (Worthington, Lakewood, NJ). The next morning, the collagenase-tissue solution was mixed via pipetting every 30 minutes until the solution appeared relatively clear, indicating the completion of the digestion process. At this point, the solution was allowed to incubate for 1.5 hours to complete digestion. The chondrocyte suspension was then filtered through a 40μm cell strainer and centrifuged at 1900rpm for 8minutes. After aspirating the supernatant, cell pellets were resuspended and centrifuged in 1X PBS. This process of centrifugation and PBS rinsing was repeated two more times. After the third round of centrifugation, the cells were resuspended in high glucose DMEM (Gibco, Auckland, New Zealand). A sample of cell suspension was microscopically analyzed for cell viability using ethidium bromide/FDA and concentration using Trypan Blue Staining (Sigma Chemical Co., St. Louis, MO). The cell suspension was then stored at 4° C until use.

3.2.1.2 Casting

0.75% and 3% agarose molds were created by pipetting 4-5ml into 35mm Petri dishes. All molds were 3-4mm thick, but varied geometrically in both inner diameter (ID) and outer diameter (OD). Molds with an ID of 5mm and an OD of 9mm were created, as well as a 9mm ID with an OD of both 12mm and 16mm. The peptide KLD-12 was custom synthesized (SynPep Corp., Dublin, CA) and lyophilized to a powder. KLD-12 powder was dissolved in a 10% sucrose solution at a concentration of 3.6mg/mL. The peptide solution was then sonicated until further use to prevent aggregation. The volume of cell suspension targeted for a cell seeding density of 10million/mL and 20million/mL was centrifuged at 1900rpm for 8 minutes. Isolated chondrocytes were then resuspended in a 10% sucrose plus 5mM HEPES buffer solution equal in volume to 10% of the final hydrogel casting volume. The peptide solution was then added to the cell suspension in volume equal to 90% of the final hydrogel casting volume. The casting solution was then lightly vortexed and injected directly into the hollow cylindrical core of the agarose mold. The samples were then submerged in 1.5X PBS without agitation for 1 hour to initiate self-assembly of the peptide hydrogel. At this point, PBS was aspirated and culture

34

medium, high-glucose DMEM with 0.2% FBS and 1% ITS, was added. Each sample received 5mL of culture medium that was changed every other day.

3.2.1.3 Cell Viability

Chondrocyte viability was assessed by removing small portions of the cylindrical core chondrocyte-seeded peptide hydrogel. A 1:1 mixture of ethidium bromide/FDA, equal in volume to 5-8μL, were added directly to the hydrogel sample submerged in 10-12 μL of culture medium. Using UV fluorescence, this assay provided a qualitative assessment of the live and dead cells in the chondrocyte-seeded peptide hydrogel.

3.2.2 Study 2 and Study 3: Gelation Time and Depth of Infiltration

3.2.2.1 Cell Isolation

The standard protocol as described in Section 3.2.1.1 was used in study 3 to isolate primary bovine chondrocytes.

3.2.2.2 PCL Fabrication

PCL scaffolds were fabricated using a Theriform™ 3DP™ machine (Therics, Inc. Princeton, NJ). An emulsion-precipitation method was used to create PCL powder (PCL MW= 65KDa, Aldrich, Milwaukee, WI) [41, 42]. Briefly, PCL was dissolved in dichloromethane (CH_2Cl_2) and then injected into a continuously stirred water bath consisting of 2.5% polyvinyl alcohol (PVA) in H_2O After the precipitation of PCL in this water bath, the spherical particles were rinsed, dried, and sieved to a particle diameter of less than 50μm. The pore size within the microarchitecture of the PCL scaffold is dictated by the NaCl particle diameter size (Mallinkrodt, Paris KY). NaCl particles were milled and sieved to a range of 50-75μm diameter (Bel-Art Products Mill, Model Number: 37252-0000, Pequannock, NJ; VWR Scientific Sieve, West Chester, PA). Particles of NaCl and PCL were mixed together in relative proportions to create the desired porosity of the scaffold. For these studies, mixture compositions included a solid PCL region and an 80% NaCl with 20% PCL powder mixture for an 80% porous PCL region. A thin layer of powder was spread by the powder spreader across the surface of the powder bed on top of a piston. An ink-jet printhead then printed the liquid binder, chloroform, thereby bonding the particles of the polymer together to form a solid (Mallinckrodt, Paris, KY). The 50μm diameter printhead nozzle created droplets of chloroform approximately 100μm in diameter. Given these printing parameters, the line resolution of these scaffolds was approximately 200-250μm. Line

spacing was defined as 185μm, layer thickness was 250μm, and the printhead velocity was 1000mm/sec. After the first layer was printed, the piston then lowered the powder bed to a fixed distance and the cycle of powder-spreading and printing was repeated. The process was repeated until a complex 3D scaffold was complete and the scaffold could then be lifted from the powder bed [25]. Scaffolds were printed 9mm in diameter and 3mm thick. The lower 2mm region was solid PCL, and the top 1mm region was 80% porous PCL. After the printing process was complete, scaffolds were placed in water on an orbital shaker to leach out the NaCl particles. The scaffolds were then frozen at -80°Celsius and lyophilized overnight to remove any residual water. The scaffolds were then autoclaved for 14 hours in ethylene oxide and ready for use (Andersen Products Autoclave, Model Number: AN74, Haw River, NC).

3.2.2.3 Casting

In study 2, agarose molds of 3% concentration were created as described in Section 3.2.1.2 with an ID of 9mm and an OD of 20mm. Synthesis of the peptide casting solution followed the standard protocol presented in Section 3.2.1.2 however an acellular peptide solution was injected directly into the porous PCL scaffold inside of the agarose mold. In order to allow for peptide infiltration and attachment to the PCL scaffold, a period of time was required to allow the molten peptide to soak the PCL scaffold. The submersion into a 1.5X PBS bath was not performed immediately in order to observe the rate and kinetics of the gelation process.

In study 3, 3% agarose molds of 9mm ID, 16mm OD, and 6mm thick were created. Standard casting protocol was followed with a cell seeding density of 20million/mL. The casting solution was injected directly into the porous PCL. The composite of the porous PCL scaffold and the molten chondrocyte-encapsulated peptide solution in the agarose mold was allowed to sit for 10 minutes before the addition of 1.5X PBS. The samples were then submerged in PBS for 45 minutes. At this point, PBS was aspirated and culture medium was added.

36

Figure 3.1 Osteochondral composites consisting of the peptide hydrogel integrated with a porous PCL scaffold. The casting of the peptide hydrogel is controlled via the 3% agarose mold. Peptide hydrogel, stained blue by Coomassie blue, is 1-2mm thick.

3.2.2.4 Cell Viability

For study 3, the standard ethidium bromide/FDA viability assay protocol described in Section 3.2.1.3 was followed. Stained cross-sections, consisting of the chondrocyte-seeded peptide hydrogel integrated into the porous PCL scaffold, were observed to study the depth of infiltration of the peptide-cell solution into the PCL scaffold.

3.2.3 Study 4: Effect of Cell Seeding Density on Chondrocyte Viability

3.2.3.1 Cell Isolation

The standard protocol, as described in Section 3.2.1.1 was used to isolate primary bovine chondrocytes.

3.2.3.2 PCL Fabrication

The standard protocol as described in Section 3.2.2.2 was used to fabricate interconnected 80% porous PCL scaffolds (9mm diameter x 3mm thick) with pore size of 50-75μm via 3DP™ technology.

3.2.3.3 Casting

In study 4, agarose molds of 3% concentration were created as described in Section 3.2.1.2 with an ID of 9mm, OD of 20mm, and thickness of 5mm. Standard casting protocol was followed with a cell seeding density of 20million/mL and 30million/mL. Casting solution was injected directly into the porous PCL scaffold placed inside of the agarose mold. The composite of the porous PCL scaffold and the molten chondrocyte-encapsulated peptide solution was

allowed to sit in the agarose mold for 15 minutes before the addition of 1.5X PBS. The samples were then submerged in PBS for 30 minutes. At this point, PBS was aspirated and 5mL of culture medium was added.
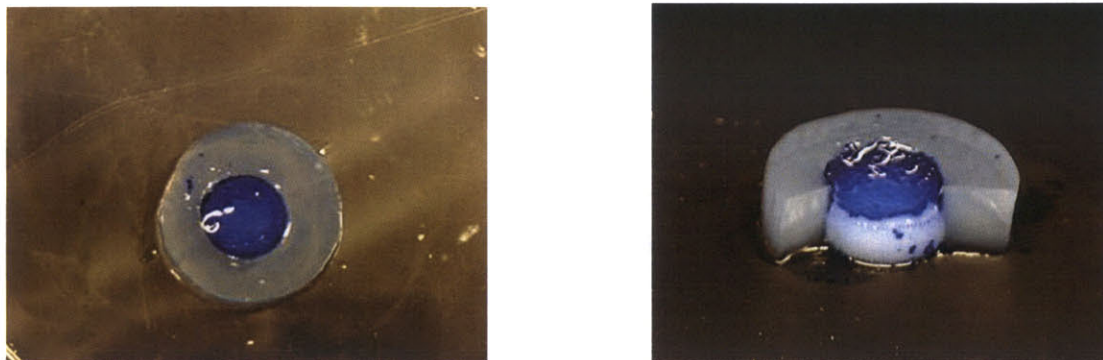
3.2.3.4 Cell Viability

The standard ethidium bromide/FDA viability assay protocol as described in Section 3.2.1.3 was followed to investigate the effects of cell seeding density on chondrocyte viability.

3.2.4 Study 5: Effect of PCL on Chondrocyte Behavior

3.2.4.1 Cell Isolation

The standard protocol as described in Section 3.2.1.1 was used to isolate primary bovine chondrocytes.

3.2.4.2 PCL Fabrication

The standard protocol as described in Section 3.2.2.2 was used to fabricate interconnected 80% porous PCL scaffolds (9mm diameter x 3mm thick) with pore size of 50-75μm via 3DP™ technology.

3.2.4.3 Casting

In study 5, agarose molds of 3% concentration were created as described in Section 3.2.1.2 with an ID of 9mm and an OD of 20mm and a thickness of 5mm. Standard casting protocol was followed with a cell seeding density of 20million/mL and 30million/mL. Casting solution was injected directly into the porous PCL scaffold placed inside of the agarose mold. The composite of the porous PCL scaffold and the molten chondrocyte-encapsulated peptide solution was allowed to sit in the agarose mold for 10 minutes before the addition of 1.5X PBS. The samples were then submerged in PBS for 30 minutes. At this point, PBS was aspirated and 5mL of culture medium was added.
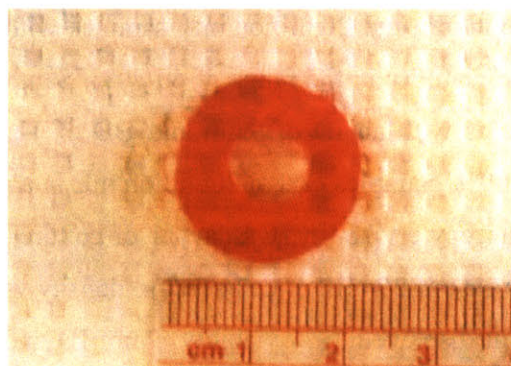
Figure 3.2 3% agarose mold, 9mm inner diameter and 20mm outer diameter, into which the porous PCL scaffold is placed. The agarose mold allows for the direct deposition of the molten chondrocyte-encapsulated peptide solution into the porous PCL scaffold in a controlled, defined, and repeatable manner without impeding on the peptide hydrogel self-assembling process. The thickness of the peptide hydrogel layer adhered to the surface of the PCL polymer is determined by the thickness of the agarose mold.

3.2.4.4 Biochemical Analysis

On days 13 and 20 of culture, the hydrogel and PCL layers of the composites were separated and 3mm plugs were taken from the peptide hydrogel portion using a disposable punch. Each plug was transferred to a 48-well tissue culture dish containing 1mL of feed medium plus $5\mu Ci/mL$ ^{35}S-sulfate and $10\mu Ci/mL$ ^{3}H-proline. Chondrocyte biosynthesis rates are described by the incorporation rates of ^{35}S-sulfate and ^{3}H-proline, which are indicative of the synthesis rates of sulfated proteoglycan and total protein, respectively. After 20 hours of incubation, the plugs were removed from the radiolabeled medium and washed 4 times over 80 minutes in PBS plus 1mM unlabeled proline and sodium sulfate (Sigma Chemical Co., St. Louis, MO and Mallinckrodt, Paris, Kentucky). Each plug was then digested in 1mL of proteinase K-TRIS HCL solution at 60°C overnight. Radiolabel incorporation rates and accumulated sulfated glycosaminoglycan (GAG) content, determined by means of DMMB dye binding, were measured as described previously [34].

3.3 Results

3.3.1 Study 1: Agarose Mold

0.75% agarose molds proved to be too difficult to work with as a potential mold material. The low concentration of the agarose was problematic in terms of creating a cylindrical core in the mold and experimental handling. The molds were repeatedly destroyed because of their fragility. All samples cast in 3% agarose molds, regardless of the variations in ID and OD of the mold, displayed a cell viability of approximately 60-80% on day 4 of culture. At both cell

seeding densities of 10million/mL and 20million/mL, samples with an ID of 5mm and OD of 9mm displayed chondrocyte viability in the range of 60-70%. Samples cast at both cell seeding densities in the agarose molds with an ID of 9mm and OD of 12mm displayed viability in a slightly higher range of 65-80%. Samples cast at 20million/mL in a mold of 9mm ID and 16mm OD displayed 75-80% chondrocyte viability. On day 11 of culture, 60-70% cell viability in all three sample configurations cast at 20mil/mL cell seeding density was observed. A sample with ID of 5mm and OD of 9mm displayed 70% viability, 9mm ID and 12mm OD displayed 70% viability, and 9mm ID and 16mm OD displayed 60% viability.

3.3.2 Study 2 and Study 3: Gelation Time and Depth of Infiltration

Because of the porous nature of the PCL scaffold, the peptide is capable of being injected directly into and on top of the PCL. Study 2 indicated that the acellular peptide was able to self-assemble and form a hydrogel when cast directly on top of the PCL scaffold. The gelation process was initiated when the peptide solution began to slowly increase in viscosity about 10-12 minutes after the peptide solution was injected into the PCL scaffold placed in the agarose mold before the sample was immersed into 1.5X PBS.

Study 3 gave a visual representation of the chondrocyte distribution in the peptide hydrogel and the PCL scaffold. On day 4 of culture, samples were cut in half and the ethidium bromide/FDA assay was able to illustrate the presence and distribution of both live and dead cells throughout the cross-section of the composite. Three distinct regions were visible with a high concentration of live cells in the peptide hydrogel layer, a lower concentration of live cells and some dead cells in the porous PCL region, and a very minimal number of cells in the solid PCL region. The solid PCL layer in the scaffold provided a clear boundary as to how far the chondrocytes had penetrated into the scaffold.

3.3.3 Study 4: Effect of Cell Seeding Density on Chondrocyte Viability

The ethidium bromide/FDA viability assay was performed on day 18 of culture on composites involving both cell seeding densities of 20million/mL and 30million/mL. Regardless of cell seeding density, the composites displayed 80-85% cell viability. However, there was a noticeable difference in the overall stiffness of the peptide hydrogel at this timepoint. Upon physical examination, it was evident that the samples with a higher cell seeding density appeared to have a higher stiffness than those with the lower cell seeding density.

40

3.3.4 Study 5: Effect of PCL on Chondrocyte Behavior

The viability of these samples on day 1 of culture was in the range of 90-95%. The GAG content of composites involving both cell seeding densities, 20million/mL and 30million/mL, increased with time. However, the amount of accumulated GAG content on both day 14 and day 21 of culture, when normalized to wet weight of the 3mm plug, was higher in the 30million/mL cell seeding density constructs than in the 20million/mL.
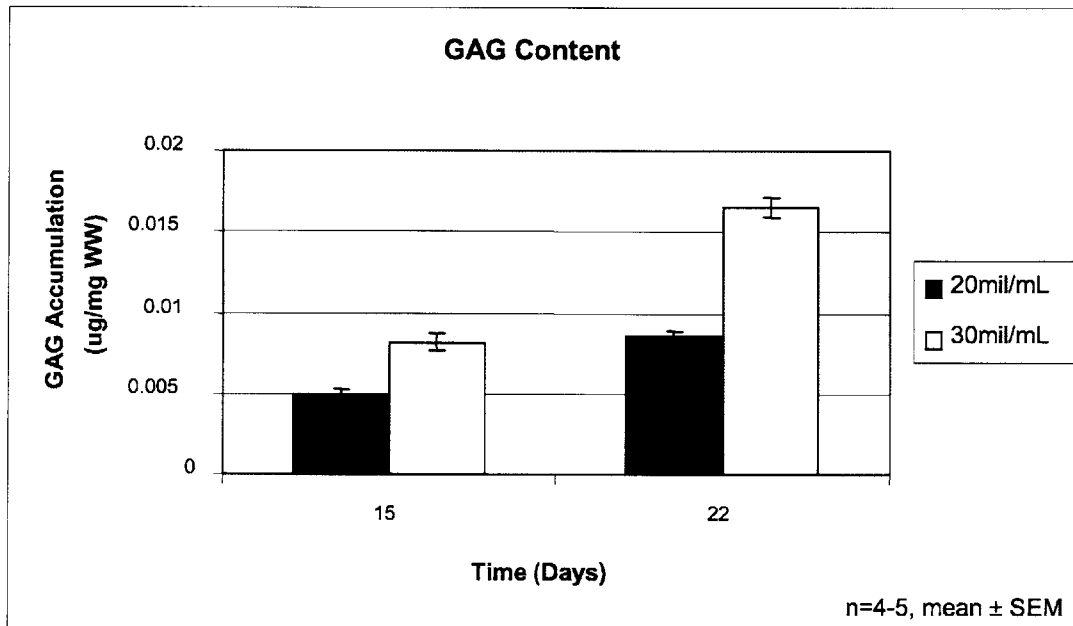
Figure 3.3 GAG accumulation measured in the peptide hydrogel region of composites. At each time point, the peptide hydrogel layer was removed from the porous PCL scaffold, and 3mm plugs were punched from this region of the composite for biochemical analysis. An increase in GAG content with respect to time and initial cell seeding density was apparent.

Although the radiolabel incorporation rates of these samples, as seen in both proline incorporation and sulfate incorporation, were similar on day 14, an increase was seen in the 30million/mL constructs and a decrease was seen in the 20million/mL constructs. These rates are indicative of protein and sulfated proteoglycan synthesis, respectively, over a 20 hour time period.
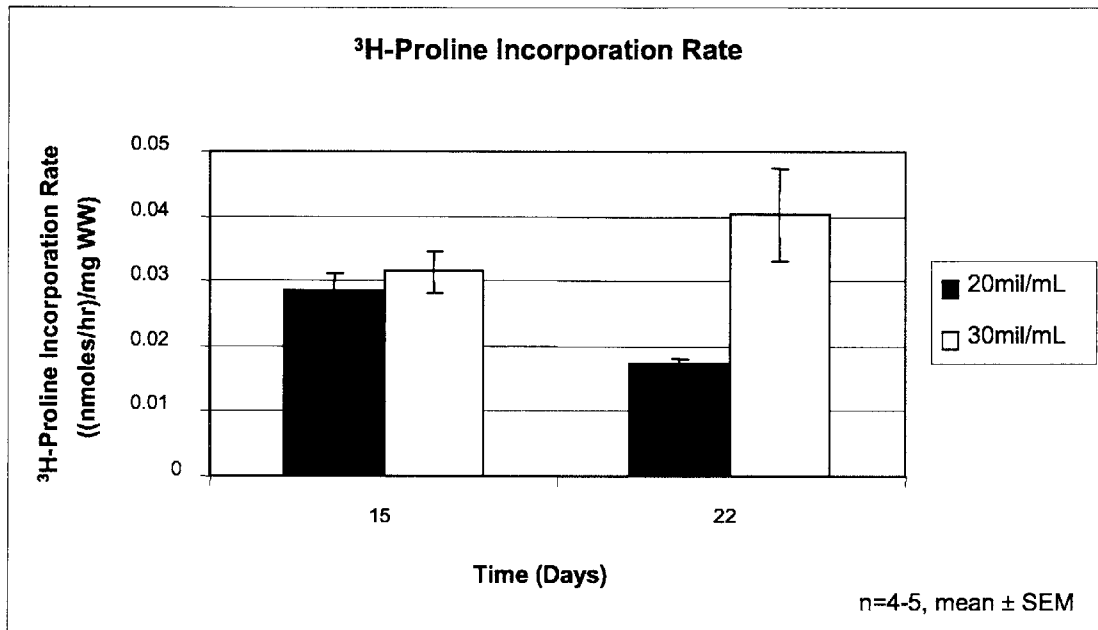
Figure 3.4 Chondrocyte biosynthesis in peptide hydrogel region of composites. ^{3}H-proline incorporation rates are indicative of protein synthesis by chondrocytes.

Figure 3.5 Chondrocyte biosynthesis in peptide hydrogel region of the composite. ^{35}S-sulfate incorporation rate is indicative of sulfated proteoglycan synthesis by chondrocytes.

3.4 Discussion

3.4.1 Study 1: Agarose Mold

This study allowed for the selection of the appropriate concentration of agarose to be used for the composite molds. 3% agarose molds proved to be consistent in maintaining acceptable levels of chondrocyte viability and were capable of providing ease of experi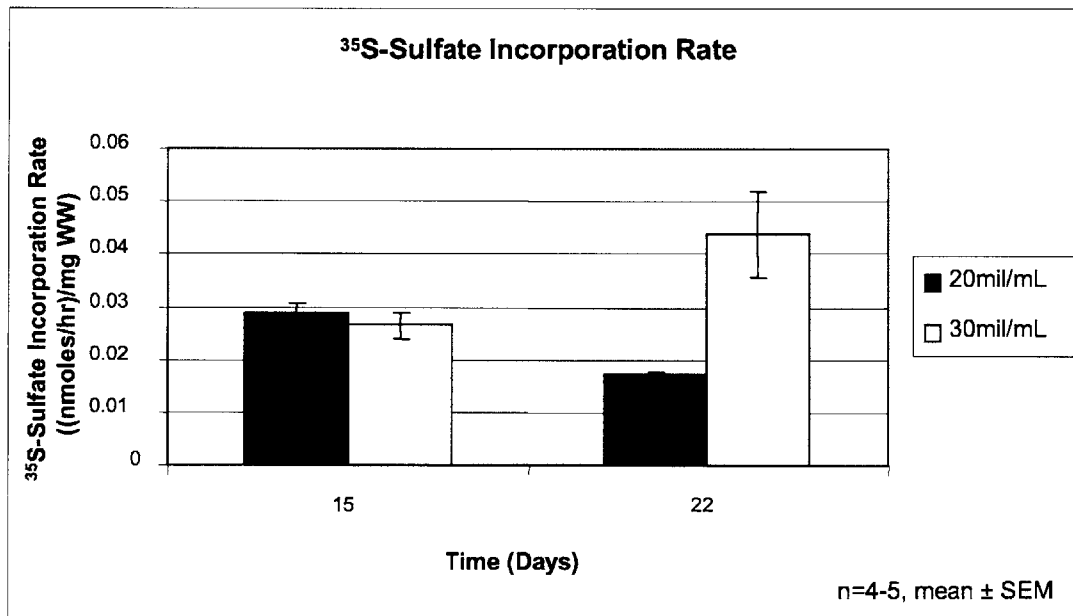mental handling and repeatability in their construction. 0.75% agarose proved to be too low of a concentration to be used in the construction of molds. The results were inconsistent and experimental handling was problematic. Cell seeding density did not appear to have a significant effect on the viability of the chondrocytes. Therefore, this experimental condition can be tailored and optimized to the confines of the composite set-up. Furthermore, chondrocyte viability remained in a relatively consistent range, regardless of variations in the geometrical constraints of the agarose mold. These results may be a consequence of the kinetics of transport and diffusion of nutrients through the agarose mold to the central chondrocyte-encapsulated peptide core.

3.4.2 Study 2 and Study 3: Gelation Time and Depth of Infiltration

Study 2 indicated that the presence of the PCL scaffold does not preclude the self-assembly process of the peptide hydrogel. The validation of this concept was crucial to confirm in order to pursue studies involving the integration of these two materials. The waiting period of approximately 10-12 minutes before submersion into PBS was conceived to allow for the infiltration of the peptide hydrogel into the porous PCL scaffold before becoming too viscous. This waiting period appeared to be an effective means of enhancing integration of the two materials.

Study 3 provided a visual means of confirming the integration of the chondrocyte-seeded peptide hydrogel into the porous PCL scaffold. This study delineated how the microarchitecture of the PCL can be utilized as a means of controlling the peptide infiltration depth into the scaffold. The integration of the two materials can be confined to a specific thickness by creating a gradient in pore size or by introducing a solid region of PCL. With this concept confirmed, future studies will focus on creating a composite involving the peptide hydrogel and only the porous region of the PCL scaffold to more closely assess chondrocyte viability, behavior, biosynthesis rates, matrix accumulation, and mechanical properties in both the peptide hydrogel and the porous PCL.

3.4.3 Study 4: Effect of Cell Seeding Density on Chondrocyte Viability

Cell seeding density is an important experimental condition to consider because of its potential effect on chondrocyte viability, and overall GAG and matrix accumulation. Study 4 revealed that the variation between 20million/mL and 30million/mL did not result in significant differences in cell viability. However, this experimental condition can be optimized in order to enhance protein and matrix accumulation and to achieve material properties of the hydrogel material that mimic that of native cartilage.

3.4.4 Study 5: Effect of PCL on Chondrocyte Behavior

Study 5 was a preliminary experiment to investigate the effects of the presence and integration with PCL on chondrocyte behavior in the hydrogel in terms of GAG accumulation and biosynthesis rates. With respect to GAG content, PCL did not appear to have any adverse effects on chondrocyte behavior. The magnitude and trends of the accumulation of GAG in the peptide hydrogel were consistent with those seen in the peptide-only systems studied by Kisiday et al [23]. Radiolabeled proline and sulfate incorporation rates in these studies were also consistent in magnitude and trend with those performed by Kisiday et al. with the chondrocyte-seeded peptide hydrogel only system [23]. Although there is a discrepancy in the overall trend in both proline and sulfate incorporation rates between the two cell seeding densities, the variations are slight enough that if additional timepoints were taken, a general trend of leveling off of the corresponding incorporation rate would most likely be observed.

Chapter 4: Characterization of Osteochondral Composite

4.1 Introduction

Although our ultimate design for the osteochondral composite involves a multi-layered PCL scaffold with distinct regions tailored towards cartilage replacement and bone ingrowth, our immediate objective is to optimize and understand the interactions between the integrated chondrocyte-seeded peptide hydrogel and the porous PCL scaffold. Studies described in Chapter 3 indicated that the thickness of this integrated region can be controlled via the PCL scaffold design. Therefore, the additional regions, the solid boundary layer and the lower porosity bone region, will be added to the fabrication process at a later date. Previous studies involving osteochondral composites have created scaffolds with a range of porosities in the cartilage replacement region. This range varies from 60% to 90% porous [17, 26, 39]. Therefore, this chapter describes an investigation into the effect of the PCL microarchitecture on chondrocyte behavior in both the peptide hydrogel and the porous PCL. In order to determine the optimal porosity level, 70% and 90% porous PCL constructs were fabricated using 3DP™ technology. A variety of pore sizes have also been incorporated into the cartilaginous region of an osteochondral composite, ranging from 106-150μm to 300-580μm [17, 39]. PCL scaffolds with pore size in the range of 106-180μm were fabricated to ensure integration of the composite materials. Characterization of the osteochondral composite was then performed through an analysis of GAG accumulation, matrix biosynthesis rates, mechanical properties, hydroxyproline content, and histology. These assays were performed on both the peptide hydrogel and porous PCL regions of the two types of composites, 70% and 90% porous PCL, in order to obtain a relative understanding of chondrocyte behavior in two distinct environments.

4.2 Methods and Materials

4.2.1 Cell Isolation

Bovine chondrocytes were harvested from the femoral condyles and femoropatellar grooves of 1-2 week old calves within a few hours of slaughter, as previously described [40]. Cartilage slices were taken from the femoral condyles and femoropatellar grooves and manually chopped into fine pieces. The tissue was then transferred to a pronase solution at a concentration of 20U/mL for 2 hours of incubation (Sigma-Aldrich, St. Louis, MO). The pronase-tissue

solution was mixed via pipetting every twenty minutes. At the end of this incubation period, the tissue was rinsed twice with 1X PBS and placed into a collagenase solution at a concentration of 200U/mL overnight (Worthington, Lakewood, NJ). The next morning, the collagenase-tissue solution was mixed via pipetting every 30 minutes until the solution appeared relatively clear, indicating the completion of the digestion process. At this point, the solution was allowed to incubate for 1.5 hours to complete digestion. The chondrocyte suspension was then filtered through a 40μm cell strainer and centrifuged at 1900rpm for 8minutes. After aspirating the supernatant, cell pellets were resuspended and centrifuged in 1X PBS. This process of centrifugation and PBS rinsing was repeated two more times. After the third round of centrifugation, the cells were resuspended in high glucose DMEM (Gibco, Auckland, New Zealand). A sample of cell suspension was microscopically analyzed for cell viability using ethidium bromide/FDA and concentration using Trypan Blue Staining (Sigma Chemical Co., St. Louis, MO). The cell suspension was then stored at 4° C until use.

4.2.2 PCL Fabrication

PCL scaffolds were fabricated using a Theriform™ 3DP™ machine (Therics, Inc. Princeton, NJ). An emulsion-precipitation method was used to create PCL powder (PCL MW= 65kDa, Aldrich, Milwaukee, WI) [41, 42]. PCL was dissolved in dichloromethane (CH_2Cl_2) and then injected into a continuously stirred water bath consisting of 95% H_2O and 5% polyvinyl alcohol (PVA). After the precipitation of PCL in this water bath, the spherical particles were rinsed, dried, and sieved a particle diameter of less than 75μm. The pore size of the PCL scaffold is dictated by the diameter size of the NaCl particles (Mallinkrodt, Paris KY). NaCl particles were milled and sieved to a range of 106-180μm diameter (Bel-Art Products Mill, Model Number: 37252-0000, Pequannock, NJ; VWR Scientific Sieve, West Chester, PA). Particles of NaCl and PCL were mixed together in relative proportions to create the desired porosity of the scaffold. For these studies, mixture compositions included 70% NaCl with 30% PCL powder, and 90% NaCl with 10% PCL powder. A thin layer of powder was spread by the powder spreader across the surface of the powder bed on top of a piston. An ink-jet printhead then printed the liquid binder, chloroform, thereby bonding the particles of the polymer together to form a solid (Mallinckrodt, Paris, KY). The 50μm diameter printhead nozzle created droplets of chloroform approximately 100μm in diameter. Given these printing parameters, the line resolution of these scaffolds was approximately 200-250μm. Line spacing was defined as

46

185μm, layer thickness was 250μm, and the printhead velocity was 1000mm/sec. After the first layer was printed, the piston then lowered the powder bed to a fixed distance and the cycle of powder-spreading and printing was repeated. The process is repeated until a complex 3D scaffold is complete and the scaffold could then be lifted from the powder bed [25]. Porous PCL cylindrical cores, 9mm in diameter and 3mm thick, were printed with a fully interconnected porous microarchitecture consisting of 70% or 90% void space. After the printing process was complete, scaffolds were placed in water on an orbital shaker to leach out the NaCl particles. The scaffolds were then frozen at -80°Celsius and lyophilized overnight to remove any residual water. The scaffolds were then autoclaved for 14 hours in ethylene oxide and ready for use (Andersen Products Autoclave, Model Number: AN74, Haw River, NC).

4.2.3 Casting

Agarose molds of 2.5% concentration were created, as described in Chapter 3, with an ID of 9mm, OD of 20mm, and thickness of 4mm. The peptide KLD-12 was custom synthesized (SynPep Corp., Dublin, CA) and lyophilized to a powder. KLD-12 powder was dissolved in a 10% sucrose solution at a concentration of 3.6mg/mL. The peptide solution was then sonicated until further use to prevent aggregation. The volume of cell suspension targeted for a cell seeding density of 30million/mL was centrifuged at 1900 rpm for 8 minutes. Isolated chondrocytes were then resuspended in a 10% sucrose plus 5mM HEPES buffer equal in volume to 10% of the final hydrogel casting volume. The peptide solution was then added to the cell suspension in volume equal to 90% of the final hydrogel casting volume. The casting solution was then lightly vortexed and injected directly into and on top of the porous PCL scaffold inside the cylindrical core of the agarose mold. After a waiting period of 10 minutes, the composite samples were then submerged in 1.5X PBS without agitation for 40 minutes to initiate self-assembly of the peptide hydrogel. At this point, PBS was aspirated and culture medium, high-glucose DMEM with 0.2% FBS and 1% ITS, was added. Each sample received 5mL of culture medium that was changed every other day.
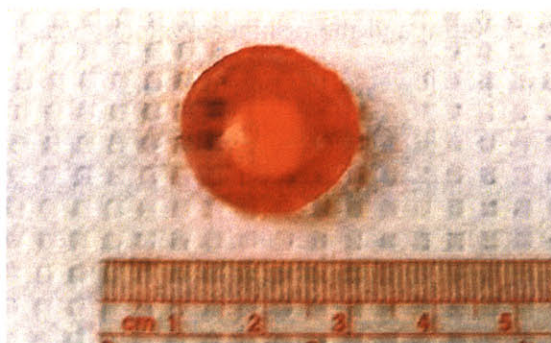
Figure 4.1 Osteochondral construct consisting of peptide hydrogel, with initial cell seeding density of 30million cells/mL, integrated into a porous PCL scaffold. The composite, 9mm diameter x 4-5mm thick, was created in a 2.5% agarose mold.

Chondrocyte-seeded peptide hydrogel slabs, without being integrated into a porous PCL scaffold, were also created to serve as a control. The casting procedure of the KLD-12 peptide into chondrocyte-seeded hydrogel slabs developed and optimized by Kisiday et al., as previously described, was employed to create these controls [22]. Briefly, isolated chondrocytes targeted for a cell seeding density of 30million/mL were resuspended in a 10% sucrose plus 5mM HEPES buffer solution equal in volume to 10% of the final hydrogel casting volume. The peptide solution was then added to the cell suspension in volume equal to 90% of the final hydrogel casting volume. The casting solution was then lightly vortexed and injected into a stainless steel frame in a molten state and subsequently placed into a 1.5X PBS bath to initiate self-assembly into a slab-like geometry. After 25-30 minutes, the casting frame was disassembled and the peptide hydrogel sheet was submerged into 15mL of culture medium in a 100mm Petri dish.

4.2.4 Biochemical Analysis

On days 5, 14, and 20 of culture, the composites were cut in half to allocate material for biochemical and mechanical analysis, as well as to histological analysis. The peptide hydrogel layer was separated from the PCL scaffold using a scalpel and 3mm plugs were taken from both regions using a disposable punch. Each plug was transferred to a 48-well tissue culture dish containing 1mL of feed medium plus 5μCi/mL ^{35}S-sulfate and 10μCi/mL ^{3}H-proline. Chondrocyte biosynthesis rates are described by the incorporation of ^{35}S-sulfate and ^{3}H-proline, which are indicative of the synthesis rates of sulfated proteoglycan and total protein, respectively. After 20 hours of incubation, the plugs were removed from the radiolabeled medium and washed 4 times over 80 minutes in PBS plus 1mM unlabeled proline and sodium

sulfate (Sigma Chemical Co., St. Louis, MO and Mallinckrodt, Paris, Kentucky). Samples designated for mechanical testing were tested at this point. Each plug was then digested in 1mL of proteinase K-TRIS HCL solution at 60°C overnight. Radiolabel incorporation rates and accumulated sulfated glycosaminoglycan (GAG) content, determined by means of DMMB dye binding, were measured as described previously [34]. The hydroxyproline assay was also performed on the digest material to measure the accumulated collagen content. 125μL aliquots of sample digest were hydrolyzed in 6N HCl at 110°C overnight. After evaporation of the acid solution was complete, the remaining solid digest was resuspended in a stock buffer consisting of citric acid monohydrate, sodium acetate trihydrate, and acetic acid to stabilize the reaction and maintain a pH of 6.1-6.2. 150μL aliquots of each sample were mixed with 75μL of 50mM Chloramine T solution. After the addition of p-dimethylaminobenzaldehyde, a spectrophotometric analysis at an absorbance of 560nm revealed the amount of collagen content in each sample [43]. The other half of each sample, designated for histological analysis, was fixed in 4% paraformaldehyde overnight at 4°C. The next morning, these intact composite samples were rinsed twice in 1X PBS and stored in 70% ethanol at 4°C until histological analysis ensued.

4.2.5 Mechanical Testing

On days 15 and 21 of culture, 3mm plugs were tested in radially confined uniaxial compression using a benchtop Incudyne to determine the equilibrium modulus and dynamic stiffness of the materials, as previously described [44] (Industrial Devices Co. LLC, Petaluma, CA, Model Number RGC-06-180-E04-X23X, Dynamic Acquisition System Software Version 9.9F). After measuring the thickness of each sample, the plug was placed into a confining cylindrical chamber clamped into the platform of the Incudyne. A porous platen was used to apply 2 sequential ramp-and-hold compressive strains of 5%, followed by 4 sequential ramp-and-hold compressive strains of 2% to the sample. Each compressive strain was applied over 30 seconds, followed by a holding period of 3 minutes to allow for stress relaxation. The ratio of the relaxed equilibrium stress to the engineering strain was used to compute the equilibrium modulus. At 18% compressive offset strain, a 1% amplitude sinusoidal dynamic strain was applied at 1, 0.5, and 0.1Hz. The dynamic compressive stiffness was calculated as the ratio of the fundamental amplitudes of stress to strain [44].

4.2.6 Histological Analysis

After being fixed in 4% paraformaldehyde overnight at 4°C, samples were rinsed in PBS, and stored in 70% ethanol at 4°C until histological assessment ensued. At the point of sample preparation for histological analysis, the intact peptide layer was removed from the porous PCL scaffold. The peptide hydrogel layer was dehydrated by means of a graded ethanol series up to 100% ethanol and cleared in xylene. These samples were then embedded in paraffin, sectioned into 5μm sections, and stained with H&E for cell content and Toluidine Blue for proteoglycan content. The porous PCL samples, however, were submerged in a gradient of sucrose solutions after being fixed as a means of cryoprotection. Embedding the samples in sucrose solutions until the sucrose solution has infiltrated the samples removes the residual water from the interior of the sample and prevents the formation of ice crystals during the freezing process of cryosectioning. The following gradient of sucrose solutions was employed: 5%, 10%, 20%, and 30% sucrose in PBS. Samples were submerged in each concentration of sucrose solution overnight at 4°C, or until the sucrose solution had completely saturated the sample; as was evident by the sinking of the sample. Samples were then embedded in 50% OCT in PBS overnight at 4°C, 100% OCT overnight at 4°C, and finally embedded into cryosectioning molds with 100% OCT and frozen at -80°C, and then sectioned into 5μm sections with a cryostat. Dry sections were mounted unstained for the visualization of the PCL architecture, while other sections were stained with H&E to visualize the presence of cells and cell morphology and with Toluidine Blue to visualize proteoglycan content.

4.2.7 Statistical Analysis

Individual 2-tail t-tests were performed at each time point to determine if the integration of the chondrocyte-seeded peptide hydrogel into the porous PCL scaffold or if the microarchitecture of the PCL scaffold produced significant effects on a given biochemical parameter.

4.3 Results

4.3.1 GAG Accumulation

At an early time point, day 6, 2-tail t-test statistical analysis indicated that there was a significant difference in GAG content in the peptide hydrogel region between composites involving the 70% and 90% porous PCL scaffolds ($p < 0.05$), as shown in Figure 4.2. While

50

GAG content in this region of the composite involving 70% porous PCL was lower on day 15, GAG accumulation in the hydrogel of the 90% porous composite increased with time, as expected. Due to experimental conditions, there were sub-optimal amounts of chondrocyte-seeded peptide hydrogel cast onto the 70% porous PCL scaffolds. Therefore, although this data was still included for each means of composite characterization, values for these specific composites and the corresponding statistical analysis may be affected by these conditions. GAG content measured in the peptide hydrogel of composites involving the 90% porous PCL samples was not significantly higher than that measured in the peptide hydrogel control sample ($p > 0.05$). GAG accumulation in 3mm plugs removed from the porous PCL region of these composites displayed similar trends as those observed in the peptide hydrogel region, as is evident in Figure 4.3. The magnitude of these values was approximately an order of magnitude less than those in the peptide hydrogel regions of the corresponding ocmposites. GAG content measured in the porous PCL scaffold ranged from approximately 8%-15% of the GAG content measured in the corresponding peptide hydrogel regions.
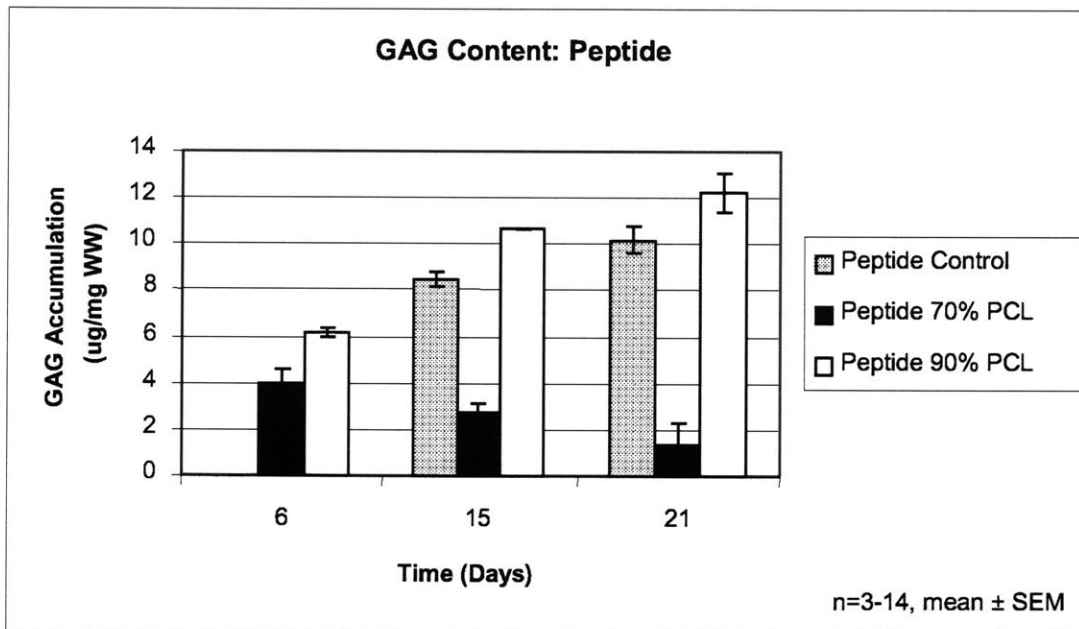

Figure 4.2 GAG accumulation measured in the peptide hydrogel region of composites at various time points throughout culture. At each time point, the peptide hydrogel layer was removed from the porous PCL scaffold, and 3mm plugs were punched from this region of the composite for biochemical and mechanical analysis. Peptide control consists of a peptide hydrogel sheet cast in slab-like geometry without a PCL scaffold.
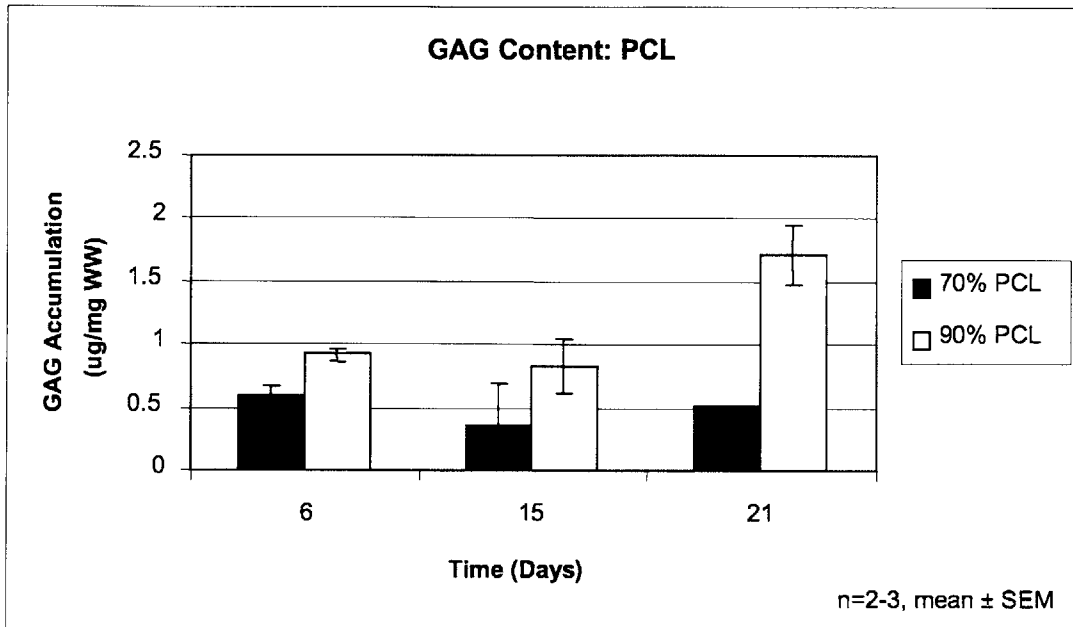
GAG Content: PCL

n=2-3, mean ± SEM

Figure 4.3 GAG content measured in 3mm plugs punched from the porous PCL scaffolds. PCL plugs were punched and digested in Proteinase K in a manner identical to the retrieval and treatment of peptide hydrogel plugs to determine the amount of matrix accumulation within the porous PCL scaffolds relative to that in the peptide hydrogel.

4.3.2 Chondrocyte Biosynthesis

Figure 4.4 indicates there was no significant difference (p > 0.05) observed in proline incorporation rates of the chondrocyte-seeded peptide hydrogel between the 70% porous PCL composite and the 90% porous PCL composite throughout the duration of culture time. The magnitudes and trends of these values remained consistent with each other throughout the time course. In the peptide hydrogel and 70% porous PCL composite, the proline incorporation rate in the peptide region decreased by 58% from day 6 to day 15 and then increased 36% from day 15 to day 21. The peptide hydrogel and 90% porous composite displayed similar trends in proline incorporation rates, decreasing by 50% from day 6 to 15 and increasing by 18% from day 15 to day 21. A peptide-only control sheet cast without a PCL scaffold served as a control for days 15 and 21. Figure 4.4 also indicates that proline incorporation rates in the peptide hydrogel region of both 70% porous and 90% porous PCL samples remained consistent with the peptide hydrogel control sheet (p > 0.05). This consistency between samples groups and the control samples implies that the presence of the PCL scaffold does not have any adverse effects on chondrocyte behavior in the peptide hydrogel. Sulfate incorporation rates within the peptide hydrogel also

52

remained consistent across composites involving the 70% and 90% porous PCL samples on day 6 ($p > 0.05$), as shown in Figure 4.5. However, the discrepancy in sulfate incorporation rates between these samples on days 15 and 21 is significant ($p < 0.05$), keeping in mind the sub-optimal experimental conditions associated with the 70% porous PCL composites. Sulfate incorporation rates displayed a slightly more pronounced decrease from its maximum value at day 6. The sulfate incorporation rate in the peptide region of the 70% porous PCL composite decreased by 69% from day 6 to day 15, and decreased an additional 30% from day 15 to day 21. Chondrocyte behavior in the peptide hydrogel region with 90% porous PCL composites displayed a similar trend with a 64% decrease in sulfate incorporation rate from day 6 to day 15, but differed after this time point with a 31% increase from day 15 to day 21. When compared to the peptide control sheet, there is a significant difference in sulfate incorporation rate in the peptide hydrogel and 70% porous PCL composite on both day 15 and 21 ($p < 0.05$), while the hydrogel integrated with the 90% porous PCL samples displayed a significant deviance from the peptide control sheet only on day 21 ($p < 0.05$). The trends in both the peptide hydrogel region and the PCL region consisted of a maximum value in incorporation rate at day 6 with a decrease and leveling off observed with time.
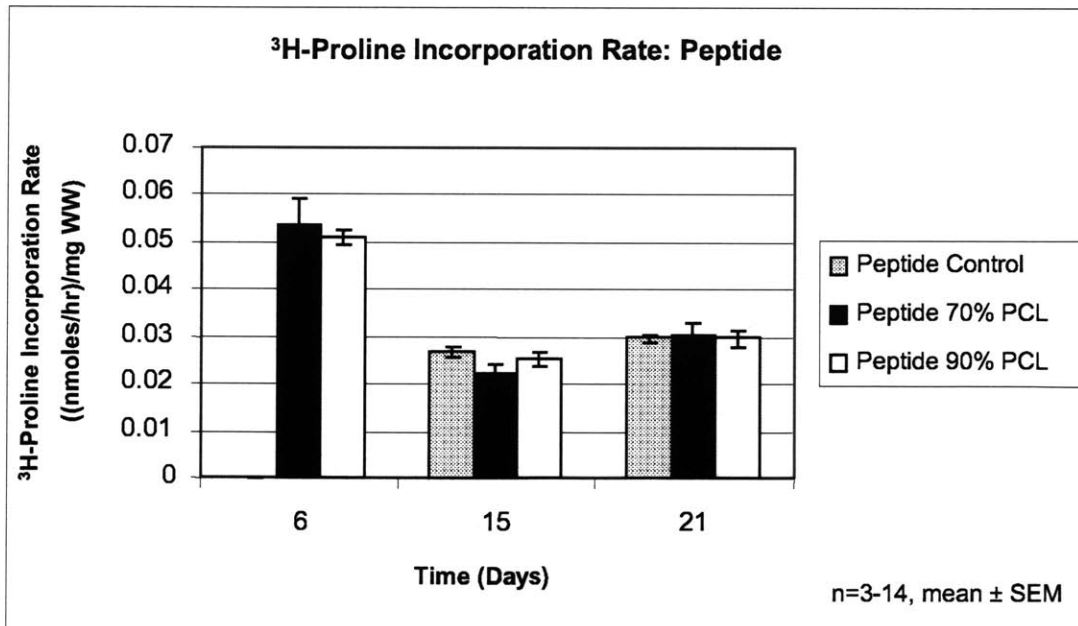

Figure 4.4 Chondrocyte biosynthesis in peptide hydrogel region of composites. [3]**H-proline incorporation rates are indicative of protein synthesis by chondrocytes. Effects of the presence of porous PCL scaffold and microarchitecture of the PCL scaffold on chondrocyte behavior in the peptide hydrogel were investigated.**
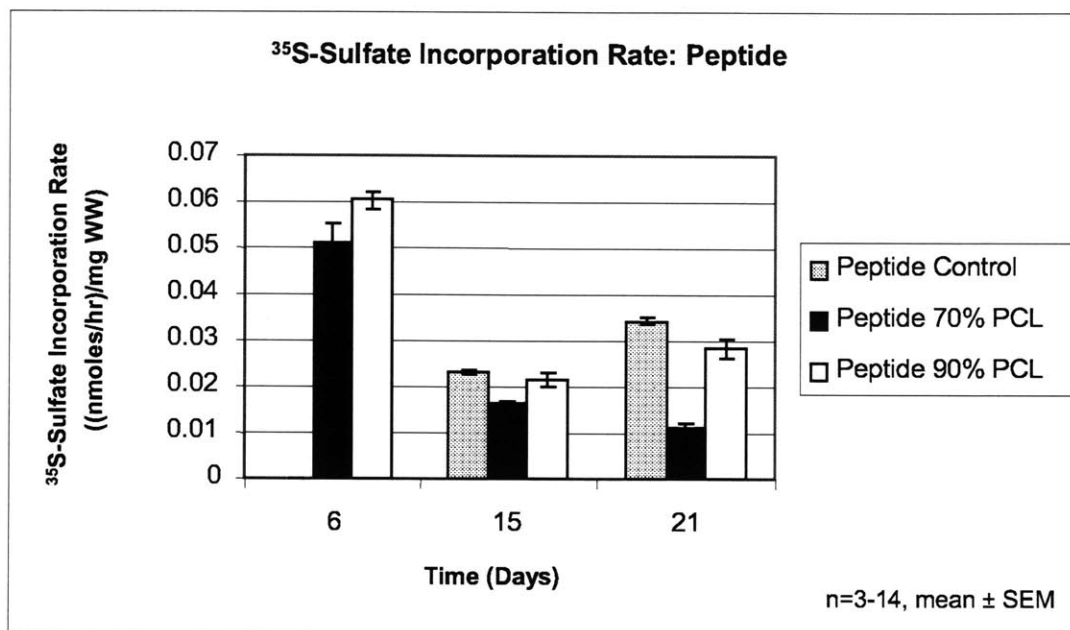
Figure 4.5 Chondrocyte biosynthesis in peptide hydrogel region of the composite. ^{35}S-sulfate incorporation rate is indicative of sulfated proteoglycan synthesis by chondrocytes. Presence of PCL does not have adverse effects on biosynthesis rates of chondrocytes in peptide hydrogel.

The radiolabel incorporation rates of the samples taken from the porous PCL regions did not display significant differences between the porosity levels at any time point ($p > 0.05$), as is evident in Figure 4.6 and Figure 4.7. The radiolabel incorporation rates displayed similar trends as those seen in the peptide hydrogel. In the 70% porous PCL region, proline incorporation rate decreased by 51% from day 6 to day 15, and decreased an additional 45% from day 15 to day 21, as shown in Figure 4.6. The 90% porous PCL region displayed a more dramatic decrease of 69% from day 6 to day 15, but appeared to stabilize after this time point with an increase of only 3% from day 15 to day 21. Figure 4.7 displays similar trends in sulfate incorporation rates as those observed in proline incorporation rates. In the 70% porous PCL region, sulfate incorporation decreased by 48% from day 6 to day 15, and decreased an additional 80% from day 15 to day 21. Similar to the proline incorporation rate, sulfate incorporation rate in the 90% porous PCL region decreased by 73% from day 6 to day 15 and decreased only an additional 2% from day 15 to day 21. The magnitudes of both proline and sulfate incorporation rates in the porous PCL region ranged from 7-23% of those seen in the peptide hydrogel region.
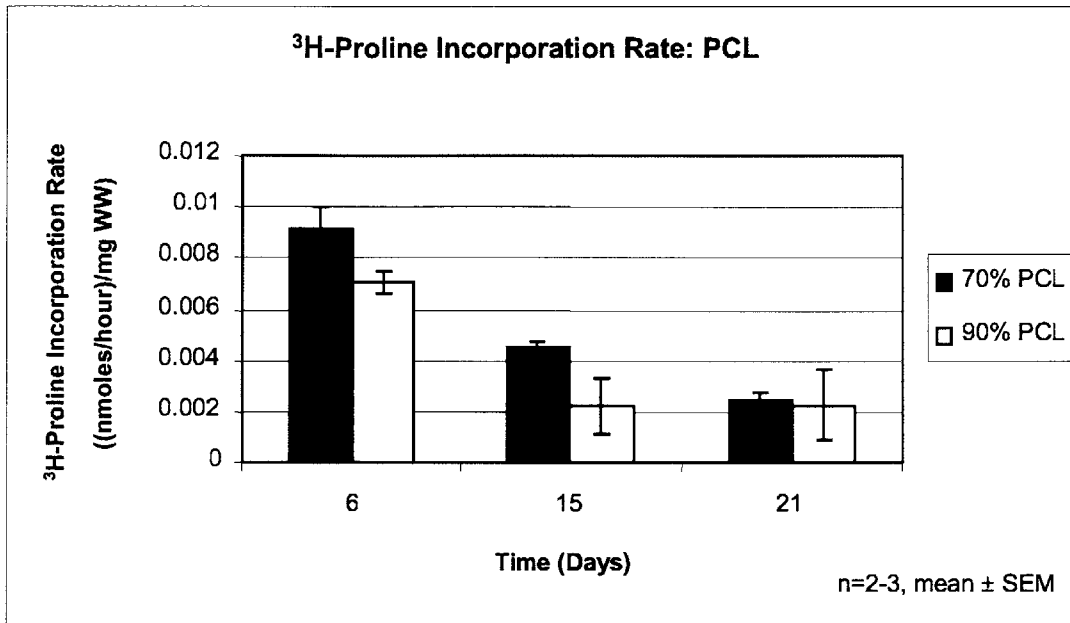
³H-Proline Incorporation Rate: PCL

Figure 4.6 Chondrocyte biosynthesis in porous PCL scaffold region of the composite. ³H-proline incorporation rate in PCL scaffolds was approximately an order of magnitude less than that measured in the peptide hydrogel, however similar trends were observed throughout the course of culture.
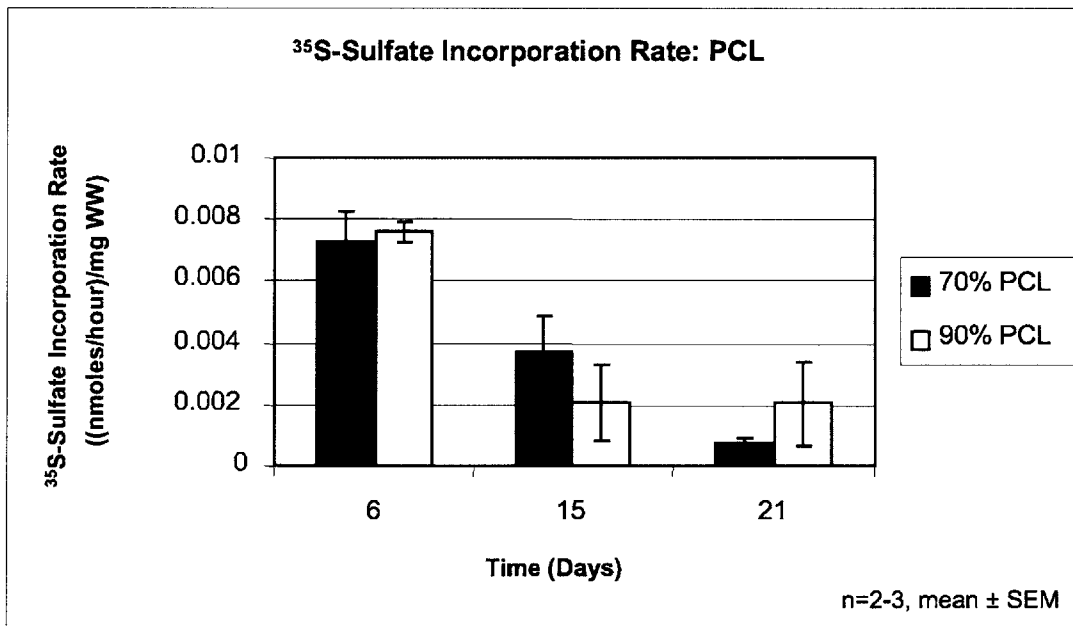

³⁵S-Sulfate Incorporation Rate: PCL

Figure 4.7 Chondrocyte biosynthesis in porous PCL scaffold region of composite. Trends in ³⁵S-sulfate incorporation rates in the porous PCL scaffold were similar to those observed in the peptide hydrogel. Distinction in porosity level of PCL scaffold did not present significant differences in ³⁵S-sulfate incorporation rate.

4.3.3 Hydroxyproline Accumulation

Hydroxyproline content in the peptide hydrogel region of the composite, which is indicative of the accumulated collagen content in the scaffolds, increased with respect to time in both types of composites. There was no significant difference in the peptide hydroxyproline content between the composites involving 70% or 90% porous PCL scaffolds at any time point ($p > 0.05$). A day 15 peptide-only control sheet was observed to be consistent with both types of composites ($p > 0.05$), as shown in Figure 4.8. A significant discrepancy from the control sheet was observed in the peptide hydrogel region of the composite involving 90% porous PCL on day 21 ($p < 0.05$), however the composite involving 70% porous PCL remained consistent with the control sheet ($p > 0.05$). Hydroxyproline content in the PCL region of the composites was negligible with no significant difference observed based on porosity level of the PCL scaffolds ($p > 0.05$).
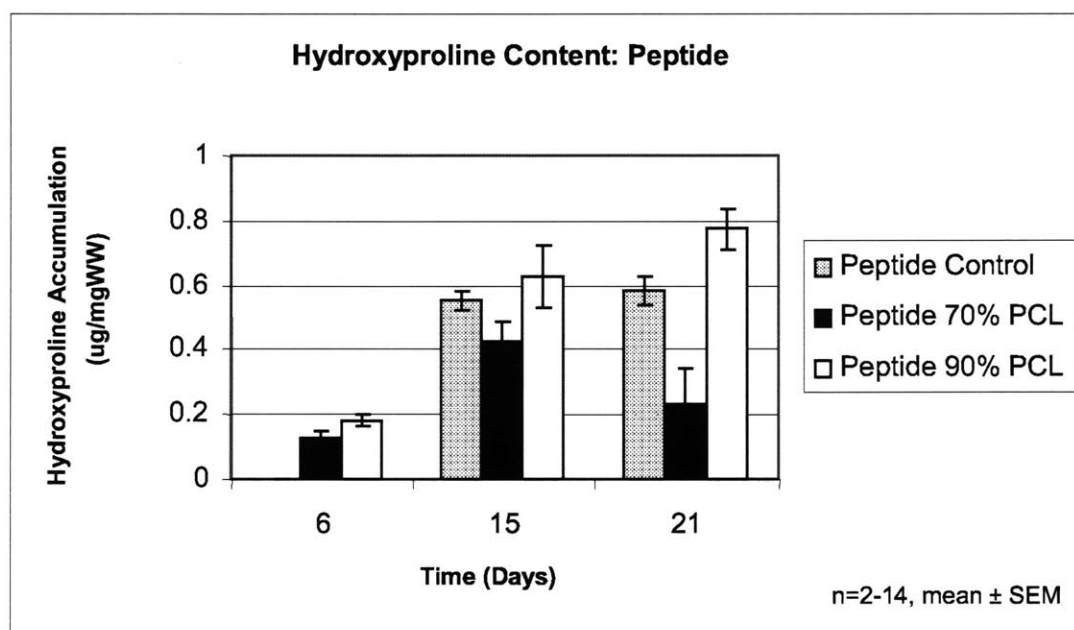

Figure 4.8 Hydroxyproline accumulation in chondrocyte-seeded peptide hydrogel region of the composite. Hydroxyproline, a hydroxylated proline residue, is a measurement of total collagen content. Presence of PCL, along with the porosity level of the PCL, did not thwart collagen synthesis.

4.3.4 Mechanical Properties

Because of the lack of sufficient sample material, mechanical properties of the peptide hydrogel and 70% porous PCL composite could only be evaluated on day 15. As Figure 4.9 shows, the average equilibrium modulus of the peptide hydrogel cultured in this composite was

25kPa on day 15. The confined compression equilibrium modulus of the peptide hydrogel samples cultured on the 90% porous PCL scaffolds increased from 41kPa to 68kPa from day 15 to day 21 of culture. These values were similar to those of the peptide control sheet for this time point ($p > 0.05$). Dynamic stiffness values for the peptide hydrogel samples were strain rate dependent as seen in Figure 4.11 and Figure 4.12. As frequency decreased from 1Hz to 0.5Hz to 0.1Hz, the dynamic stiffness values also decreased, which is characteristic of poroelastic tissues. The magnitude of the dynamic stiffness values increased from day 15 to day 21 across all frequencies [44]. As seen in Figure 4.10, mechanical testing of the PCL regions of the composite was also performed to characterize the material properties of the porous PCL scaffold. The equilibrium modulus of the 70% porous PCL samples increased from 296kPa to 403kPa from day 15 to day 21, while that of the 90% porous PCL samples increased from 253kPa to 403kPa. The dynamic stiffness values of the PCL samples also increased from day 15 to day 21 for all frequencies, as is evident in Figure 4.13 and Figure 4.14.
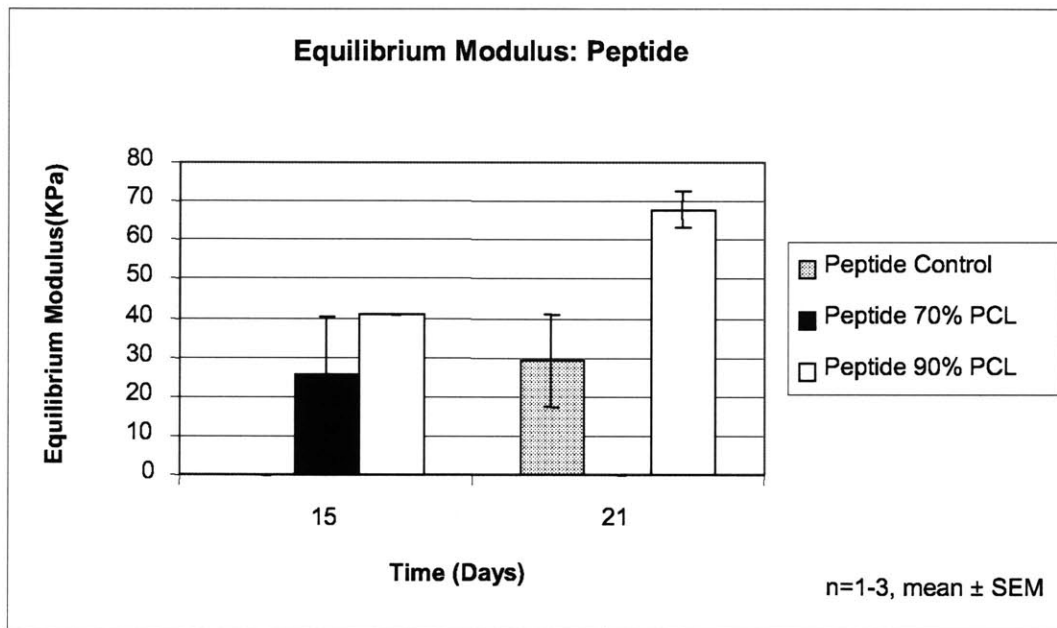

Figure 4.9 Mechanical properties of chondrocyte-seeded peptide hydrogel region of composite. Uniaxial confined compressive mechanical testing of 3mm peptide hydrogel plugs from 5% compressive strain to 18% compressive strain was performed to determine the equilibrium modulus.
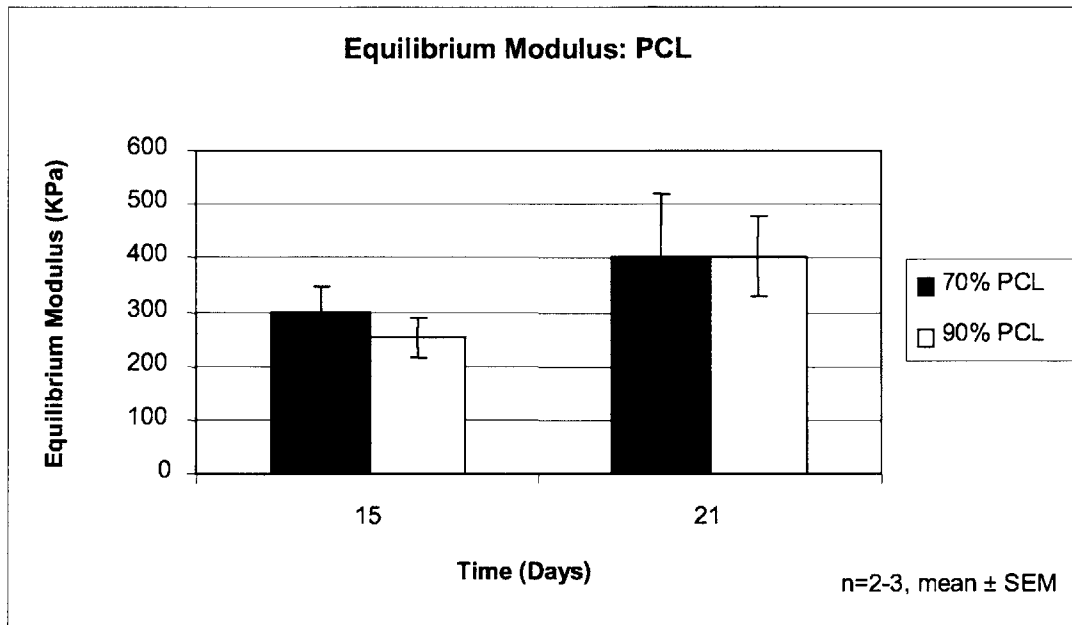
Figure 4.10 Mechanical properties of porous PCL region of composite. 3mm plugs of porous PCL scaffolds were retrieved from osteochondral composites. Uniaxial confined compressive mechanical testing performed to determine effect of scaffold porosity on mechanical properties.

Figure 4.11 Mechanical properties of dynamically compressed chondrocyte-seeded peptide hydrogel on day 15 of culture. Poroelastic material properties of peptide hydrogel are displayed as dynamic stiffness decreases with decreasing frequency.

58

Figure 4.12 Mechanical properties of dynamically compressed chondrocyte-seeded peptide hydrogel on day 21 of culture. In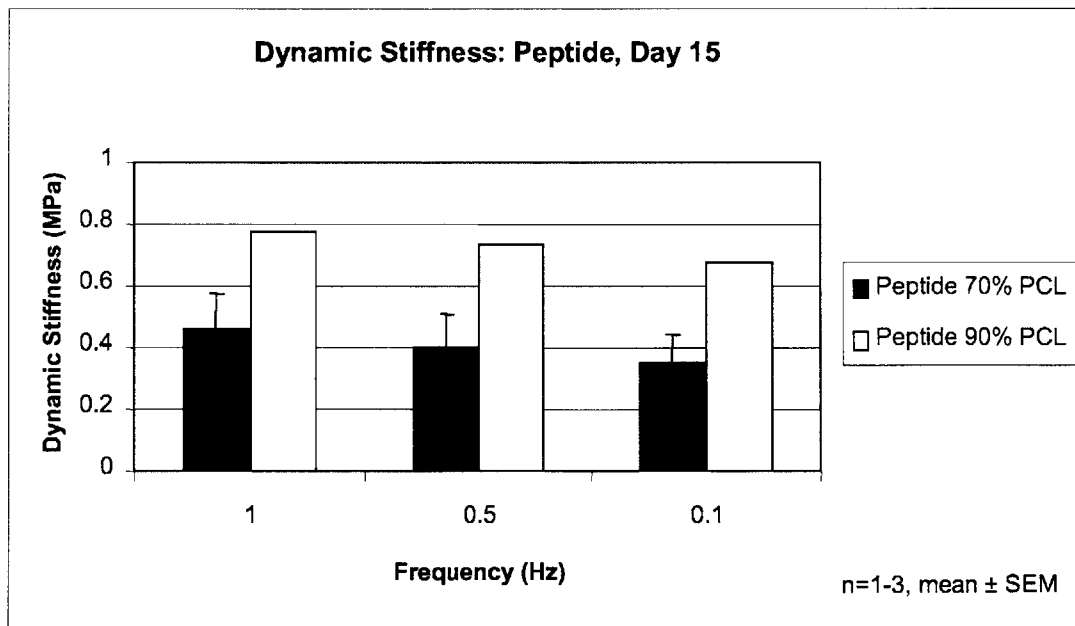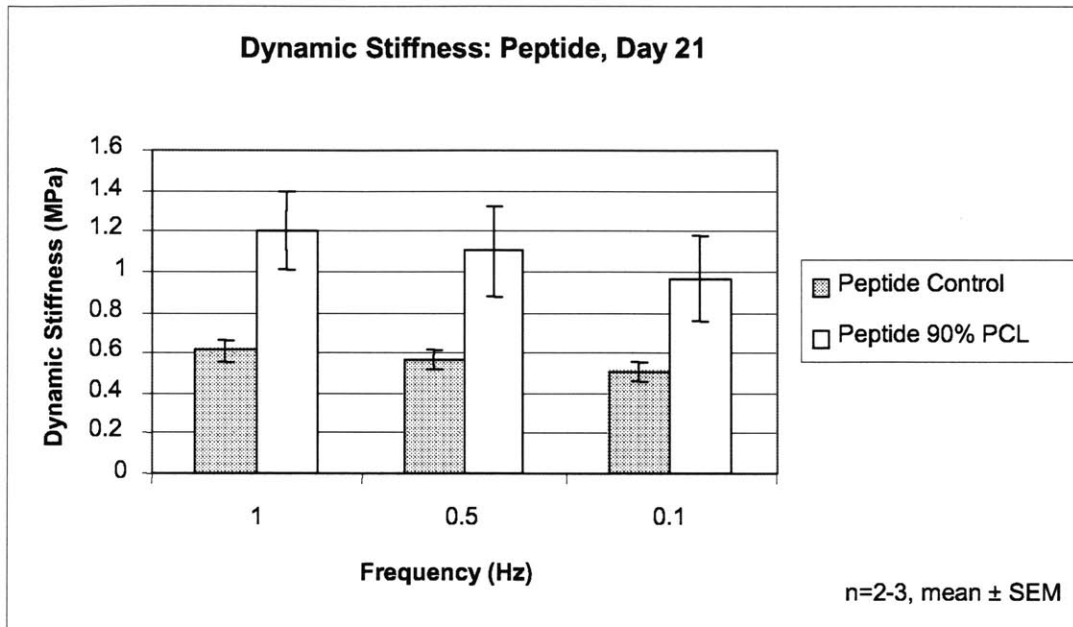crease in dynamic stiffness of chondrocyte-seeded peptide hydrogel is apparent relative to day 15 measurements of material properties.
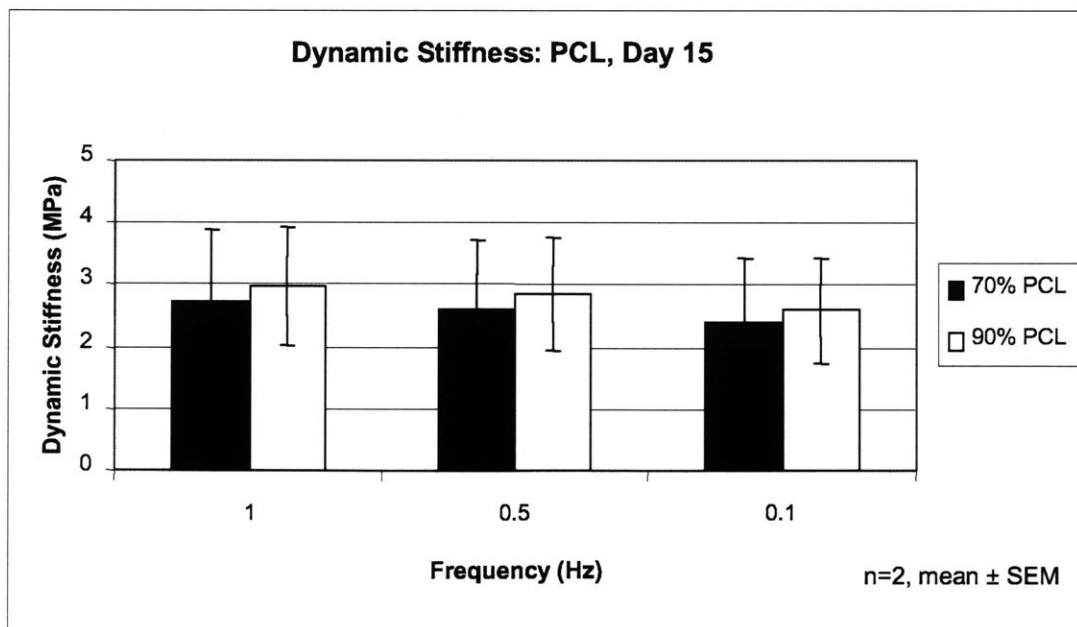

Figure 4.13 Mechanical properties of dynamically compressed porous PCL scaffolds on day 15 of culture.
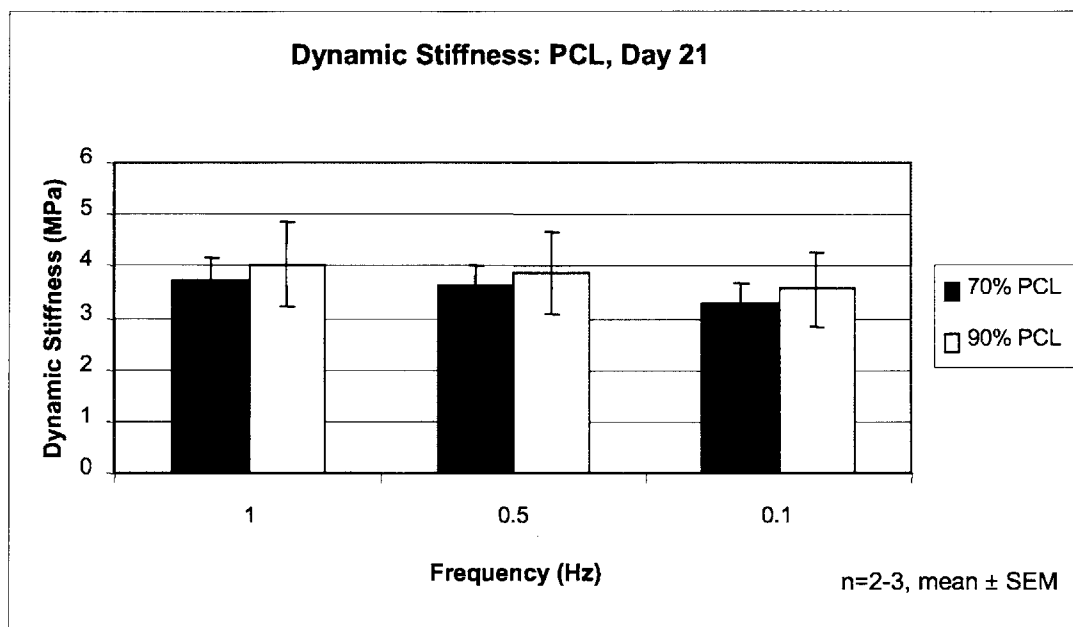
Figure 4.14 Mechanical properties of dynamically compressed porous PCL scaffolds on day 21 of culture. Dynamic stiffness values remained relatively constant with respect to frequency, however appeared to increase with respect to time.

4.3.5 Histological Analysis

Histological analysis was performed to provide a visual and qualitative confirmation of the integration of the chondrocyte-encapsulated peptide solution into the porous PCL and to depict the development of ECM inside the pores of the PCL scaffold. Unstained PCL sections were dry-mounted to provide a visual representation of the PCL scaffold architecture as seen in Figure 4.15. Due to histological processing techniques, entire cross-sections of the PCL regions of the composites were difficult to obtain. Therefore, by comparing stained images to those of the unstained PCL sections, it is clear that the areas that have been stained with H&E or Toluidine Blue are within the interconnected porous regions of the PCL scaffolds and the surrounding network of lighter regions are the PCL polymer.

60
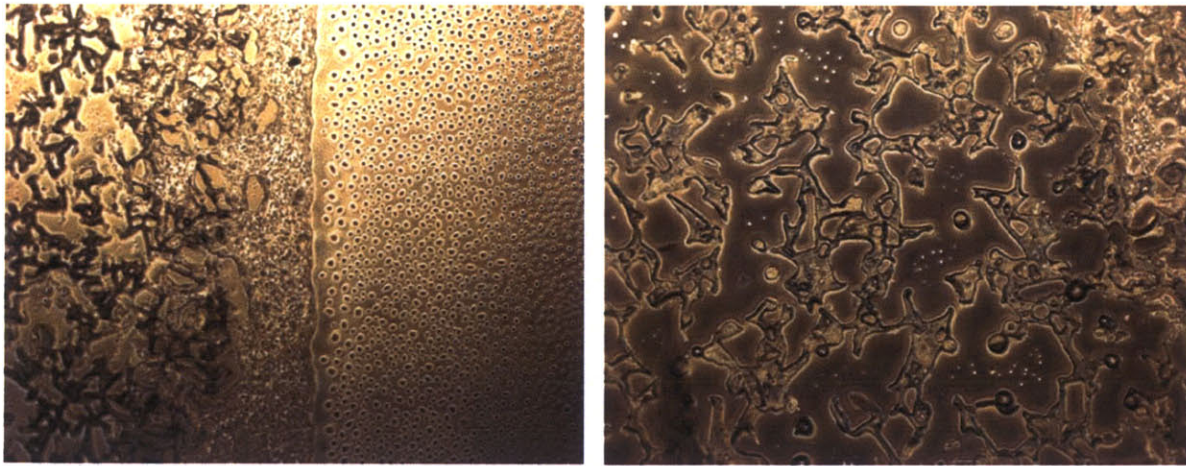
Figure 4.15 Unstained 5μm PCL section from a 70% porous composite integrated with a chondrocyte-seeded peptide hydrogel at (a) 4X and (b) 10X. Both figures depict the microarchitecture and fully interconnected porous structure of the PCL scaffold.

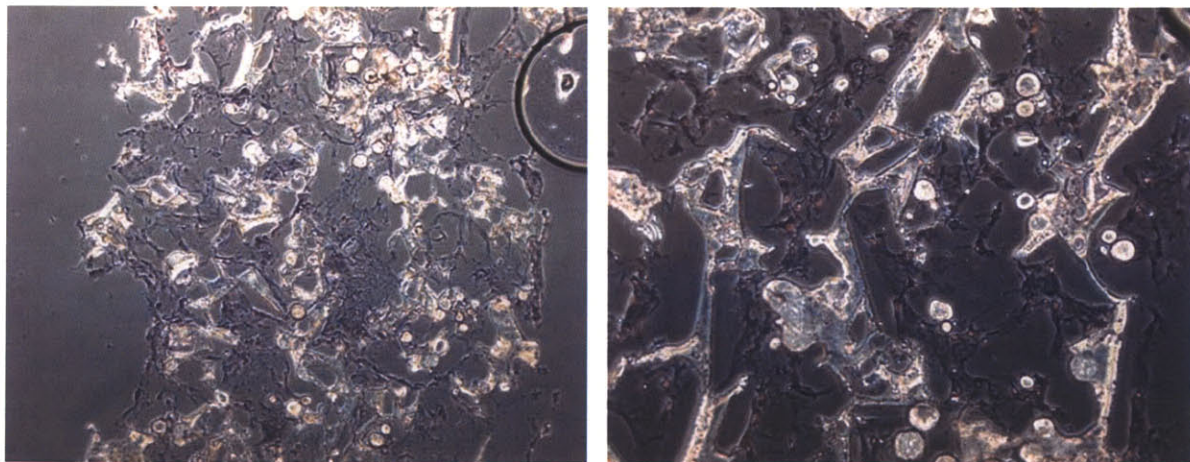Figure 4.16 5μm PCL section from a 70% porous PCL and chondrocyte-seeded peptide hydrogel composite at (a) 4X and (b) 10X. H&E staining on day 21 of culture illustrates the integration of the chondrocyte-seeded peptide hydrogel into the pores of the PCL scaffold. The light interconnected regions are the PCL polymer, and the dark spots within the pores of the PCL scaffold are chondrocyte nuclei.
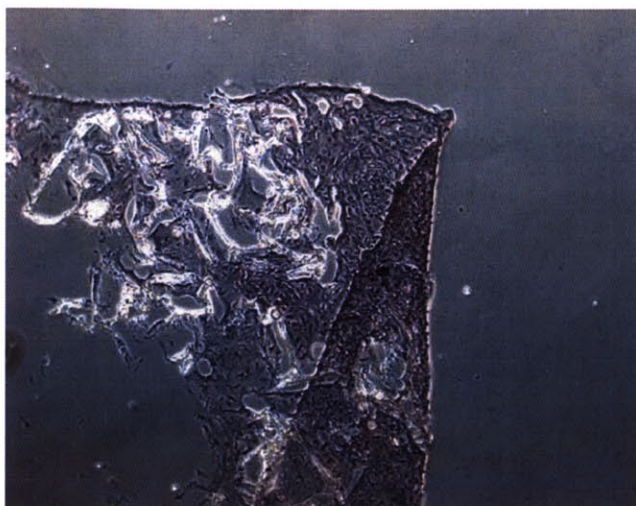
Figure 4.17 5μm PCL section from a 90% porous PCL and chondrocyte-seeded peptide hydrogel composite at 4X. H&E staining on day 21 of culture illustrates the gradient of integration of the chondrocyte-seeded peptide hydrogel into the pores of the PCL scaffold. Higher concentration of H&E staining on the right edge of the image, indicating the top surface of the PCL scaffold, may be remnants of the peptide hydrogel on this surface of the PCL.

4.4 Discussion

Biochemical and mechanical analyses of the chondrocyte-seeded peptide hydrogel and porous PCL composites have verified the potential use of these materials in an integrated osteochondral construct. The initial objective in testing the validity of such a composite was to investigate whether the presence of the PCL scaffold had any adverse effects on chondrocyte viability and behavior in both the peptide hydrogel and the porous PCL regions. As is evident in the biochemical analysis, the PCL scaffold did not introduce any detrimental impacts on chondrocyte behavior. Although there was a slight difference in the composite involving the peptide hydrogel and 70% porous PCL scaffold on day 15, GAG content in the peptide hydrogel for both types of composites was similar to earlier studies performed by Kisiday et al. involving peptide hydrogel-only systems [23]. However, additional studies are needed to confirm whether this discrepancy between the peptide hydrogel and 70% porous PCL composite and the peptide hydrogel-only systems was a result of the sub-optimal experimental conditions experienced in this study or whether there is indeed a difference. This consistency between studies indicates that the PCL appears to have behaved as an inert material with respect to the capability of the chondrocytes to produce ECM. The validation of this conclusion is significant to achieve in order to pursue PCL as a viable bone substitute material in an osteochondral composite.

Similarly, biosynthesis rates also suggested that the PCL scaffold had innocuous effects on chondrocyte behavior. A peptide sheet was cast without integration into a PCL scaffold to serve as the control on day 15. Both proline and sulfate incorporation rates were consistent with this chondrocyte-seeded peptide sheet control at this time point. Furthermore, proline and sulfate incorporation rates appeared to be consistent in magnitude and trend with peptide hydrogel-only systems studied by Kisiday, et al. [23]. Therefore, integration of the peptide hydrogel with PCL did not cease chondrocytes' capability to produce ECM or the rate at which they produce protein and sulfated proteoglycan. Furthermore, with regard to hydroxyproline accumulation, the overlap between these composite studies and peptide hydrogel-only studies was at a single time point, day 15. This biochemical assay also proved to be analogous between the two studies. Each of these assays not only characterizes the osteochondral construct, but also serves as a means of validation when compared to the peptide-hydrogel only studies. Because of the parallels between these studies, with respect to peptide scaffold material, cell seeding density, culture medium, and experimental conditions, the initial objective of determining whether or not the presence of the PCL scaffold has adverse effects on chondrocyte behavior was achieved.

The next objective of this study was to investigate the effects of PCL microarchitecture on chondrocyte behavior. Because a range of porosities have been utilized for the cartilaginous region of osteochondral composites in current studies, determination of the optimal scaffold design may enhance integration and adhesion of the two materials in the composite, chondrocyte viability, ECM accumulation, and biosynthetic activity. From this study, it is difficult to ascertain whether the PCL microarchitecture had an effect on GAG accumulation. There was a significant difference in GAG content between composites involving the 70% porous and the 90% porous PCL scaffolds at all time points ($p < 0.05$). However, the GAG content in the peptide hydrogel for this 70% porous composite decreased unexpectedly between time points. Therefore, it is difficult to determine whether this discrepancy in GAG content between the two distinct PCL scaffold designs was due to the difference in the level of porosity of the scaffolds or if it was an artifact of sub-optimal experimental conditions. Radiolabel incorporation rates appear to provide a more thorough assessment of the minimal effect of PCL microarchitecture. As is evident through both proline incorporation rate and sulfate incorporation rate, the level of porosity of the PCL scaffold bears little impact on these values over time, as is seen in both the peptide hydrogel region and the PCL region. Similar results are also observed regarding

hydroxyproline content, which appears to be similar between the two porosities and with controls at all time points ($p > 0.05$), except the hydrogel and 90% porous PCL composite which is significantly higher than controls ($p < 0.05$). Mechanical testing, similar to the GAG assay, is a challenging characterization to use in assessing the effect of microarchitecture. Peptide hydrogel samples from 70% porous PCL scaffolds were unavailable for day 21 testing. The equilibrium moduli of the hydrogels from 70% and 90% porous PCL were not significantly different ($p > 0.05$). Although this assessment is based on one time point, the porosity of the PCL scaffold does not appear to impact material properties of the peptide hydrogel.

These studies suggest that porous PCL fabricated through 3DP™ technology is a viable option for use in an osteochondral composite involving the peptide hydrogel. Both chondrogenic and osteogenic cells have previously been shown to attach, proliferate, and develop cell-specific ECM in PCL [17]. This porous PCL does not interfere with the viability, matrix production, or biosynthesis rates of chondrocytes typical of chondrocyte-seeded peptide hydrogel-only systems. Therefore, the PCL material can function as a means of anchorage and mechanical support for the peptide hydrogel when implanted into the native defect without thwarting optimal chondrocyte behavior. Furthermore, biochemical and mechanical analysis provide a preliminary understanding of the impact of PCL scaffold design on material integration and chondrocyte behavior. Although these preliminary studies indicate that the microarchitecture of the PCL scaffold does not grossly affect chondrocyte behavior in an osteochondral composite, a more thorough investigation will provide a deeper understanding of the impact of the PCL scaffold porosity level.

Chapter 5: Effect of PCL Microarchitecture and Hydrogel Material on Chondrocyte Behavior

5.1 Introduction

The studies reported in the previous chapter indicated that porous PCL fabricated through 3DP™ technology is a viable option for the bone scaffold component of an osteochondral composite with regard to its effects on chondrocyte behavior in the peptide hydrogel. This scaffold material does not appear to interfere with the matrix production or biosynthesis rates of chondrocytes typical of chondrocyte-seeded peptide hydrogel-only systems. Although these preliminary studies indicated that the microarchitecture of the PCL scaffold does not grossly impact chondrocyte behavior in an osteochondral composite, a more thorough investigation was needed to provide a deeper understanding of the effect of porosity level.

One objective of this study was to repeat and corroborate the results presented in the previous chapter. The microarchitecture appeared to have little effect on biosynthesis rates; however, a validation study was necessary to thoroughly ascertain the impact of porosity and pore size on GAG accumulation and mechanical properties. PCL scaffolds with pore size in the range of 105-180μm and porosity levels of 70% and 90% porous were fabricated via 3DP™ technology. An additional means of characterization was introduced to further the investigation of PCL effect on chondrocyte viability. The MTS assay, as previously described, was incorporated into this study to monitor the viability of chondrocytes in the hydrogel region of the composite throughout the period of culture [22, 23].

Another objective of this study was to probe the selection of the hydrogel material. To delineate the efficacy of the peptide hydrogel as a scaffold material for maintaining chondrocyte phenotype, viability, and matrix production, analogous osteochondral composites were created incorporating an agarose hydrogel. Through the use of an agarose hydrogel, a more traditionally accepted means of studying chondrocyte behavior, a reference scale was established for the analysis of chondrocyte behavior in the peptide hydrogel.

This study also provided a visual characterization and high resolution analysis of the distinctions in PCL microarchitecture. Scanning electron microscopy (SEM) creates visual images of material surfaces at high magnification and resolution. These images provide insight

into the internal architecture of the porous PCL scaffolds, depicting the layer by layer feature of the 3DP™ fabrication process and the effect of porosity level on PCL polymer binding.

Therefore, this study attempts to validate the potential of the peptide hydrogel and porous PCL osteochondral composite through its characterization of chondrocyte viability, GAG accumulation, biosynthesis rates, mechanical properties, and histology. These assays were performed on both the hydrogel and porous PCL regions of the two types of composites, 70% and 90% porous PCL, in order to obtain a relative understanding of chondrocyte behavior in two distinct environments. A reference scale for these analyses is established through the incorporation of agarose hydrogel and porous PCL osteochondral constructs, and a visual understanding of the impact of PCL porosity level is provided through SEM images.

5.2 Methods and Materials

5.2.1 Cell Isolation

Bovine chondrocytes were harvested from the femoral condyles and femoropatellar grooves of 1-2 week old calves within a few hours of slaughter, as previously described [40]. Cartilage slices were taken from the femoral condyles and femoropatellar grooves and manually chopped into fine pieces. The tissue was then transferred to a pronase solution at a concentration of 20U/mL for 2 hours of incubation (Sigma-Aldrich, St. Louis, MO). The pronase-tissue solution was mixed via pipetting every twenty minutes. At the end of this incubation period, the tissue was rinsed twice with 1X PBS and placed into a collagenase solution at a concentration of 200U/mL overnight (Worthington, Lakewood, NJ). The next morning, the collagenase-tissue solution was mixed via pipetting every 30 minutes until the solution appeared relatively clear, indicating the completion of the digestion process. At this point, the solution was allowed to incubate for 1.5 hours to complete digestion. The chondrocyte suspension was then filtered through a 40μm cell strainer and centrifuged at 1900 rpm for 8 minutes. After aspirating the supernatant, cell pellets were resuspended and centrifuged in 1X PBS. This process of centrifugation and PBS rinsing was repeated two more times. After the third round of centrifugation, the cells were resuspended in high glucose DMEM (Gibco, Auckland, New Zealand). A sample of cell suspension was microscopically analyzed for cell viability using ethidium bromide/FDA and concentration using Trypan Blue Staining (Sigma Chemical Co., St. Louis, MO). The cell suspension was then stored at 4° C until use.

66

5.2.2 PCL Fabrication

PCL scaffolds were fabricated using a Theriform™ 3DP™ machine (Therics, Inc. Princeton, NJ). An emulsion-precipitation method was used to create PCL powder (PCL MW= 65KDa, Aldrich, Milwaukee, WI) [41, 42]. PCL was dissolved in dichloromethane (CH_2Cl_2) and then injected into a continuously stirred water bath consisting of 95% H_2O and 5% polyvinyl alcohol (PVA). After the precipitation of PCL in this water bath, the spherical particles were rinsed, dried, and sieved a particle diameter of less than 75μm. The pore size of the PCL scaffold is dictated by the diameter size of the NaCl particles (Mallinkrodt, Paris KY). NaCl particles were milled and sieved to a range of 106-180μm diameter (Bel-Art Products Mill, Model Number: 37252-0000, Pequannock, NJ; VWR Scientific Sieve, West Chester, PA). Particles of NaCl and PCL were mixed together in relative proportions to create the desired porosity of the scaffold. For these studies, mixture compositions included 70% NaCl with 30% PCL powder, and 90% NaCl with 10% PCL powder. A thin layer of powder was spread by the powder spreader across the surface of the powder bed on top of a piston. An ink-jet printhead then printed the liquid binder, chloroform, thereby bonding the particles of the polymer together to form a solid (Mallinckrodt, Paris, KY). The 50μm diameter printhead nozzle created droplets of chloroform approximately 100μm in diameter. Given these printing parameters, the line resolution of these scaffolds was approximately 200-250μm. Line spacing was defined as 185μm, layer thickness was 250μm, and the printhead velocity was 1000mm/sec. After the first layer was printed, the piston then lowered the powder bed to a fixed distance and the cycle of powder-spreading and printing was repeated. The process was repeated until a complex 3D scaffold is complete and the scaffold could then be lifted from the powder bed [25]. Porous PCL cylindrical cores, 9mm in diameter and 3mm thick, were printed with a fully interconnected porous microarchitecture consisting of 70% or 90% void space. After the printing process was complete, scaffolds were placed in water on an orbital shaker to leach out the NaCl particles. The scaffolds were then frozen at -80°Celsius and lyophilized overnight to remove any residual water. The scaffolds were then autoclaved for 14 hours in ethylene oxide and ready for use (Andersen Products Autoclave, Model Number: AN74, Haw River, NC).

5.2.3 Casting

2.5% agarose molds were created by pipetting 5ml into 35mm Petri dishes. All molds were 4mm thick with an inner diameter (ID) of 9mm and an outer diameter (OD) of 20mm. The

peptide KLD-12 was custom synthesized (SynPep Corp., Dublin, CA) and lyophilized to a powder. KLD-12 powder was dissolved in a 10% sucrose solution at a concentration of 3.6mg/mL. The peptide solution was then sonicated until further use to prevent aggregation. The volume of cell suspension targeted for a cell seeding density of 30million/mL was centrifuged at 1900rpm for 8 minutes. Isolated chondrocytes were then resuspended in a 10% sucrose plus 5mM HEPES buffer solution equal in volume to 10% of the final hydrogel casting volume. The peptide solution was then added to the cell suspension in volume equal to 90% of the final hydrogel casting volume. The casting solution was then lightly vortexed and injected directly into and on top of the porous PCL scaffold inside the cylindrical core of the agarose mold. After a waiting period of 10 minutes, the composite samples were then submerged in 1.5X PBS without agitation for 30 minutes to initiate self-assembly of the peptide hydrogel. At this point, PBS was aspirated and culture medium, high-glucose DMEM with 0.2% FBS and 1% ITS, was added. Each sample received 5mL of culture medium that was changed every other day.

Chondrocyte-seeded peptide hydrogel slabs, without integration into a porous PCL scaffold, were also created to serve as a control. The casting procedure of the KLD-12 peptide into chondrocyte-seeded hydrogel slabs developed and optimized by Kisiday et al., as previously described, was employed to create these controls [22]. Briefly, isolated chondrocytes targeted for a cell seeding density of 30million/mL were resuspended in a 10% sucrose plus 5mM HEPES buffer solution equal in volume to 10% of the final hydrogel casting volume. The peptide solution was then added to the cell suspension in volume equal to 90% of the final hydrogel casting volume. The casting solution was then lightly vortexed and injected into a stainless steel frame in a molten state and subsequently placed into a 1.5X PBS bath to initiate self-assembly into a slab-like geometry. After 25-30 minutes, the casting frame was disassembled and the chondrocyte-seeded peptide hydrogel sheet was submerged into 15mL of culture medium in a 100mm Petri dish. Culture medium was changed every other day.

Osteochondral constructs consisting of a 2% agarose hydrogel layer and porous PCL scaffold were also created using similar methods. For these samples, isolated chondrocytes were re-suspended in warm culture medium equal in volume to one-third of the final casting volume. This re-suspended cell suspension was then mixed with molten 3% agarose equal in volume to two-thirds of the final casting volume and lightly vortexed to ensure an even distribution of cells. The casting solution was then injected directly into and on top of the porous PCL scaffold inside

68

the cylindrical core of the agarose mold. Composite samples were then submerged in 1X PBS without agitation for 10 minutes to allow for gelation of the agarose hydrogel. At this point, PBS was aspirated and culture medium, high-glucose DMEM with 0.2% FBS and 1% ITS, was added. Each sample received 5mL of culture medium that was changed every other day.

Chondrocyte-seeded agarose hydrogel slabs, without being integrated into a porous PCL scaffold, were also created to serve as controls. This casting procedure is analogous to that of the KLD-12 peptide hydrogel slabs as previously described [22]. Briefly, isolated chondrocytes targeted for a cell seeding density of 30million/mL were re-suspended in warm culture medium equal in volume to one-third of the final casting volume. This re-suspended cell suspension was then mixed with molten 3% agarose equal in volume to two-thirds of the final casting volume and lightly vortexed to ensure an even distribution of cells. The casting solution was then injected into a stainless steel frame in a molten state and subsequently placed into a 1X PBS bath to initiate gelation of the agarose hydrogel. After 10 minutes, the casting frame was disassembled and the chondrocyte-seeded agarose hydrogel sheet was submerged into 15mL of culture medium in a 100mm Petri dish. Culture medium was changed every other day.

5.2.4 Chondrocyte Viability

On days 7, 15, and 18 of culture, chondrocyte viability was assessed both qualitatively through ethidium bromide/FDA analysis as well as quantitatively via the MTS assay. This assay estimates the number of viable cells through spectrophotometric means. The compound (3-(4,5-dimethylthiazol-2-yl)-5-(3-carboxymethoxyphenyl)-2-(4-sulfophenyl)-2H-tetrazolium (MTS) (Promega Corp., Madison, WI) is taken up and metabolized by the cells into a formazan compound. When this product is released from the cell through the addition of 10% SDS, the absorbance of the culture medium can be measured at 490nm using a microplate spectrophotometer. At each time point, samples 4-6mg in wet weight were taken from the peptide hydrogel region of the composites. Each sample was cultured in 0.5mL high glucose DMEM without phenol red supplemented with the MTS assay solution. The samples were incubated on a shaker table for 1.5 hours, at which point 10% SDS at a concentration equal to 2% of the final volume was added. After approximately three hours of incubation, ensuring the complete equilibration of bioreduced MTS, 100μL aliquots of culture medium were assayed for absorbance. Absorbance values were normalized to wet weight of the plugs and provide a measure of viable cells for each sample relative to each other [22].

5.2.5 Biochemical Analysis

On days 5, 13, and 18 of culture, the composites were cut in half to allocate material for biochemical and mechanical analysis, as well as to histological analysis. The peptide hydrogel layer was separated from the PCL scaffold using a scalpel and 3mm plugs were taken from both regions using a disposable punch. Each plug was transferred to a 48-well tissue culture dish containing 1mL of feed medium plus $5\mu Ci/mL$ ^{35}S-sulfate and $10\mu Ci/mL$ ^{3}H-proline. Chondrocyte biosynthesis rates are described by the incorporation of ^{35}S-sulfate and ^{3}H-proline, which are indicative of the synthesis rates of sulfated proteoglycan and total protein, respectively. After 20 hours of incubation, the plugs were removed from the radiolabeled medium and washed 4 times over 80 minutes in PBS plus 1mM unlabeled proline and sodium sulfate (Sigma Chemical Co., St. Louis, MO and Mallinckrodt, Paris, Kentucky). Samples designated for mechanical testing were tested at this point. Each plug was then digested in 1mL of proteinase K-TRIS HCL solution at 60°C overnight. Radiolabel incorporation rates and accumulated sulfated glycosaminoglycan (GAG) content, determined by means of DMMB dye binding, were measured as described previously [34]. The other half of each sample, designated for histological analysis, was fixed in 4% paraformaldehyde overnight at 4°C. The next morning, these intact composite samples were rinsed twice in 1X PBS and stored in 70% ethanol at 4°C until histological analysis ensued.

5.2.6 Mechanical Testing

On days 14 and 19 of culture, 3mm plugs were tested in a radially confined uniaxial compression set-up using a benchtop Incudyne to determine the equilibrium modulus and dynamic stiffness of the materials, as previously described [44]. (Industrial Devices Co. LLC, Petaluma, CA, Model Number RGC-06-180-E04-X23X, Dynamic Acquisition System Software Version 9.9F). After measuring the thickness of each sample, the plug was placed into a confining cylindrical chamber clamped into the platform of the Incudyne. A porous platen was used to apply 2 sequential ramp-and-hold compressive strains of 5%, followed by 4 sequential ramp-and-hold compressive strains of 2% to the sample. Each compressive strain was applied over 30 seconds, followed by a holding period of 3 minutes to allow for stress relaxation. The ratio of the relaxed equilibrium stress to the engineering strain was used to compute the equilibrium modulus. At 18% compressive offset strain, a 0.2% amplitude sinusoidal dynamic

70

strain was applied at 1, 0.5, and 0.1Hz. The dynamic compressive stiffness was calculated as the ratio of the fundamental amplitudes of stress to strain [44].

5.2.7 Histological Analysis

After being fixed in 4% paraformaldehyde overnight at 4°C, samples were rinsed in PBS, and stored in 70% ethanol at 4°C until histological assessment ensued. At the point of sample preparation for histological analysis, the intact peptide layer was removed from the porous PCL scaffold. The peptide hydrogel layer was dehydrated by means of a graded ethanol series up to 100% ethanol and cleared in xylene. These samples were then embedded in paraffin, sectioned into 5μm sections, and stained with H&E for cell content and Toluidine Blue for proteoglycan content. The porous PCL samples, however, were submerged in a gradient of sucrose solutions after being fixed as a means of cryoprotection. Embedding the samples in sucrose solutions until the sucrose has infiltrated the samples removes the residual water from the interior of the sample and prevents the formation of ice crystals during the freezing process of cryosectioning. The following gradient of sucrose solutions was employed: 5%, 10%, 20%, and 30% sucrose in PBS. Samples were submerged in each concentration of sucrose solution overnight at 4°C, or until the sucrose solution had completely saturated the sample; as was evident by the sinking of the sample. Samples were then embedded in 50% OCT in PBS overnight at 4°C, 100% OCT overnight at 4°C, and finally embedded into cryosectioning molds with 100% OCT and frozen at -80°C, and then sectioned into 5μm sections with a cryostat. Dry sections were mounted unstained for the visualization of the PCL architecture, while other sections were stained with H&E to visualize the integration of the two materials and the presence of cells and with Toluidine Blue to visualize proteoglycan content.

5.2.8 Scanning Electron Microscopy

Scanning electron microscopy (SEM) provides visual images of material surfaces at high magnification and resolution. SEM characterization of control PCL samples that were not chondrocyte-seeded or cultured was performed at the W.M. Keck Microscopy Facility of the Whitehead Institute at MIT. Two porous PCL samples of each porosity level were sectioned, one with a horizontal orientation to characterize the material from a top-down view and one with a vertical orientation to provide a cross-section perspective of the scaffold. Samples were palladium coated for 2 minutes at 15mAmps and 7 volts (LADD Research Industries, Hummer

6.2 Sputter Coater, Williston, VT). This coating instrument is capable of uniformly coating irregularly shaped specimens with metal atoms without causing any thermal damage to the sample material. After the palladium coating was complete, SEM images of the 70% and 90% porous PCL samples were obtained (Jeol, JSM-5600LV, Peabody, MA).

5.2.9 Statistical Analysis

2-way ANOVA statistical analysis was performed to determine the effect of time and PCL porosity on a given biochemical parameter. If a statistically significant difference was observed, then individual 2-tail t-tests were performed at each time point to determine when the discrepancy based on PCL porosity arose throughout the time course. Individual 2-tail t-tests were also performed for a given biochemical parameter on each hydrogel region removed from a composite and its corresponding control hydrogel sheet to determine the significance of integrating the hydrogel material into a PCL scaffold.

5.3 Results

5.3.1 Chondrocyte Viability

A relative assessment of chondrocyte viability in the control sheets and hydrogel region of each composite can be made from the MTS assay, as shown in Figure 5.1. The initial values appeared to be slightly lower than expected based on previous studies performed with the MTS assay. 2-way ANOVA indicated that there was a significant difference in chondrocyte viability in the peptide hydrogel region of composite samples based on the porosity of the underlying PCL scaffold ($p < 0.05$). However, chondrocyte viability in the agarose region of the composite samples appeared to be independent of the PCL scaffold porosity ($p > 0.05$).
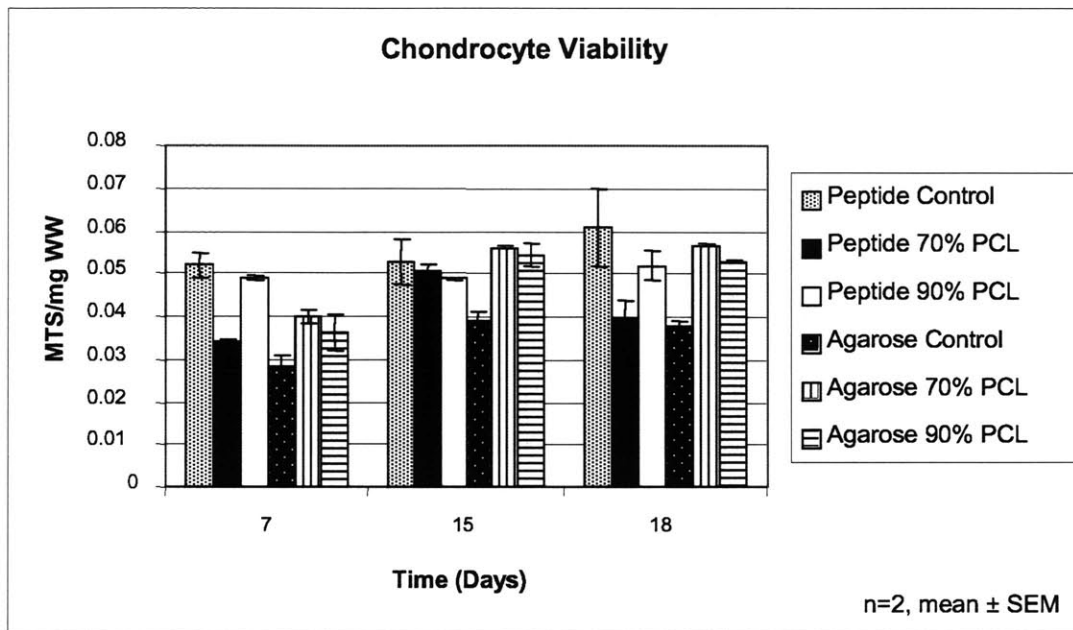
72

Figure 5.1 Cell viability in chondrocyte-seeded peptide and agarose hydrogel controls and regions of composites. MTS absorbance at 490nm provided relative measurement of viable chondrocytes in peptide and agarose hydrogels integrated with PCL scaffolds of 70% and 90% porosity. Presence of PCL, material selection for hydrogel region of osteochondral composite, and porosity level of PCL scaffold do not appear to produce marked discrepancies in chondrocyte viability in hydrogel region.

5.3.2 GAG Accumulation

In the composites comprised of the peptide hydrogel and porous PCL scaffold, 2-way ANOVA revealed that there was a significant difference in GAG accumulation in the peptide hydrogel region based on the porosity of the underlying PCL scaffold ($p < 0.05$). A post-hoc 2-tail t-test analysis indicated that this sensitivity to the porosity of the PCL scaffold became apparent on day 19 ($p < 0.05$), as shown in Figure 5.2. 2-tail t-tests demonstrated a significant difference in GAG content in the peptide hydrogel layer of the composite samples when compared to the chondrocyte-seeded peptide hydrogel control sheet ($p < 0.05$); however this result may be a reflection of the quality of the control sheet. The peptide hydrogel control sheet possessed a high concentration of air bubbles upon gelation, and the stiffness of this control sheet did not increase in the same manner as that of the hydrogel layer of the composite samples. The trends displayed an expected increase in GAG content over time.
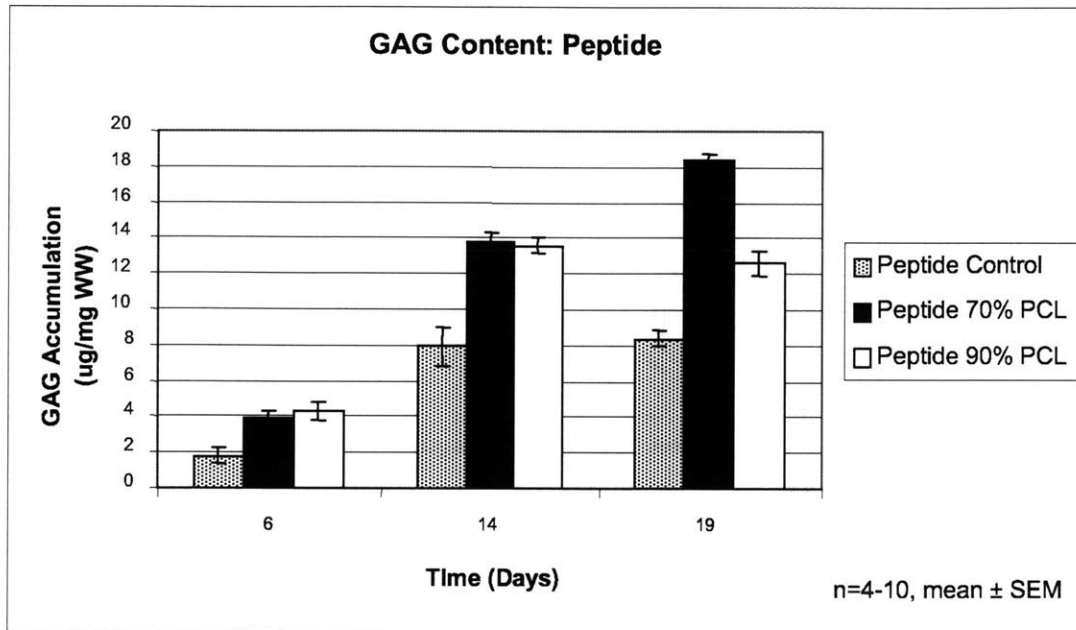
Figure 5.2 GAG accumulation measured in the peptide hydrogel region of the composite at various time points throughout culture. Integration with a porous PCL scaffold did not hinder matrix accumulation in hydrogel region of composite.

Unlike composites involving a peptide hydrogel layer, GAG accumulation in composites comprised of an agarose hydrogel and porous PCL scaffold appeared to be independent of the porosity of the PCL scaffold ($p > 0.05$), as is evident in Figure 5.3. In comparison to the chondrocyte-seeded agarose only control sheet, GAG content in the agarose layer of the composite samples was significantly higher at all time points ($p < 0.05$), with the exception of the composite consisting of an agarose hydrogel and 70% porous PCL scaffold on day 19. The trends observed in GAG content in agarose were similar to those seen in the peptide hydrogel, with an increase in GAG content observed over time. The overall magnitude of GAG content measured in the peptide hydrogel control samples was consistent with that observed in the agarose hydrogel control samples at all time points ($p > 0.05$).

74

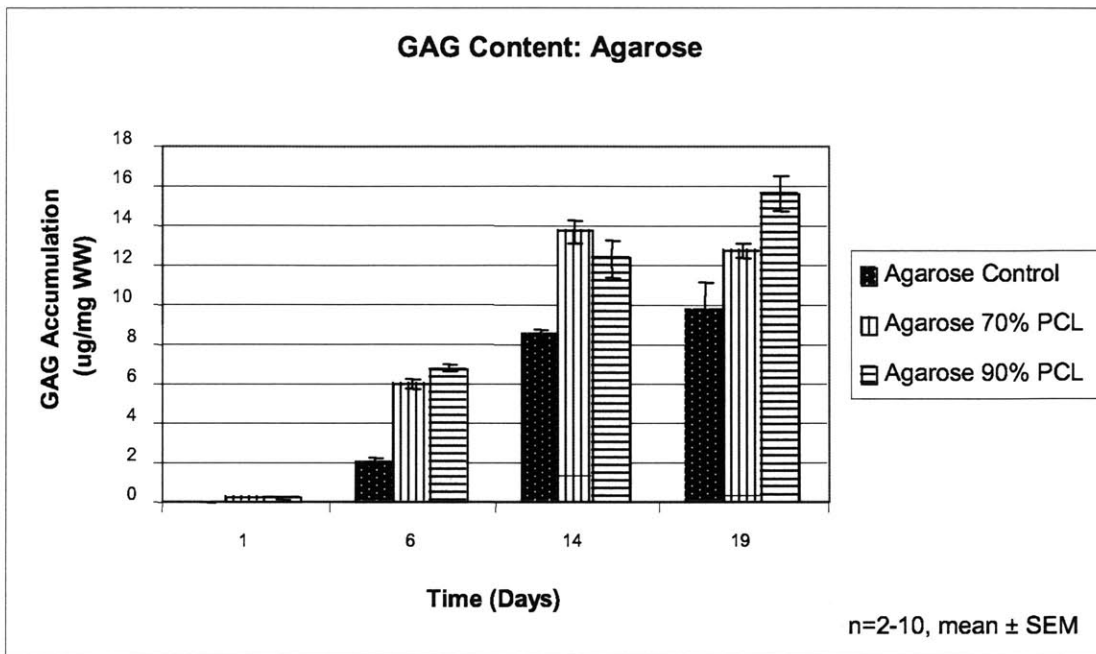**GAG Content: Agarose**

n=2-10, mean ± SEM

Figure 5.3 GAG accumulation was measured in the agarose hydrogel region of the composites at various time points throughout culture. GAG content in agarose hydrogel was consistent with that measured in peptide hydrogel in terms of magnitude and trend. Material selection for the hydrogel region, presence of PCL, and porosity level of PCL did not hinder matrix accumulation in hydrogel region.

GAG accumulation in 3mm plugs removed from the porous PCL region of these composites displayed similar trends as those observed in the peptide hydrogel region, with an increase in GAG content seen over time as shown in Figure 5.4. The magnitude of these values was approximately an order of magnitude less than those observed in the hydrogel region. 2-way ANOVA delineated a significant difference in GAG accumulation inside the PCL scaffolds in composites involving the peptide hydrogel based on the porosity of the PCL ($p < 0.05$). A post-hoc 2-tail t-test revealed that this dependence on PCL porosity became apparent on day 19 ($p < 0.05$). PCL portions of the composites involving the agarose hydrogel layer did not display a significant difference in GAG accumulation between the 70% porous PCL scaffolds and the 90% porous PCL scaffolds ($p > 0.05$). With the exception of the 70% porous PCL samples on day 6, a 2-tail t-test revealed no significant difference in GAG content in the porous PCL region based on the choice of hydrogel material ($p > 0.05$).
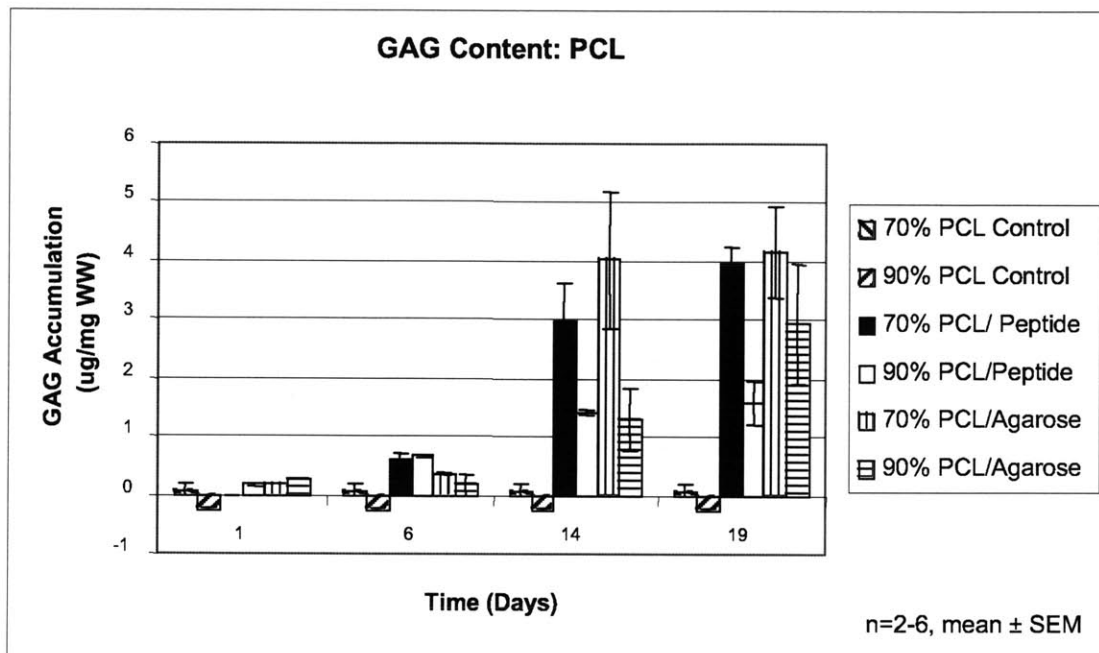
Figure 5.4 GAG accumulation measured in porous PCL controls and regions of the composites at various time points throughout culture. Unseeded porous PCL constructs were cultured in an agarose mold, in an identical manner as those that were seeded, to measure any residual background in biochemical assays. Choice of hydrogel material did not significantly impact GAG accumulation in the porous PCL scaffold.

5.3.3 Chondrocyte Biosynthesis

With respect to the porosity of the PCL scaffold in composites involving the peptide hydrogel, 2-way ANOVA indicated that there was a significant difference in both proline incorporation rate and sulfate incorporation rate in the peptide hydrogel region ($p < 0.05$). Post-hoc 2-tail t-tests demonstrated that this sensitivity of radiolabel incorporation rates to the porosity of the PCL scaffold existed on day 6 ($p < 0.05$), as is evident in Figure 5.5. When compared to the chondrocyte-seeded peptide hydrogel only control sheet, 2-tail t-tests displayed a significant difference in proline incorporation rate in the peptide hydrogel region integrated with the 70% porous PCL scaffolds on day 19 ($p < 0.05$). In composites comprised of the peptide hydrogel layer and the 90% porous PCL scaffolds, a significant difference in proline incorporation rates between the composite samples and the control sheet was observed on day 6 ($p < 0.05$). Unlike the study described in Chapter 4, proline incorporation rates in both the peptide control sheet and the peptide hydrogel composite samples remained relatively constant throughout the time of culture. 2-tail t-tests demonstrated that only the composite involving the peptide hydrogel and 70% porous PCL displayed a significant deviation from the peptide

76

hydrogel control samples in sulfate incorporation rate on day 19 (p < 0.05), as depicted in Figure 5.6.
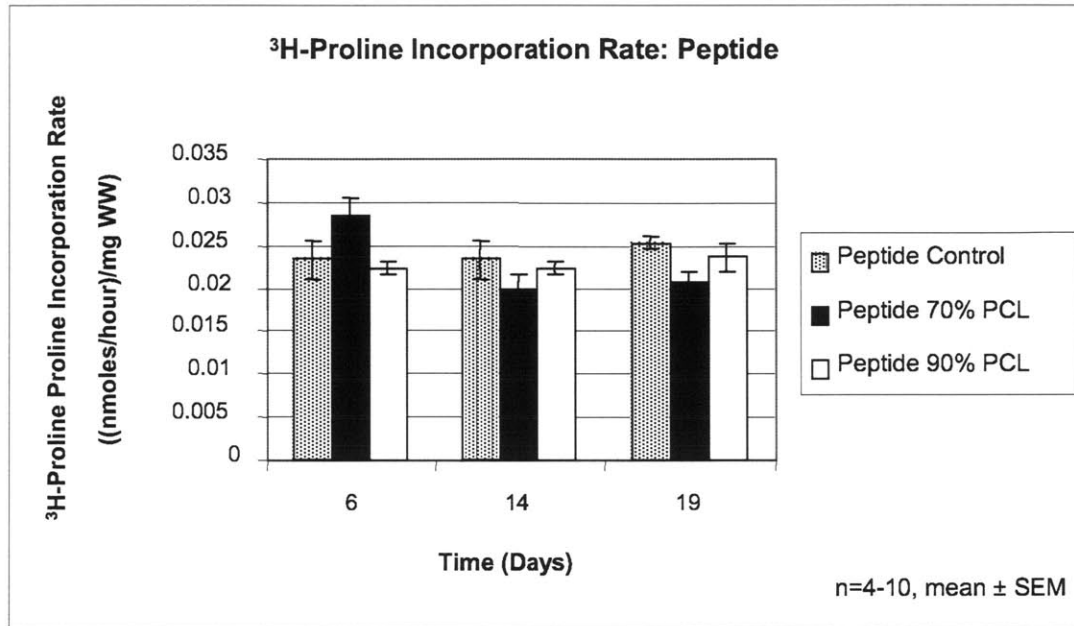

Figure 5.5 Chondrocyte biosynthesis in peptide hydrogel region of the composites. ^{3}H-proline incorporation rates, indicative of protein synthesis by chondrocytes, were affected by PCL scaffold presence and microarchitecture. The initial ^{3}H-proline incorporation rates appeared to be slightly lower than previous studies.
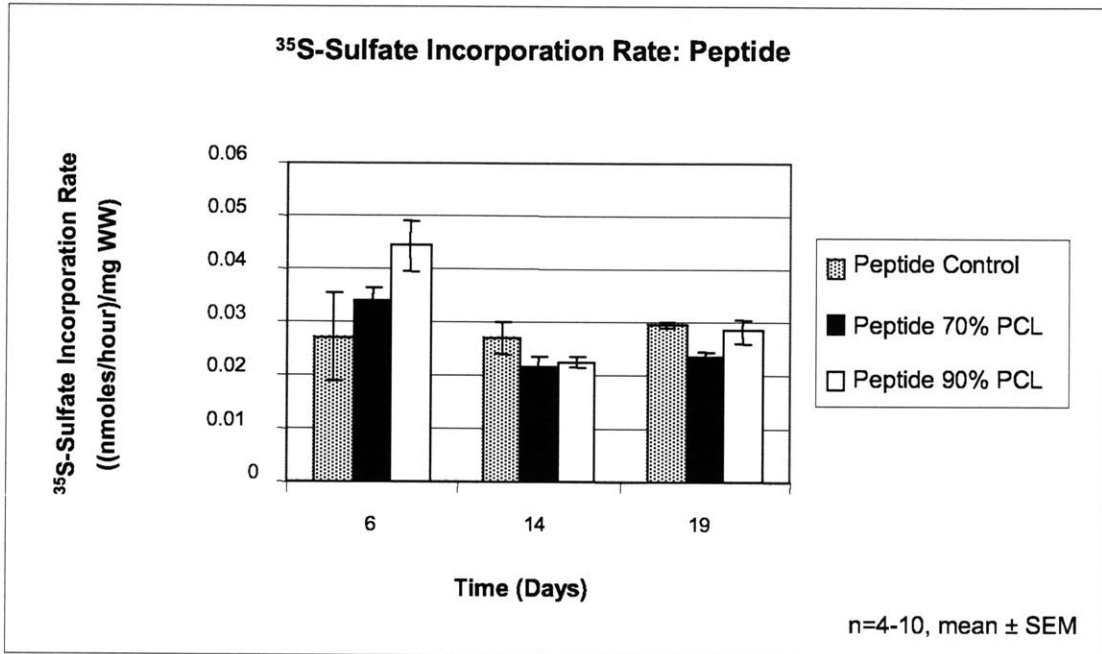
Figure 5.6 Chondrocyte biosynthesis in peptide hydrogel region of composites. ^{35}S-sulfate incorporation rate, indicative of sulfated proteoglycan synthesis by chondrocytes, also displayed lower values than expected based on previous studies. Presence of PCL did not have adverse effects on biosynthesis rates of chondrocytes and distinctions in porosity level did impact sulfated proteglycan synthesis by chondrocytes in peptide hydrogel.

Composite samples involving the agarose hydrogel displayed similar trends in proline incorporation rates as those seen in the peptide hydrogel region. Figure 5.7 indicates that these values were relatively constant in magnitude across all time points. No significant difference was observed in proline incorporation rate in the agarose hydrogel region of the composite samples based on the porosity of the PCL scaffold ($p > 0.05$). 2-tail t-tests displayed significantly higher values of proline incorporation rate in both types of composites when compared to the chondrocyte-seeded agarose only control sheet ($p < 0.05$). 2-way ANOVA described a significant difference in sulfate incorporation rates in the agarose hydrogel region of the composite samples based on the porosity of the underlying PCL scaffold ($p < 0.05$). Post-hoc 2-tail t-tests indicated that this significant discrepancy in sulfate incorporation rates in the agarose hydrogel region occurred on days 6 and 19 ($p < 0.05$), as seen in Figure 5.8. Furthermore, a significant deviation existed in sulfate incorporation rates between the agarose control sheet and agarose composite hydrogels, regardless of PCL porosity ($p < 0.05$). When comparing peptide hydrogel control sheet to agarose control sheet, it is evident that there was a significant

difference in proline incorporation rates at all time points ($p < 0.05$). A significant difference in sulfate incorporation rates between the peptide hydrogel control sheet and agarose control sheet was observed only on day 19 ($p < 0.05$).
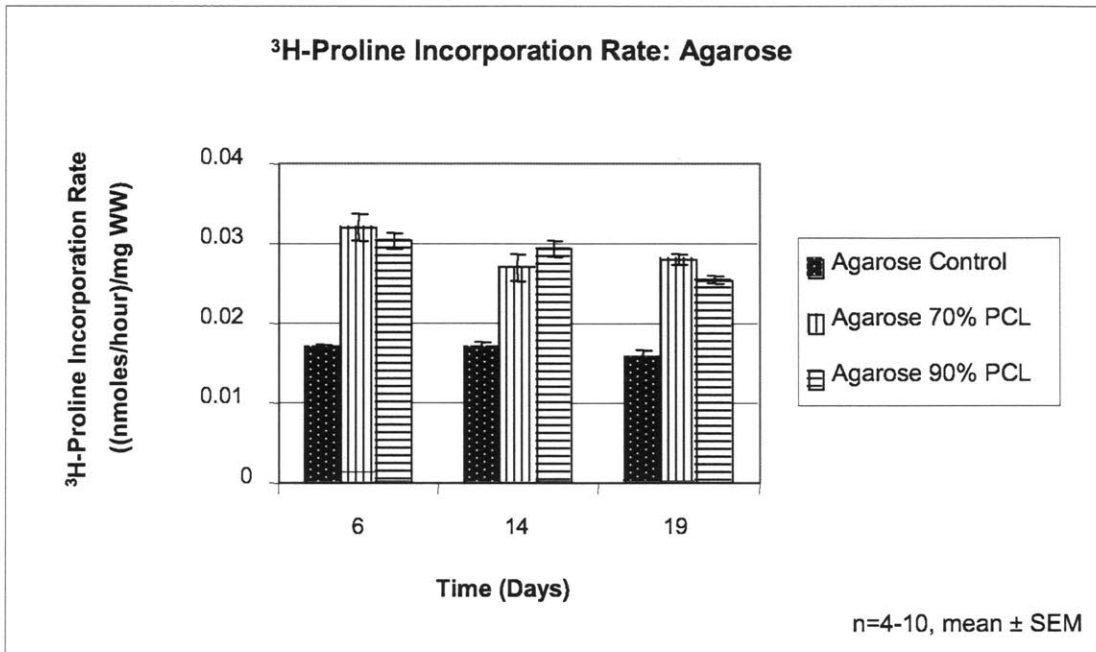

Figure 5.7 Chondrocyte biosynthesis in agarose hydrogel region of composite. ^{3}H-proline incorporation rates in the hydrogel region were independent of porosity level of PCL scaffold. Similar to the ^{3}H-proline incorporation rates in the peptide hydrogel, the initial values appeared to be slightly lower than previous studies.
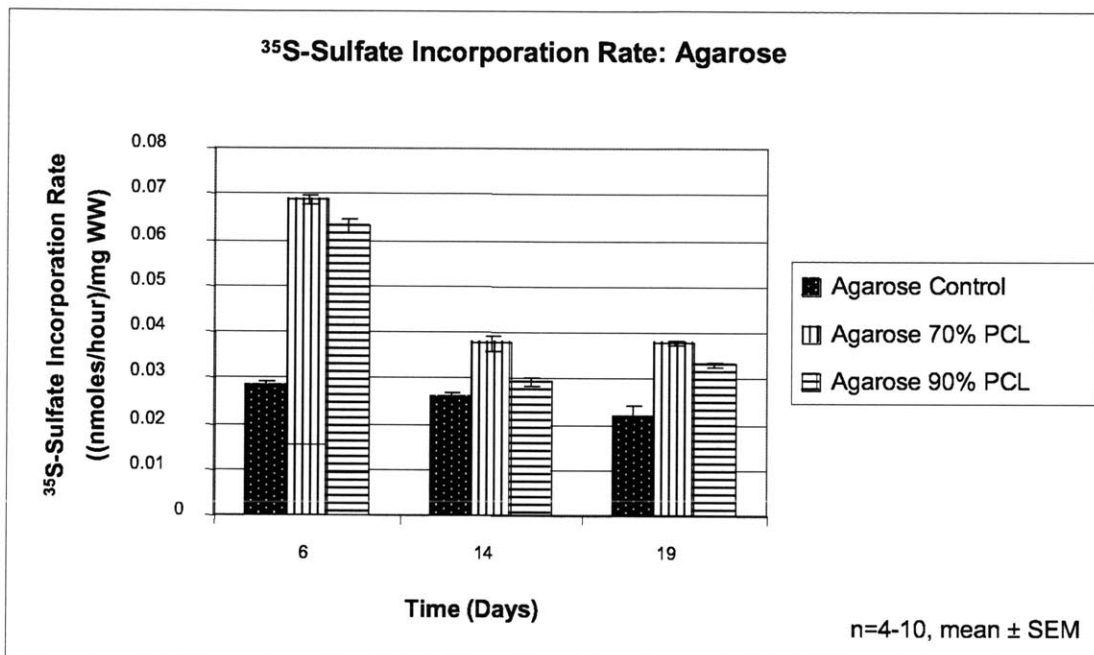
Figure 5.8 Chondrocyte biosynthesis in agarose hydrogel region of composite. Sulfated proteoglycan synthesis in agarose hydrogel was not hindered by integration of the hydrogel with a porous PCL scaffold with either 70% porosity or 90% porosity.

The trend in sulfate incorporation rates was similar in both types of hydrogels, displaying a distinct drop in magnitude from day 6 to day 14, as shown in Figure 5.6 and Figure 5.8. In the peptide hydrogel composites, the sulfate incorporation rate in the 70% porous composite and 90% porous composite decreased 37% and 49%, respectively, from day 6 to day 14, and increased 9% and 26% from day 14 to day 19. In the agarose hydrogel composites, sulfate incorporation rate in the 70% porous composite and 90% porous composite decreased 46% and 54%, respectively, from day 6 to day 14, and increased 0.3% and 12% from day 14 to day 19.

Radiolabel incorporation rates in the samples taken from the porous PCL regions were approximately an order of magnitude less than those seen in the hydrogel regions and appeared to be independent of the porosity of the PCL. 2-way ANOVA indicated that there was no significant difference in radiolabel incorporation rates inside the PCL region of composites involving either a peptide hydrogel layer or an agarose hydrogel layer ($p > 0.05$), as shown in Figure 5.9 and Figure 5.10. This result may be affected by the relatively large standard error of the mean values and by the relatively small magnitude of the radiolabel incorporation rates.

80

Proline incorporation rates in the PCL portions of the composite ranged from 1% to 18% of the values observed in the corresponding hydrogel regions. The magnitude of the sulfate incorporation rates in the PCL samples ranged from 2% to 17% of those values measured in the corresponding hydrogel regions of the composites.
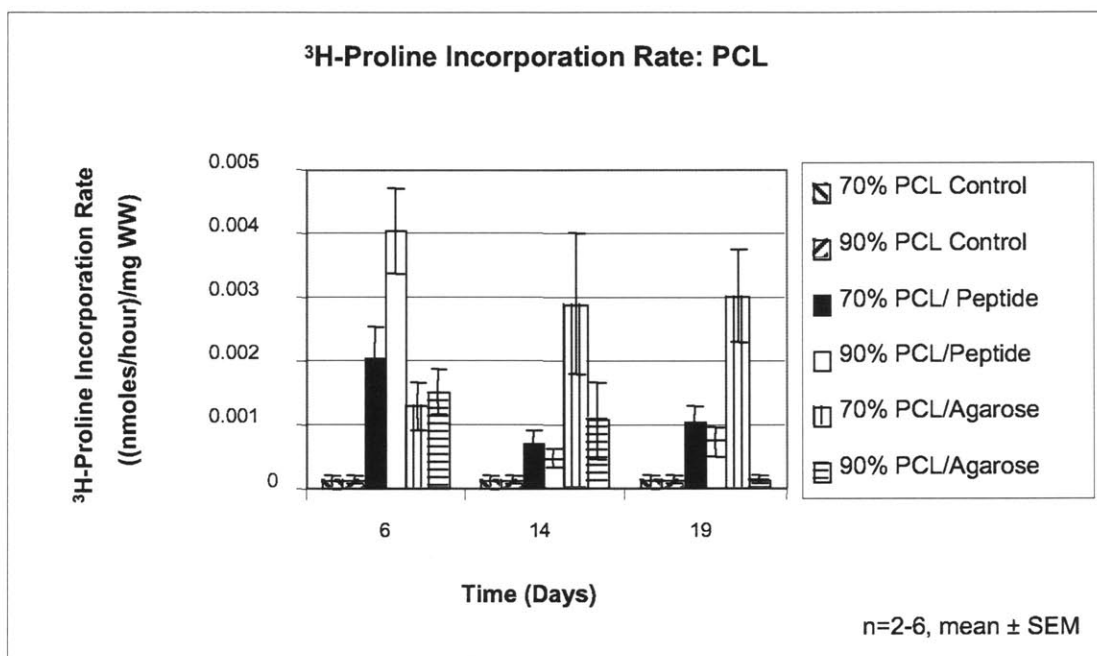

Figure 5.9 Chondrocyte biosynthesis in porous PCL scaffold region of composite. ^{3}H-proline incorporation rates in the porous PCL scaffolds were approximately an order of magnitude less than those measured in the hydrogel region. ^{3}H-proline incorporation rates observed in the PCL region of the composite were 1%-18% of those measured in the corresponding hydrogel regions.
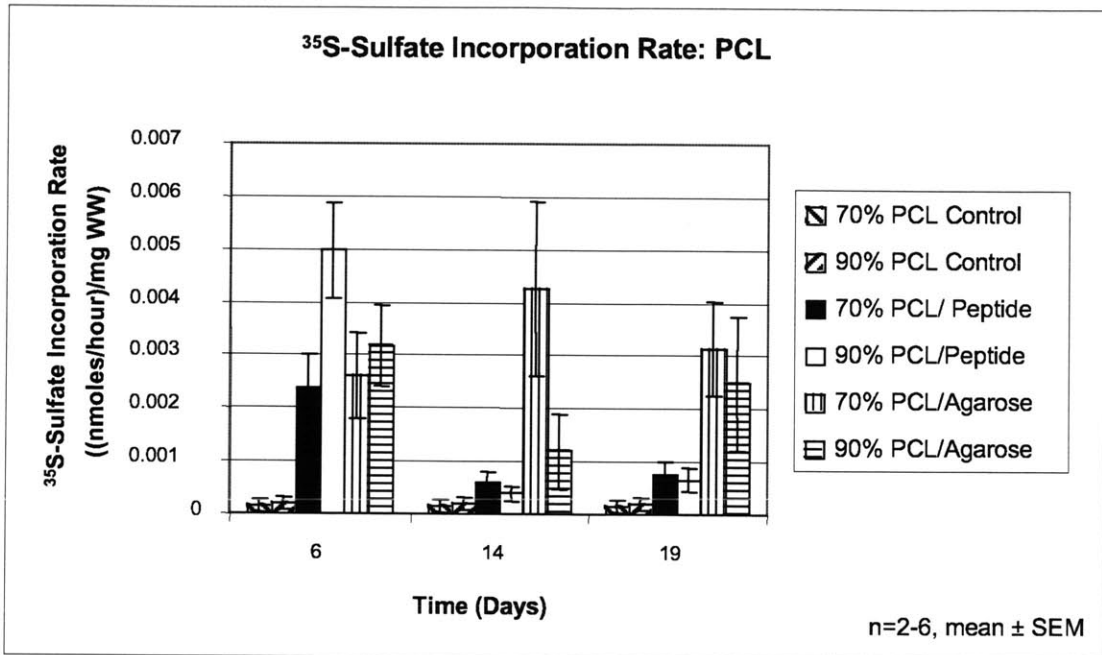
Figure 5.10 Chondrocyte biocynthesis in porous PCL scaffold region of composite. ^{35}S-sulfate incorporation rates were 2%-17% of ^{35}S-sulfate incorporation rates of corresponding hydrogel regions.

5.3.4 Mechanical Properties

The confined compression equilibrium modulus of the peptide hydrogel samples cultured on the 70% porous PCL scaffolds, as shown in Figure 5.11, decreased slightly from 61kPa to 56kPa from day 14 to day 19 of culture. The moduli of the peptide hydrogel samples cultured on the 90% porous PCL scaffolds also decreased from 79kPa to 37kPa from day 14 to 19. Despite these variations in changes in equilibrium moduli from day 14 to 19, there was no significant discrepancy in peptide hydrogel equilibrium modulus based on PCL porosity at either time point ($p > 0.05$). The equilibrium moduli of the agarose hydrogel samples cultured on 70% porous PCL samples, as depicted in Figure 5.12, also decreased slightly from 46kPa to 36kPa from day 14 to 19. The agarose hydrogel samples involving the 90% porous PCL samples also displayed a slight decrease in equilibrium modulus from 41kPa on day 14 to 39kPa on day 19. There was no significant difference in moduli values of the agarose hydrogel samples due to the distinction in PCL porosity on both days 14 and 19 ($p > 0.05$). Dynamic stiffness values for the peptide and agarose hydrogel samples were strain rate dependent, as shown in Figures 5-13 through 5-16. As frequency decreased from 1Hz to 0.5Hz to 0.1Hz, the dynamic stiffness values also decreased,

82

which is characteristic of poroelastic tissues. The magnitude of the dynamic stiffness values slight decreased from day 15 to day 21 across all frequencies [44].
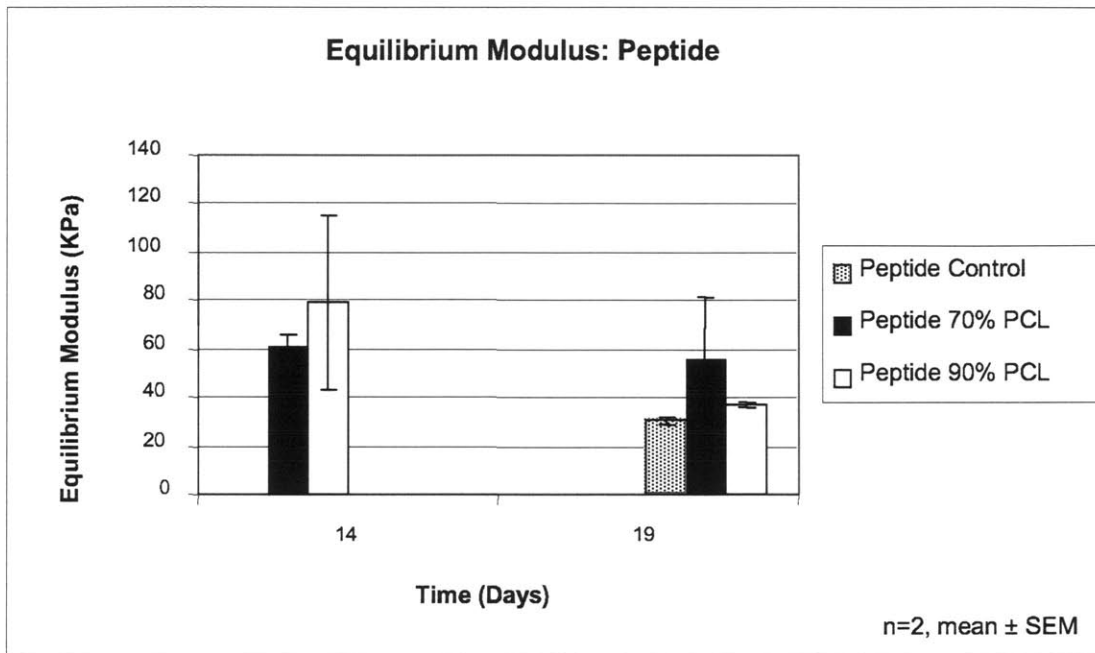

Figure 5.11 Mechanical properties of chondrocyte-seeded peptide hydrogel region of composite. Mechanical testing of 3mm plugs was performed in uniaxial confined compression. Equilibrium modulus was computed as the ratio of the relaxed equilibrium stress to the engineering strain for compressive strains of 5% to 18%. PCL porosity did not have significant effects on peptide hydrogel equilibrium modulus.
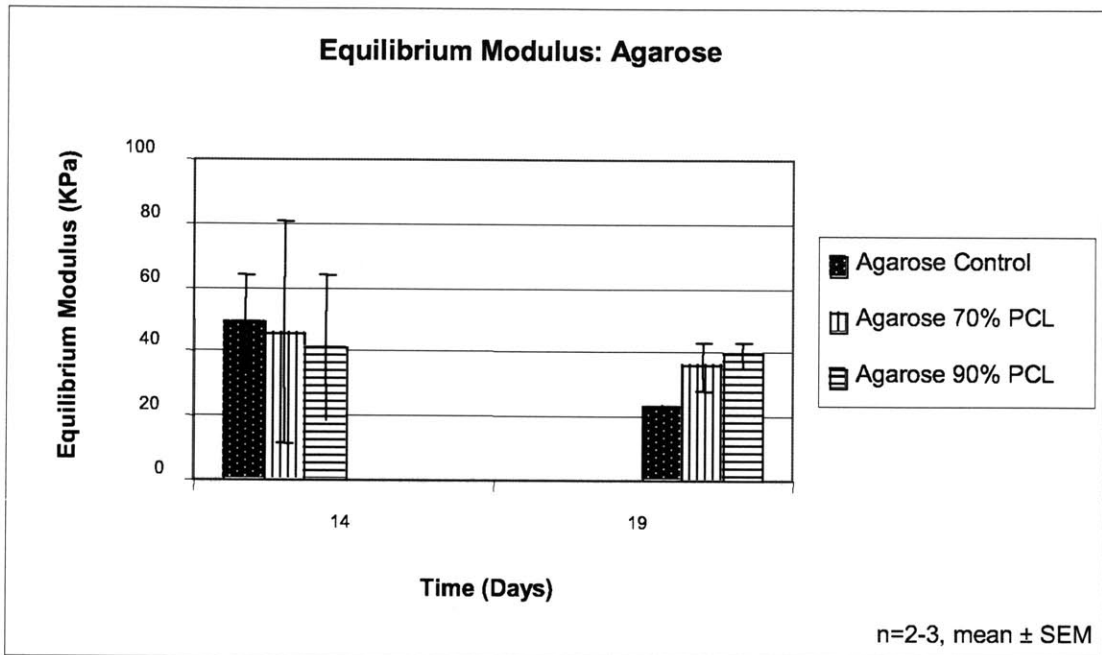
Figure 5.12 Mechanical properties of chondrocyte-seeded agarose hydrogel. PCL porosity did not have significant effects on agarose hydrogel layer equilibrium modulus.
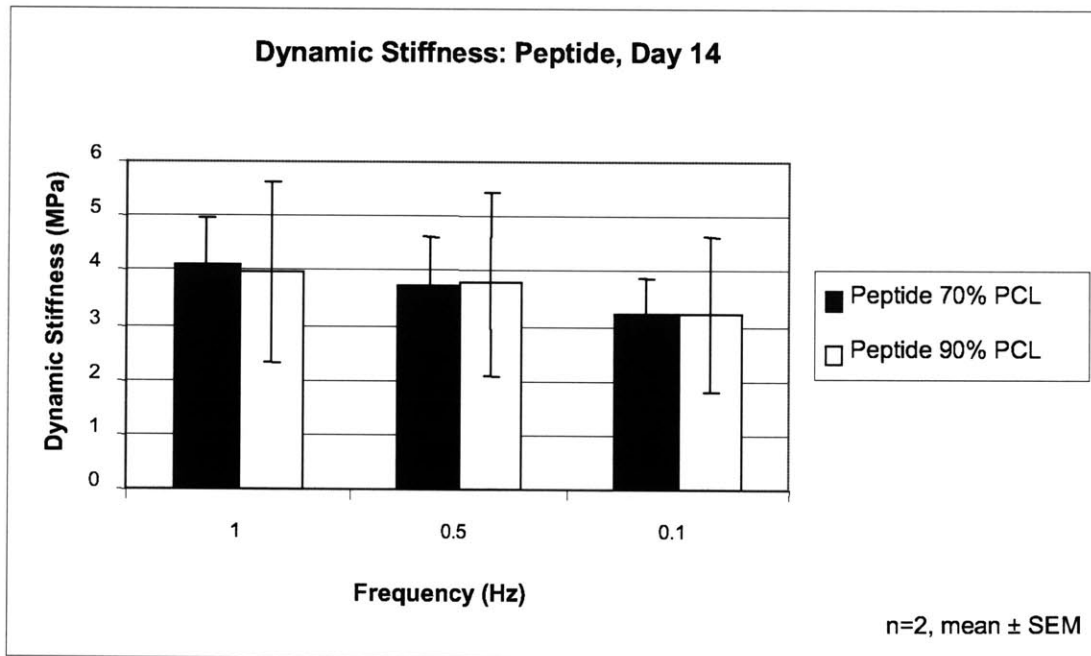

Figure 5.13 Mechanical properties of dynamically compressed chondrocyte-seeded peptide hydrogel on day 14 of culture. Dynamic compressive stiffness was computed as the ratio of the fundamental amplitudes of stress to strain with a dynamic strain amplitude of 0.2%. No apparent distinction was made in peptide hydrogel dynamic stiffness based on the porosity level of the PCL scaffold with which it was integrated.
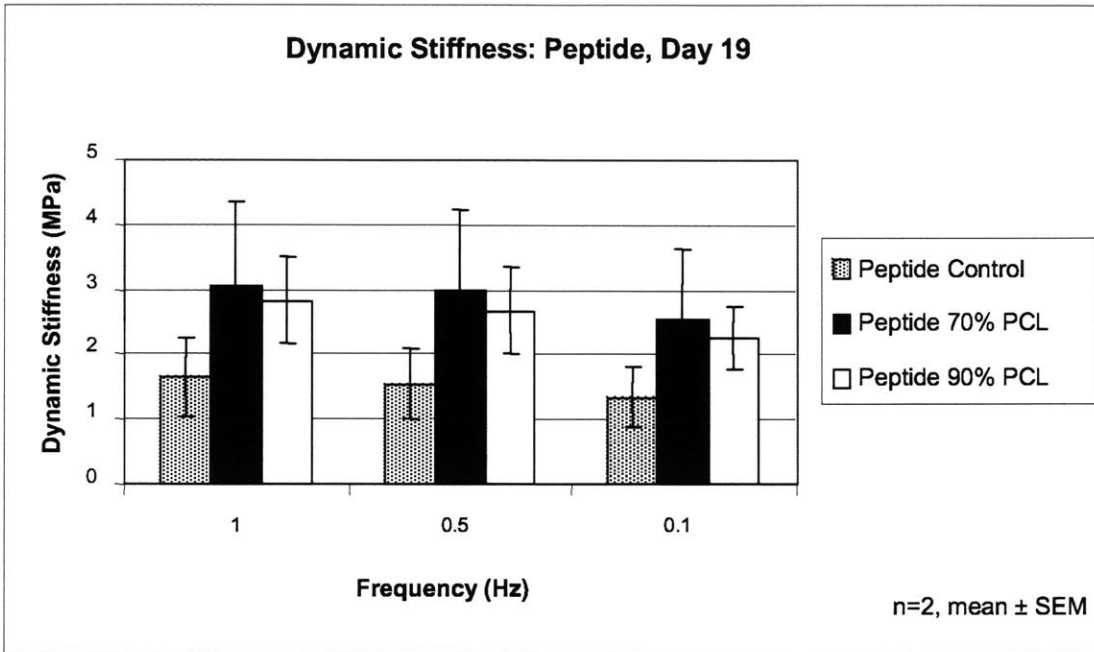
Figure 5.14 Mechanical properties of dynamically compressed chondrocyte-seeded peptide hydrogel on day 19 of culture.
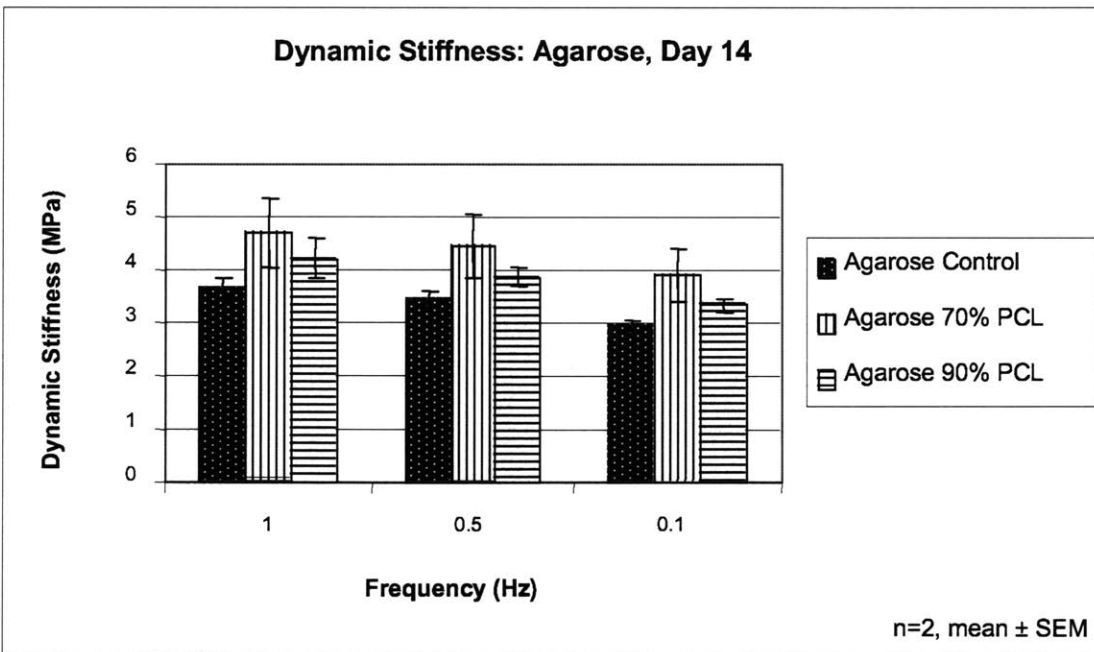

Figure 5.15 Mechanical properties of dynamically compressed chondrocyte-seeded agarose hydrogel on day 14 of culture. Dynamic stiffness was computed utilizing a dynamic strain amplitude of 0.2%. Poroelastic material properties of agarose hydrogel were displayed as dynamic stiffness decreased with decreasing frequency.
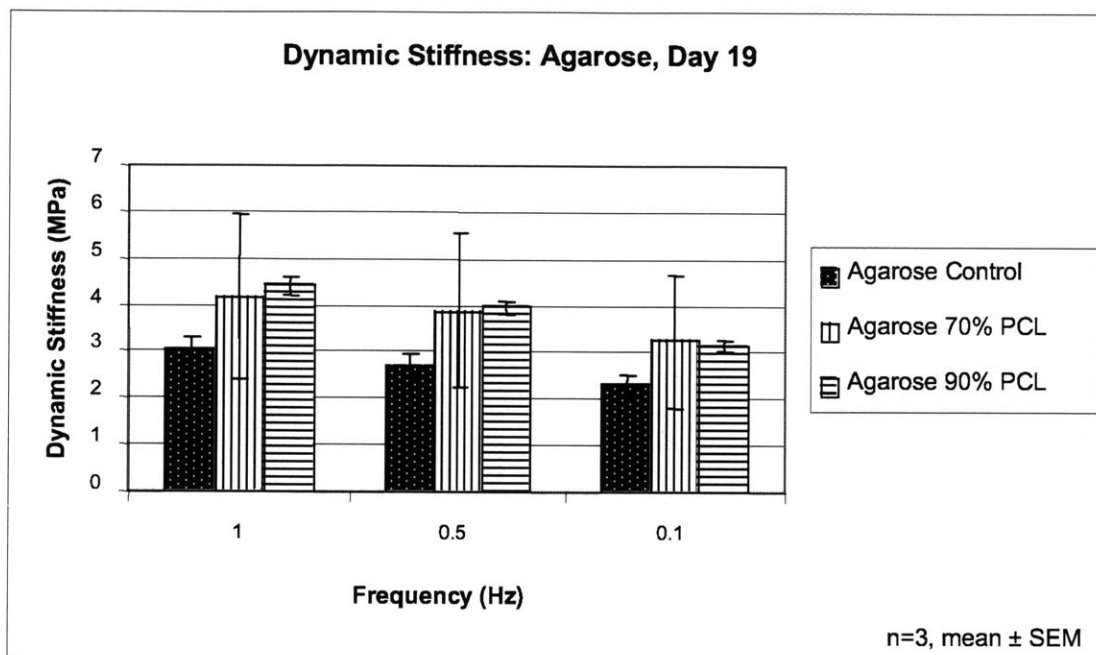
Figure 5.16 Mechanical properties of dynamically compressed chondrocyte-seeded agarose hydrogel on day 19 of culture. No marked distinction was apparent based on the integration of the agarose hydrogel with a porous PCL scaffold, or with respect to the variation in PCL microarchitecture.

The equilibrium modulus values of PCL samples cultured without an integrated chondrocyte-seeded hydrogel were measured as controls, shown in Figure 5.17. The 70% porous PCL samples displayed an equilibrium modulus of 796KPa, while that of the 90% porous PCL samples was lower at 371KPa. The equilibrium modulus of the 70% porous PCL samples integrated with the peptide hydrogel increased from 559KPa to 770KPa from day 14 to day 19 while that of the 90% porous PCL samples decreased from 438KPa to 320KPa. In the composites involving the agarose hydrogel, the equilibrium modulus of the 70% porous PCL samples decreased from 582KPa to 538KPa from day 14 to 19, while those involving the 90% porous PCL samples displayed an increase in moduli from 228KPa to 275KPa. The dynamic stiffness values of the PCL samples also appeared to be frequency dependent as they decreased with decreasing frequency, as is evident in Figure 5.18 and Figure 5.19.
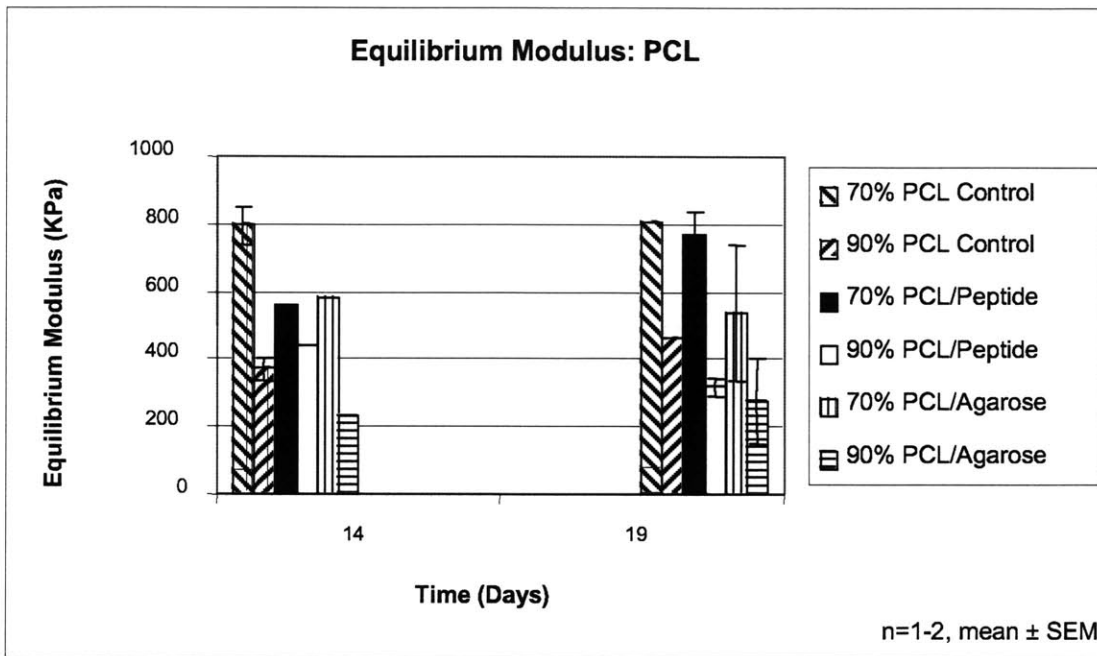
Figure 5.17 Mechanical properties of porous PCL scaffold. PCL controls were not integrated with a chondrocyte-seeded hydrogel. 70% porous PCL scaffolds, equating to 30% PCL polymer, possessed higher equilibrium moduli than 90% porous PCL scaffolds, equating to 10% polymer.

Figure 5.18 Mechanical properties of dynamically compressed porous PCL scaffold on day 14 of culture. Dynamic strain amplitude of 0.2% was utilized to remain consistent with mechanical testing of hydrogel materials.

Figure 5.19 Mechanical properties of dynamically compressed porous PCL scaffold on day 19 of culture.

5.3.5 Histological Analysis
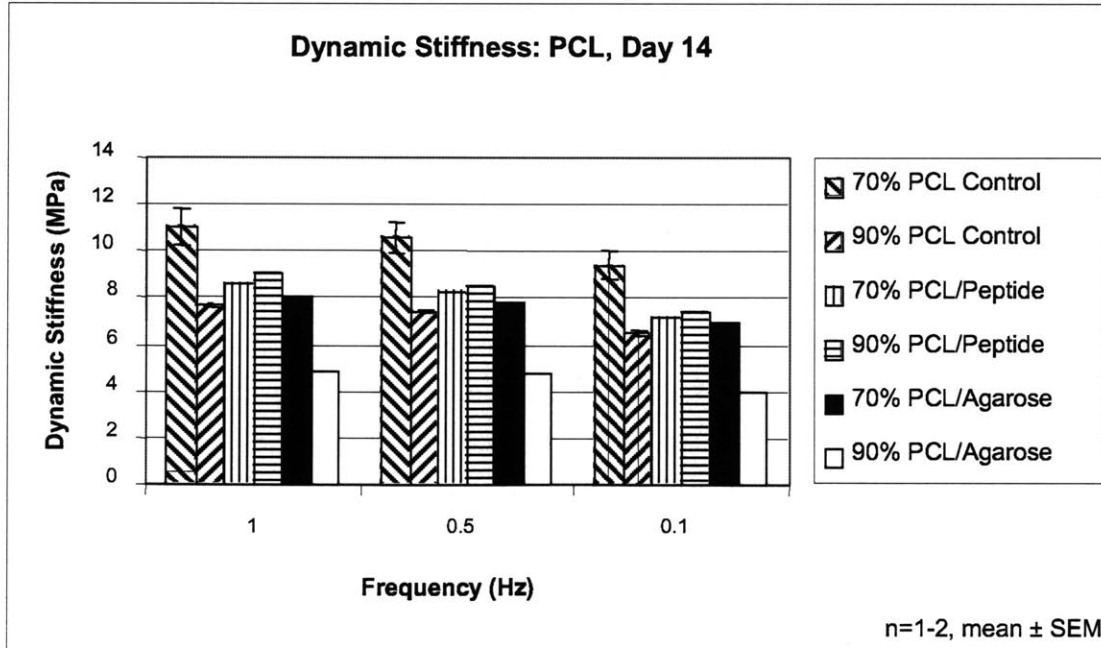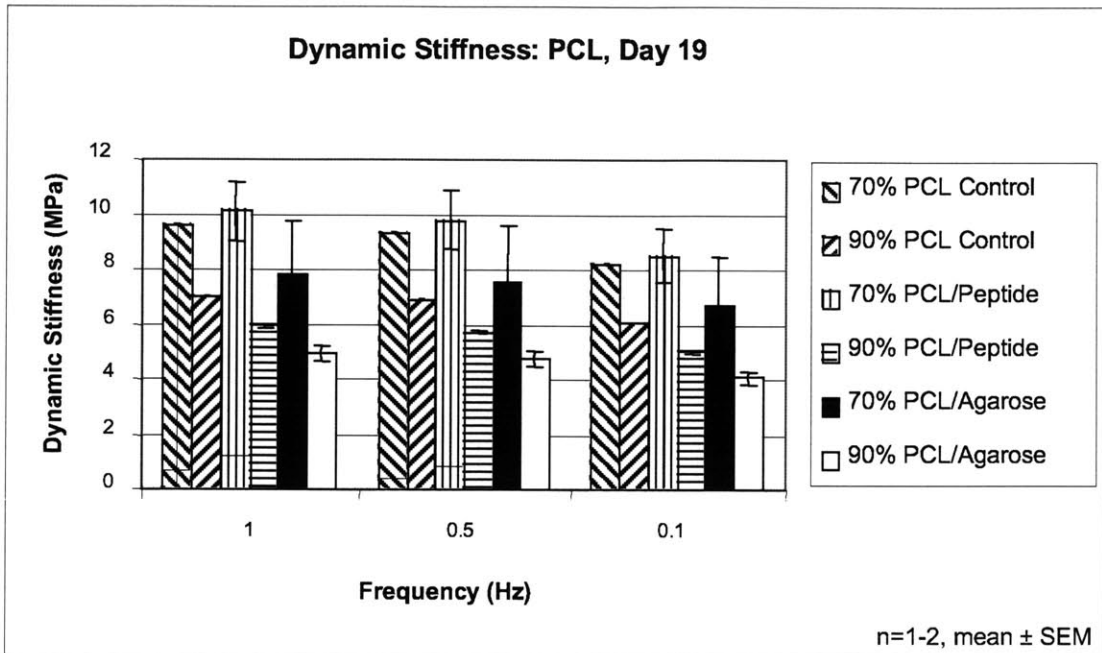
Histological analysis was performed to provide a visual and qualitative confirmation of the integration of the chondrocyte-encapsulated peptide solution into the porous PCL and to depict the development of ECM inside the pores of the PCL scaffold. Figure 5.20 depicts unstained PCL sections that were dry-mounted to provide a visual representation of the PCL scaffold architecture. Therefore, by comparing stained images to those of the unstained PCL sections, it is clear that the areas that have been stained with H&E or Toluidine Blue are within the interconnected porous regions of the PCL scaffolds and the surrounding network of lighter regions are the PCL polymer. H&E staining illustrates the integration of the chondrocyte-seeded peptide hydrogel into the PCL scaffold, with dark spots indicating the presence of chondrocyte nuclei as shown in Figure 5.21. Toluidine blue staining, which binds to proteoglycans, reveals the deposition of proteoglycans within the pores of the PCL scaffold, as illustrated in Figure 5.22. These images can be contrasted to those of the peptide hydrogel region of the composites. Both H&E and Toluidine blue staining of the hydrogel, as shown in Figure 5.23 and Figure 5.24, depict the cell and proteoglycan distribution in the peptide hydrogel. In contrast to the staining of PCL regions of the composite, these figures depict a dense and continuous network of cells and

88

proteoglycan accumulation. Therefore, the peptide hydrogel appears to be an appropriate choice of material for an osteochondral composite because it not only allows for a continuous deposition of matrix, but it also allows for integration into the porous PCL scaffold.
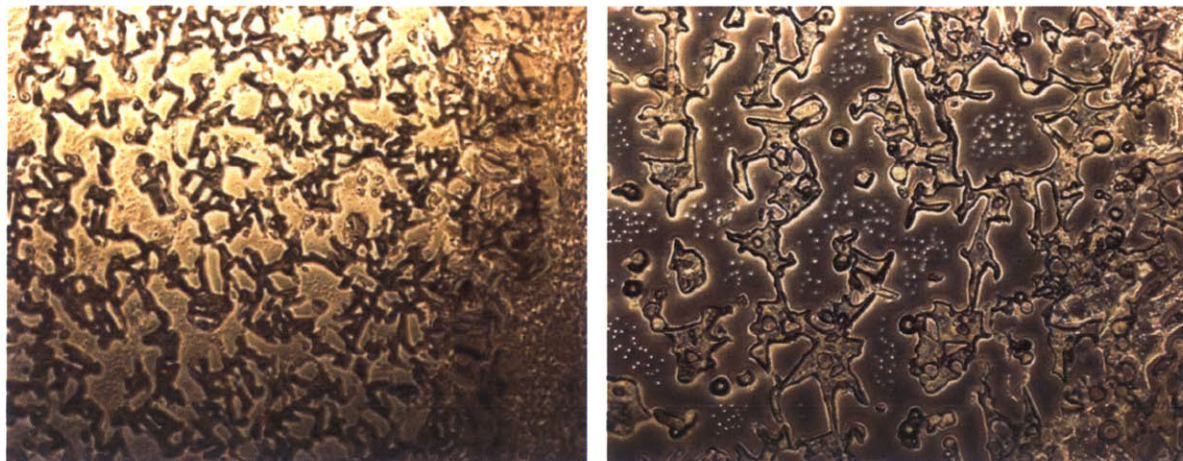
Figure 5.20 (a) Unstained 5μm PCL section from a 70% porous composite integrated with a chondrocyte-seeded peptide hydrogel, 4X. (b) Unstained 5μm PCL section from a 90% porous composite integrated with a chondrocyte-seeded peptide hydrogel, 10X. Both figures depict the microarchitecture and fully interconnected porous structure of the PCL scaffold.

Figure 5.21 5μm PCL section from a 90% porous PCL and chondrocyte-seeded peptide hydrogel composite, 10X. H&E staining done on day 19 of culture illustrates the integration of the chondrocyte-seeded peptide hydrogel into the pores of the PCL scaffold. The dark spots, nuclei of chondrocytes, within the pores of the PCL indicate the presence of chondrocytes.

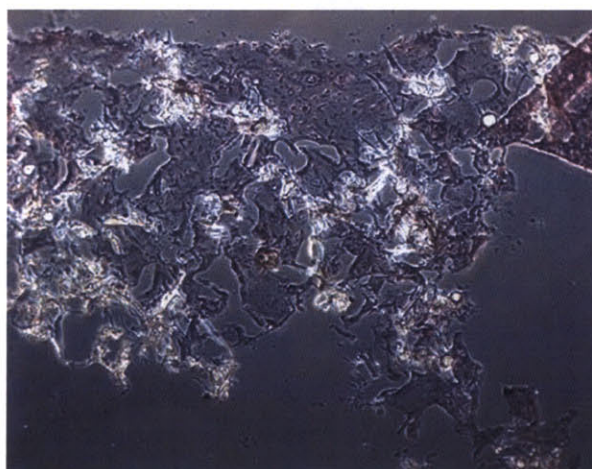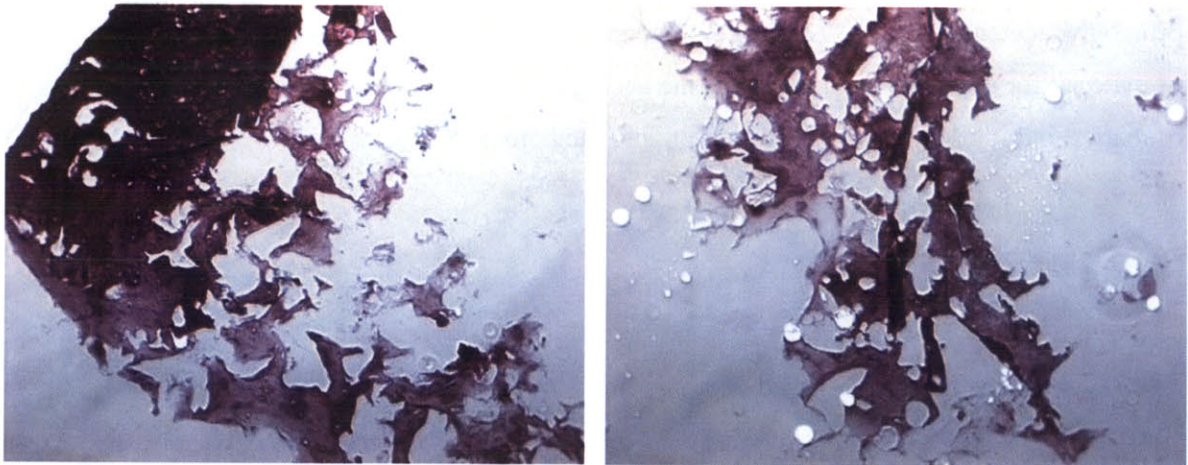Figure 5.22 Both figures depict PCL sections stained with Toluidine Blue to indicate the presence of proteoglycans on day 19 of culture. (a) 5μm PCL section from a 90% porous PCL and chondrocyte-seeded peptide hydrogel composite, 10X. Top dense region of Toludine Blue staining may indicate the presence of peptide hydrogel remnants on the superior surface of the PCL scaffold, while the staining at the edge indicates the presence of proteoglycan within the pores of the PCL scaffold. (b) 5μm PCL section from a 70% porous PCL and chondrocyte-seeded peptide hydrogel composite, 10X. Toludine Blue staining provides a qualitative assessment of the deposition of proteoglycans within the pores of the PCL scaffold.

Figure 5.23 (a) 5 μm section of the chondrocyte-seeded peptide hydrogel region of a composite consisting of a 90% porous PCL scaffold, 10X. H&E staining reveals the dense and homogenous distribution of chondrocytes within the peptide hydrogel on day 19. (b) 5 μm section of the chondrocyte-seeded peptide hydrogel region of a composite consisting of a 90% porous PCL, 20X.

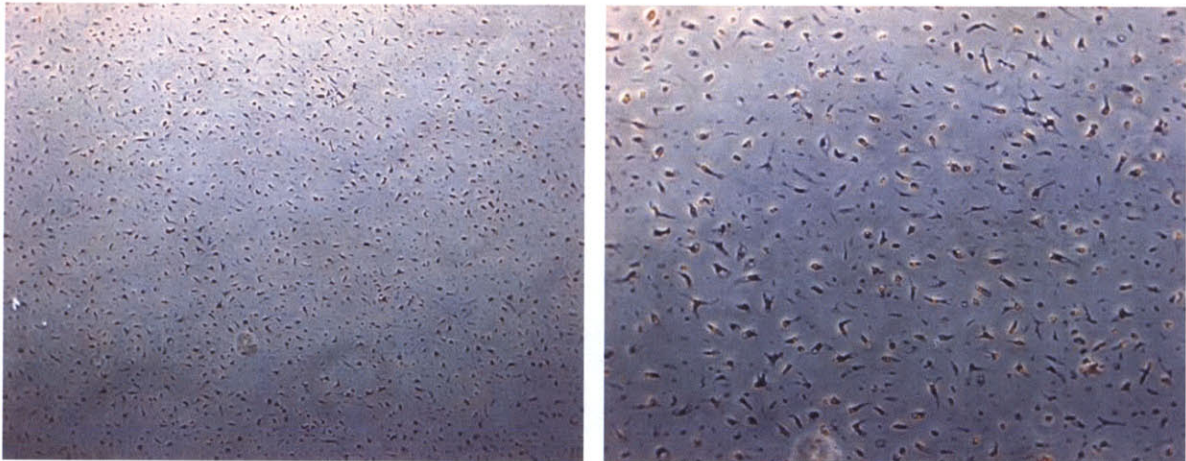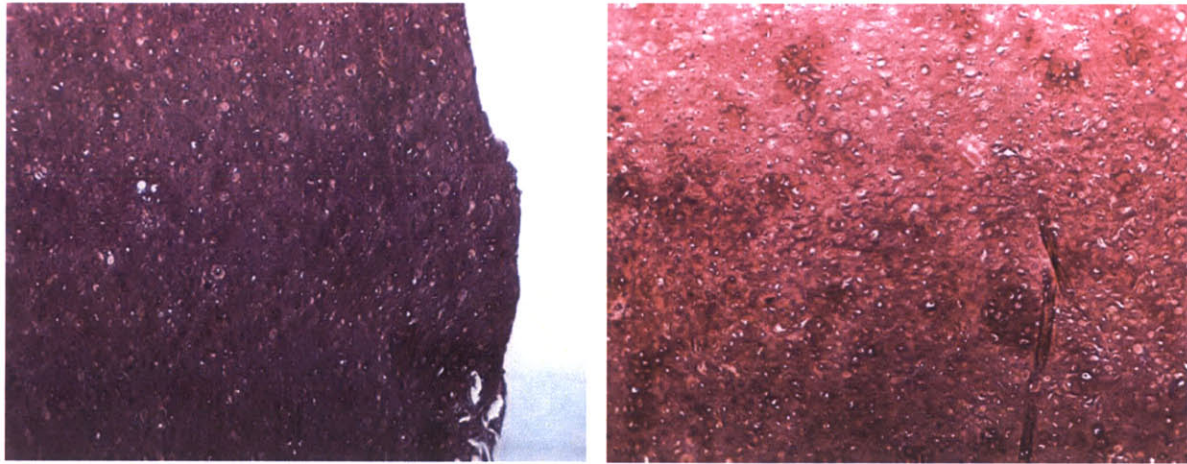Figure 5.24 (a) 5μm section of the chondrocyte-seeded peptide hydrogel region of a composite involving a 90% porous PCL scaffold, 10X. Toludine Blue staining on day 19 of culture reveals the dense and continuous proteglycan accumulation within the peptide hydrogel. (b) 5μm section of the chondrocyte-seeded peptide hydrogel region of a composite involving a 90% porous PCL scaffold, 20X.

5.3.6 SEMS

SEM images provide an effective means of visualizing the microarchitecture of the porous PCL scaffolds. The layer by layer fabrication process was represented in cross-section images. The interconnectivity of the microarchitecture, pore size, and distinctions in porosity level were also well characterized through these means. The cross-section images delineated the discrepancy in the dissolution process based on the porosity level. As seen in Figure 5.27, spherical beads were present throughout the cross-section of the samples. These beads are PCL particles that were not completely dissolved by chloroform during the printing process. The effect of porosity level on the dissolution process becomes evident when the cross-section images of the 70% porous PCL samples are compared to those of the 90% porous PCL samples, as seen in Figure 5.30. Because of a 20% reduction in the concentration of PCL in the printing powder mixture, these undissolved spherical beads were absent in the cross-section images of the 90% porous PCL samples. However, the higher concentration of void space in these 90% porous PCL samples hindered the sectioning capacity of the scaffolds. Therefore, the pores in the images of the 90% porous PCL samples appeared to be slightly more collapsed than those seen in the 70% porous PCL scaffold images.
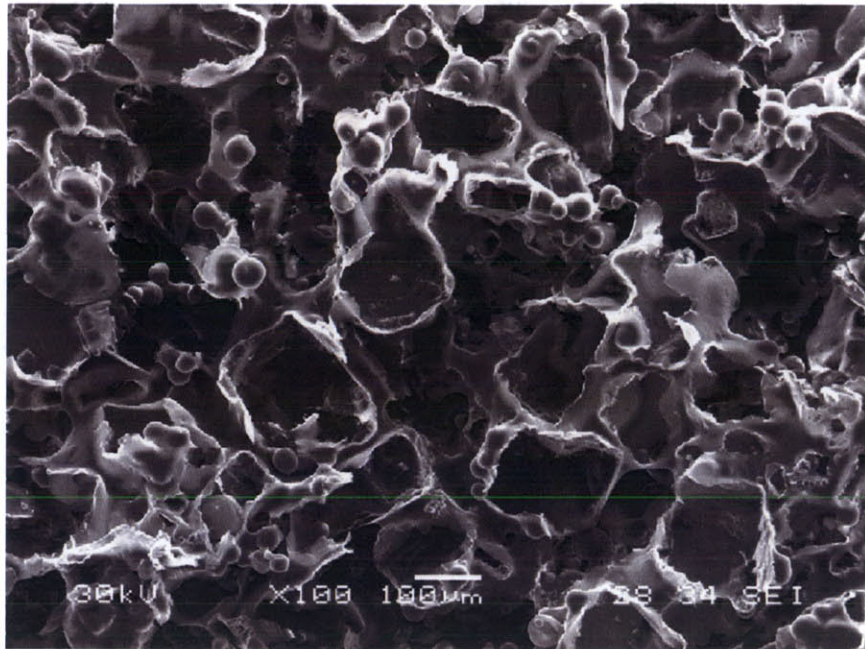
Figure 5.25 SEM image of 70% porous unseeded PCL scaffold with 108μm - 150μm pore size. Top-down view at 100X magnification.
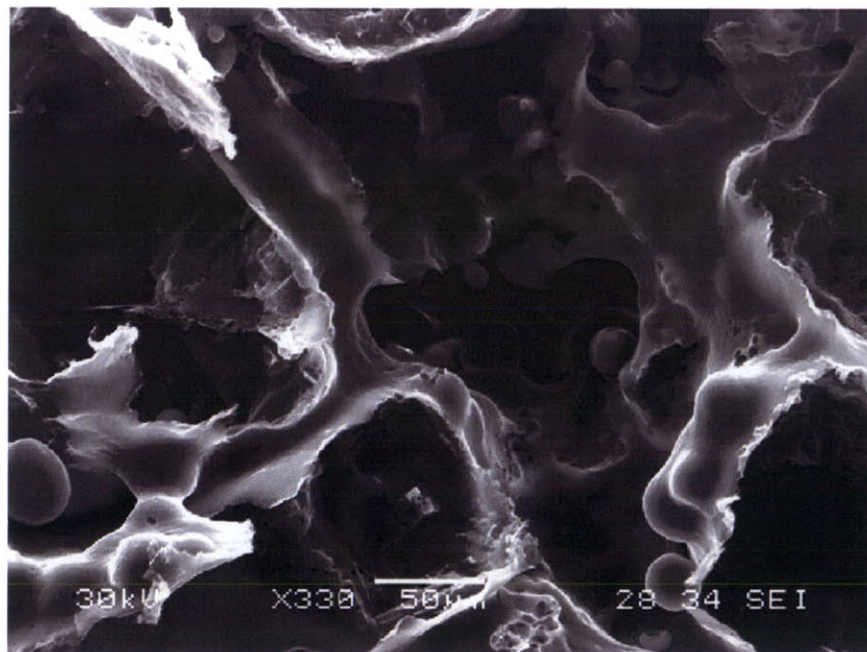
Figure 5.26 Higher magnification SEM image of 70% porous PCL scaffold from top-down view. Fully interconnected scaffold architecture is depicted in this image at 330X magnification.
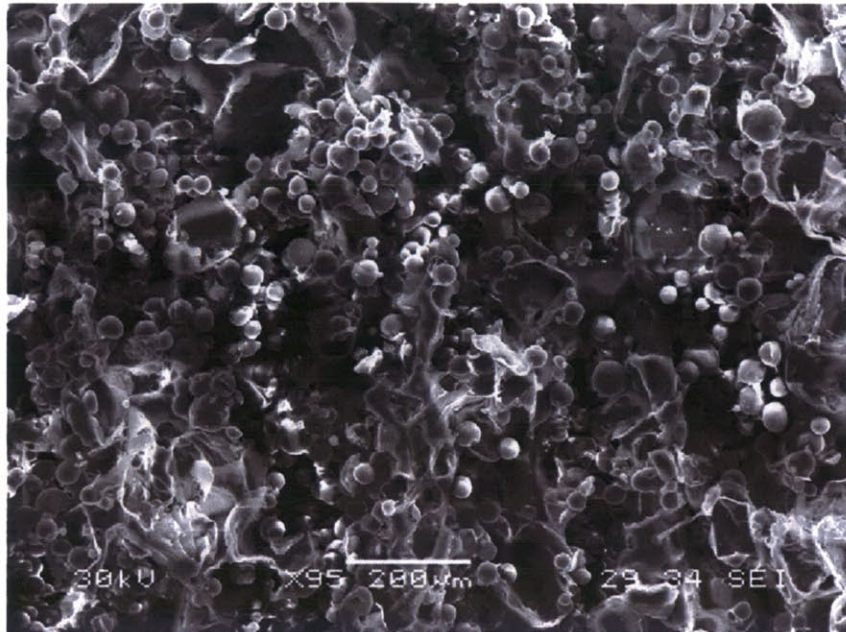
Figure 5.27 Cross-section SEM image of 70% porous PCL scaffold at 95X magnification. Incomplete dissolution of PCL particles due to 30% polymer concentration are depicted as spherical beads throughout the cross-section of the scaffold.
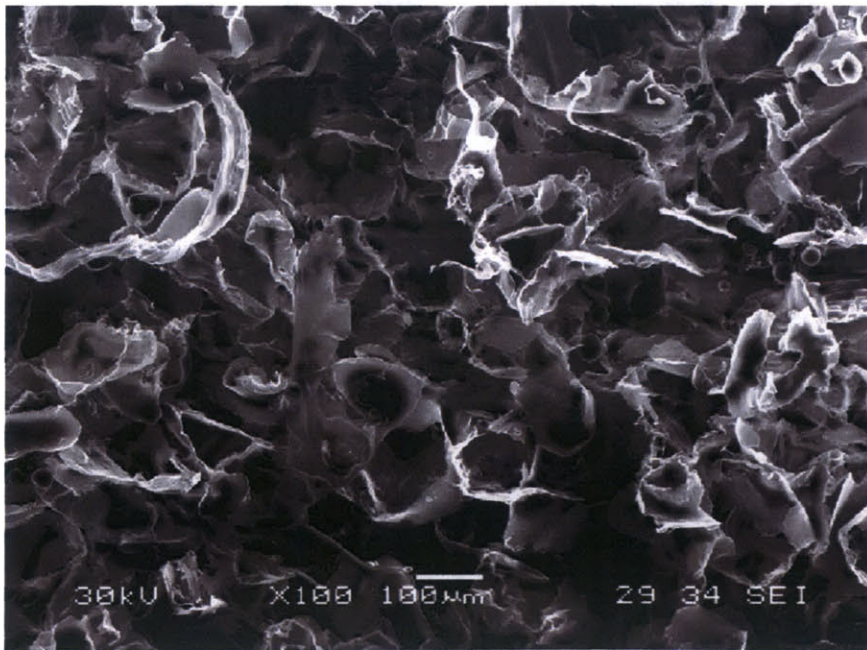
Figure 5.28 SEM image of 90% porous unseeded PCL scaffold at 100X magnification from top-down view.
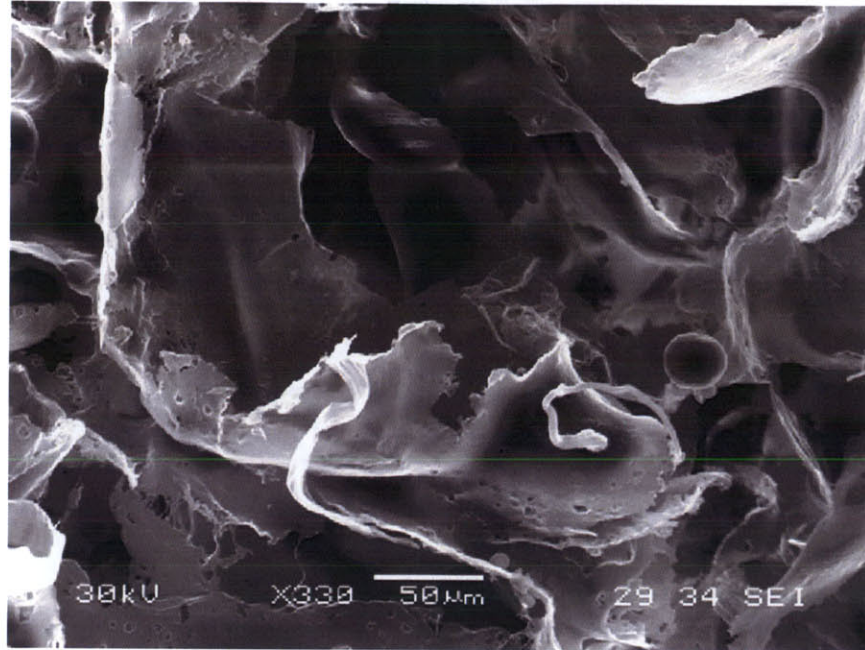
Figure 5.29 Higher magnification (330X) image of 90% porous PCL scaffold from top-down view.
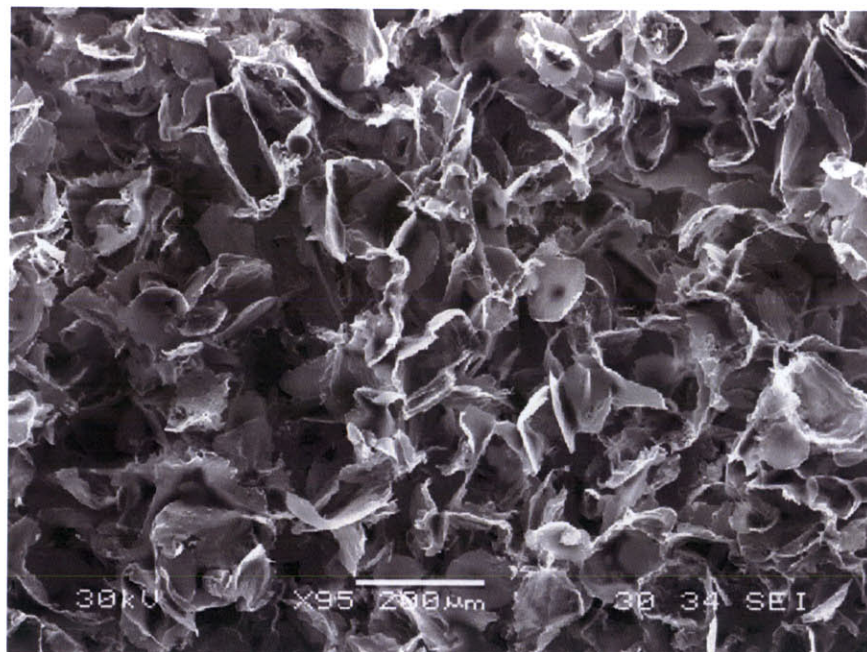
Figure 5.30 SEM image of 90% porous PCL scaffold at 95X magnification. Inherent challenges in sectioning scaffold of such high porosity are evident in the appearance of collapsed void space throughout the cross-section.

94

5.4 Discussion

The characterization of the osteochondral composites through biochemical, mechanical, and histological means allowed for the validation of the studies presented in Chapter 4 and further probed the effect of PCL microarchitecture on chondrocyte viability and behavior. The introduction of the agarose hydrogel as an analogous component in the osteochondral composite provided a reference scale to which chondrocyte behavior in the peptide hydrogel could be compared. Integration of a chondrocyte-seeded hydrogel into a porous PCL scaffold did not appear to adversely affect chondrocyte behavior in the hydrogel region. Whether or not the PCL microarchitecture affects chondrocyte behavior in the hydrogel region of the composite appears to be dictated by the choice of hydrogel material. The porosity of the PCL scaffold had a more pronounced impact on chondrocyte biosynthesis in the cell-seeded peptide hydrogel than in the cell-seeded agarose hydrogel. The effect of PCL microarchitecture may be more prominent in the composites consisting of the peptide hydrogel because of the lowered concentration of the peptide suspension used, 0.36% as opposed to the 2.0% concentration of the agarose hydrogel, or may be a result of distinct material property differences between the two hydrogels.

Monitoring the cell viability of these osteochondral composites throughout the time course of the study indicated that the initial cell viability was slighter lower than expected when compared to previous studies utilizing the MTS assay. This slight discrepancy in cell viability may be a result of the quality of the peptide powder used in this study. Cell viability appeared to be relatively comparable when comparing the two distinct hydrogels, peptide and agarose. When investigating the impact of the PCL porosity on chondrocyte viability in the hydrogel region of the composite, statistical analysis indicated that only the composites involving the peptide hydrogel showed a significant distinction in cell viability as a result of this variable.

Matrix accumulation, as indicated by GAG content, also displayed a dependence on hydrogel material regarding the effect of PCL microarchitecture. Statistical analysis indicated that GAG accumulation in the hydrogel region of composites involving a chondrocyte-seeded peptide hydrogel was affected by PCL porosity. However, matrix accumulation in the agarose region of these composites appeared to be independent of the porosity of the underlying PCL scaffold. The choice of hydrogel material, peptide versus agarose, displayed negligible effects on both the magnitude and trend of the overall GAG content throughout the time course of the study. An increase in GAG content with respect to time, as expected, was apparent in each type

of composite. The porosity of the PCL scaffold also had a significant impact on GAG accumulation within the PCL region of the composite, however only in composites consisting of the peptide hydrogel. An increase with respect to time in measured GAG content was also observed in this region of the composites.

Radiolabel incorporation, which is indicative of chondrocyte biosynthesis rates, was also investigated. Proline incorporation rates in the hydrogel region of these composites, involving either a peptide hydrogel or agarose hydrogel, appeared to be slightly lower on day 6 than expected based on previous studies. A more distinct drop in proline incorporation rates is usually evident from day 6 to day 14 of a time course. However, the proline incorporation rates in this study appeared to be relatively constant throughout the duration of the time course, independent of the type of composite investigated. This decreased initial magnitude of proline incorporation rates may be linked to the slightly lower cell viability that was evident in both types of composites. Similar to the trends observed in GAG content, the porosity of the PCL scaffold produced a significant impact on proline incorporation rates only in the hydrogel region of composites involving the peptide hydrogel. PCL porosity did not appear to have an effect on proline incorporation into the PCL region of the composite, regardless of the hydrogel material used. This observation may be linked to the relatively large standard errors of these mean values and the relatively small magnitude of the proline incorporation rates for these samples.

Unlike the proline incorporation rates, the sulfate incorporation rates in the hydrogel regions of the composites displayed a slightly more distinct decrease in magnitude from day 6 to day 14, as expected. Sulfate incorporation rates in both the agarose and peptide hydrogel regions of these composites appeared to be dependent on the PCL microarchitecture. Sulfate incorporation rates in the porous PCL region were similar in behavior to the proline incorporation rates of this region, as they were not significantly affected by PCL porosity. Again, this statistical assessment may be a result of the size of the standard errors of the mean values and the magnitude of the mean values.

Mechanical characterization of the samples is also crucial to their viability as osteochondral composite materials. Consistent with the previously described biochemical characterizations of these materials, porosity of the PCL scaffold did not appear to impact the mechanical properties of the hydrogel material. However, an unexpected result was the slight decrease in equilibrium moduli of the hydogel materials from day 14 to day 19. This slight

96

decrease in equilibrium moduli from day 14 to day 19 may be associated with either the sample variation on day 14, or the slightly lowered sulfate incorporation rates. As would be expected due to the higher amount of polymer, the 70% porous PCL samples displayed higher equilibrium moduli than the 90% porous PCL samples, regardless of the choice of hydrogel material.

The calculation of the dynamic stiffness values revealed the need for further investigation into this means of characterizing a material. The objective of the data presented in Section 5.3.4 is one of relative analysis only. Dynamic stiffness values in this section appeared to be higher than those presented in Section 4.3.4 which may be a reflection of the change in the dynamic strain amplitude. The dynamic strain amplitude of the mechanical tests performed in Section 4.3.4 was 1.0%; however, those performed in Section 5.3.4 were at 0.2% dynamic strain amplitude. Strain amplitude was decreased to prevent lift off during dynamic compression and to eliminate harmonic distortion that was present at the 1.0% strain amplitude due to the softness of the hydrogel material. Therefore, a comprehensive study investigating the dynamic stiffness of a hydrogel material at a wide range of frequencies and dynamic strain amplitudes is necessary to determine the optimal testing parameters for a given material. Despite the inability to compare the magnitude of this data across studies, valid comparisons can be drawn within this study. The dynamic stiffness values of the peptide hydrogel samples and the agarose hydrogel samples can be compared to clarify the effect of hydrogel material selection. The effect of culture of a chondrocyte-seeded hydrogel that has been integrated into a porous PCL scaffold can also be investigated by assessing the dynamic stiffness values of hydrogel only control sheets with those of the corresponding hydrogel and PCL composites. Within a given set of data, the effect of PCL microarchitecture on the dynamic stiffness values of the corresponding hydrogel region or PCL region can be examined by comparing the values of composites consisting of 70% porous PCL scaffolds to those consisting of 90% porous PCL scaffolds. Therefore, dynamic stiffness values of the hydrogel region of composites involving the peptide hydrogel and those involving the agarose hydrogel appeared to be independent of the hydrogel material selection. The effect of the presence of PCL on the dynamic stiffness of the peptide hydrogel region of these composites can be assessed by comparison to the control chondrocyte-seeded peptide hydrogels that lacked an underlying PCL scaffold. The dynamic stiffness of the peptide hydrogel samples cultured on PCL in composite form appeared to be higher than the peptide hydrogel control samples. This observation may also be a reflection of the quality of the control sheet. The peptide hydrogel

control sheet possessed a high concentration of air bubbles upon gelation, and the stiffness of this control sheet did not increase in the same manner as that of the hydrogel of the composite samples. In composites involving an agarose hydrogel region, dynamic stiffness of the chondrocyte-seeded agarose hydrogel control sheets were slightly lower than those cultured on the PCL scaffolds. Therefore, the presence of PCL does not appear to have any adverse effects on the compressive integrity, or matrix accumulation, of the chondrocyte-seeded hydrogel region. Furthermore, an analysis with respect to the porosity of the PCL scaffold indicated that dynamic stiffness of the peptide or agarose hydrogel region of the composite was independent of the PCL porosity level. The dependence of dynamic stiffness on porosity level was portrayed in the mechanical testing of the samples retrieved from the PCL scaffold region of the composite. As would be expected, porosity does affect stiffness values, as 70% porous PCL samples possess 20% more PCL polymer than the 90% porous PCL samples. Therefore, the stiffness values of the 70% porous PCL scaffolds were higher than those of the 90% porous PCL scaffolds.

The ultimate objective of the osteochondral composite is a significant issue to consider for the selection of the final composite materials and parameters. As stated in Section 2.11 the overall design of the osteochondral composite consists of a hydrogel region integrated into a porous PCL scaffold that possesses a gradient of porosity. The hydrogel material will serve as a cartilage substitute, the top porous region of the PCL scaffold functions to integrate the hydrogel and PCL scaffold, and the lower porous region of the PCL scaffold serves as a bone substitute material with appropriate microarchitecture. For this purpose, the peptide hydrogel would be the material of choice because of its superior integration into the porous PCL scaffold observed throughout the duration of culture time. Although the biochemical characterizations may portray slightly superior chondrocyte behavior in the hydrogel region of composites involving the agarose hydrogel than the peptide hydrogel, these slight increases may be a result of the quality of the specific batch of peptide used in this study. Furthermore, poor integration of the chondrocyte-seeded agarose hydrogel into the porous PCL scaffold hinders the efficacy of the overall osteochondral composite in terms of integration and anchorage of the individual materials.

98

Chapter 6: Summary and Future Work

6.1 Summary

The aim of these studies was to create a novel osteochondral construct, consisting of a chondrocyte-seeded self-assembling peptide hydrogel and an interconnected porous 3DP™ PCL scaffold. Although the procedure for casting KLD-12 peptide into chondrocyte-seeded hydrogel slabs had been developed and optimized by Kisiday et al., there were many challenges to overcome in order to integrate this material with a porous PCL scaffold to form an osteochondral composite. Therefore, a means of casting the molten peptide onto and into the cylindrical PCL cores in a controlled and repeatable manner that would result in the integration of the two materials was investigated. An agarose mold in which the peptide could be cast directly onto the PCL core was conceived and implemented as an effective means of addressing these issues. The concentration of agarose utilized to create this mold, as well as the optimal geometry, were significant issues to address because of their potential effects on chondrocyte viability, and diffusion and transport of nutrients to the chondrocytes.

The effects of a PCL scaffold on chondrocyte viability, phenotype, and behavior both in the peptide hydrogel and the PCL scaffold were critical components to study in order to prove the efficacy of such a composite. PCL was chosen as the underlying scaffold material because it is bioresorbable and biocompatible. Studies have shown that both osteogenic and chondrogenic cells attach, migrate, and develop cell-specific ECM in PCL scaffolds, thereby indicating its potential as an ostechondral scaffold material [17]. The advantage of the 3DP™ technology is the ability to control the microarchitecture of the PCL scaffold and to create a multi-layer design [39]. Porosity of the PCL scaffold material was varied to investigate the effects of PCL scaffold microarchitecture on chondrocyte behavior. The interconnected porous structure of this material allows for nutrient transport and cell migration into the scaffold. The depth of infiltration of the peptide hydrogel into the PCL can be controlled by varying the porosity of the scaffold. The ultimate PCL scaffold design consists of a porous top region, a solid or very small pore size thin middle region, and a porous bottom region. The porous top region will allow for peptide infiltration down to the solid region, while the bottom region will contain pores of the optimal size for bone ingrowth.

These studies indicated the viability of a chondrocyte-seeded peptide hydrogel and an inter-connected porous PCL composite. The self-assembling peptide hydrogel has been shown to provide an environment that maintains chondrocyte phenotype and viability. Furthermore, the 3D scaffold fosters extracellular matrix production and chondrocyte division [22]. This choice of material selection for the cartilaginous region of the osteochondral composite was compared to a more traditional hydrogel material, agarose, commonly used to investigate chondrocyte behavior. The peptide hydrogel material proved to be superior in terms of integration into the porous PCL scaffold when compared to the agarose hydrogel.

Through various means of characterization, including biochemical, mechanical, and histological analyses, this osteochondral composite has been shown to maintain chondrocyte phenotype, viability, and biosynthesis rates analogous to those seen in the chondrocyte-seeded peptide hydrogel only systems. Biochemical anlaysis provided insight into the biosynthesis rates of the chondrocytes by evaluating extracellular matrix production and total protein content. Mechanical analysis characterized the compressive properties of the individual components of the composite over time. Histological analysis provided a visual representation of the integration of the cell-seeded peptide solution into the PCL scaffold, the presence of cells within the interconnected porous network of the PCL, and the deposition of proteoglycan within the pores of the PCL scaffold. Therefore, the PCL scaffold does not impose any adverse effects on chondrocyte behavior.

The effect of the PCL scaffold microarchitecture was investigated by studying two distinct porosities, 70% porous and 90% porous PCL. Whether or not the PCL microarchitecture affects chondrocyte behavior in the hydrogel region of the composite appears to be dictated by the choice of hydrogel material. Porosity level of the PCL scaffold produced a more pronounced impact on chondrocyte biosynthesis in the cell-seeded peptide hydrogel than in the cell-seeded agarose hydrogel. The microarchitecture of the PCL scaffold had less of an impact on chondrocyte behavior in the agarose hydrogel because this material behaved more as a separate entity, as indicated by its poor integration into the PCL scaffold. In order to optimize the efficacy of an integrated osteochondral composite, a chondrocyte-seeded peptide hydrogel region appears to be a more effective choice of hydrogel material, while simultaneously maintaining chondrocyte viability, matrix accumulation, biosynthesis rates, and mechanical properties analogous to chondrocyte-seeded hydrogels created without an underlying PCL scaffold.

6.2 Future Work

There are many future directions that can be pursued based on this study. Along with seeding the peptide hydrogel with chondrocytes, the bone scaffold material can also be seeded with osteoblasts. Another consideration is to seed the entire osteochondral composite with one cell type, such as stem cells, and to induce differentiation into chondrocytes and osteoblasts for each respective region. This differentiation may require the use of growth factors to create the appropriate environment in each region. Shear mechanical testing can also be performed between the two layers of the construct to assess the magnitude of the attachment forces between the two materials. The biomechanical properties of the implanted composite scaffold would also have to be comparable to those of the natural surrounding tissues. This area of research can be further expanded by investigating the stimulatory or inhibitory effects of various combinations of compressive and shear mechanical loading. On another level, the effects of mechanical loading can also be described through its impact on gene expression. Furthermore, in vivo studies would allow for the analysis of integration of the osteochondral composite into native cartilage and bone in the physiological environment. This research topic depicts the vastness of tissue engineering and its broad scope of potential impacts because of the various directions through which it can be pursued.

Appendix A: Culture Medium Investigation

An investigation into the choice of culture medium was carried out to assess the effectiveness of DMEM and its supplements. Kisiday et al. delineated the efficacy of DMEM supplemented with 0.2% FBS and 1% ITS in the culture of chondrocyte-seeded peptide hydrogels [23]. These supplements were chosen, as opposed to the more traditionally used 10% serum medium, to prevent surface de-differentiation and fibrous capsule formation. However, the studies presented in this section explored the use of F12, as opposed to DMEM, and its effects on chondrocyte behavior in an agarose hydrogel.

F12 was originally developed for the serum-free clonal growth of Chinese Hamster Ovary (CHO) cells, lung cells, and mouse L-cells. It is the medium of choice for supporting the growth of cells of rodent origin. Due to the lack of serum in this medium, F12 is often supplemented with dialyzed serum, hormones, selenium, and other supplements frequently used in conjunction with serum-free cultures. This medium lacks L-glutamine, and has much lower sulfate content than DMEM.

Primary chondrocytes were seeded into 2% agarose hydrogels using the stainless steel frame, as described earlier, to produce hydrogels of a slab-like geometry. 12mm plugs were punched from the hydrogel sheets and cultured in two groups, DMEM and F12, for time points of 5, 10, 15, and 21 days. The supplements for both groups included 1% ITS, 0.2% FBS, 0.4% proline, 1.0% PenStrep, and 4μl/mL ascorbate added at the time of medium change every other day. The samples were characterized biochemically for DNA content, GAG content, and biosynthesis rates, as well as mechanically for material properties.

In the DMEM cultured sample group, the maximum cell number attained was 50,000 cells when normalized to the wet weight of 3mm plugs, however F12 samples displayed a maximum of only 33,500 cells. A 50% increase in cell number over the 21 days of culture was observed in the DMEM group, but there was only a 12% increase seen in the F12 group.
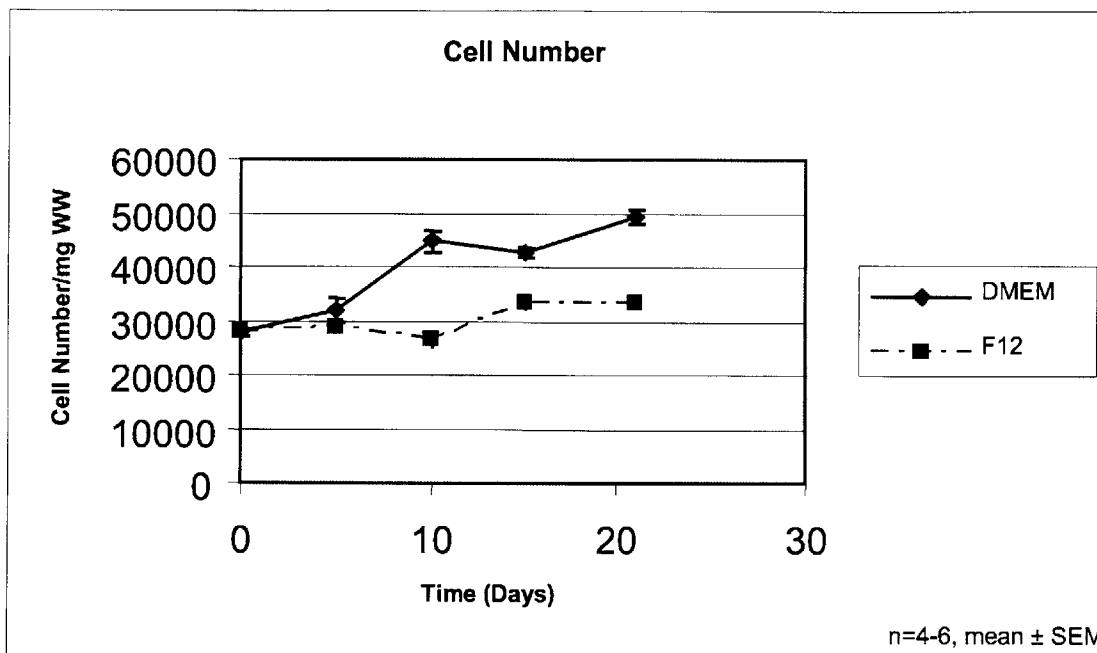
Figure A.1 Cell number in agarose hydrogel. Hoechst dye analysis quantified DNA content in chondrocyte-seeded agarose hydrogels. 50% increase in cell number was evident in DMEM-cultured samples, while only a 12% increase was observed in cell number of the F12-cultured samples.

Although the increase in GAG content from day 10 to day 21 appeared to be comparable between the two groups, there was a much larger increase in GAG content over the first 10 days of culture in the DMEM group than in the F12 group. This discrepancy led to a two-fold increase in GAG content in DMEM samples on day 21 when compared to the F12 samples. Radiolabel incorporation provided insight into the biosynthesis rates of the chondrocytes. The proline incorporation rate, indicative of protein synthesis, was lower in the F12 group than the DMEM group throughout the time of culture. Sulfate incorporation rates, indicative of sulfated proteoglycan synthesis, was higher in F12 than in DMEM samples. The information provided by the sulfate incorporation rates conflicts with the fact that GAG content was consistently higher in DMEM samples than in F12 samples, unless there is an underlying mechanism of GAG loss to the medium. The data provided by the DMMB assay is a measure of total GAG content at any given time, which accounts for synthesis and loss of GAG. If synthesis rates in the F12 samples are higher and yet the measured GAG accumulation is less, a valid hypothesis would be that there is higher GAG loss to the medium in the F12 samples than in the DMEM samples. Mechanical testing of the samples on day 21 corroborates the data provided by the DMMB

104

assay. The average equilibrium modulus of the DMEM samples, 27kPa, was three-fold higher than that of the F12 samples, 9.1kPa.
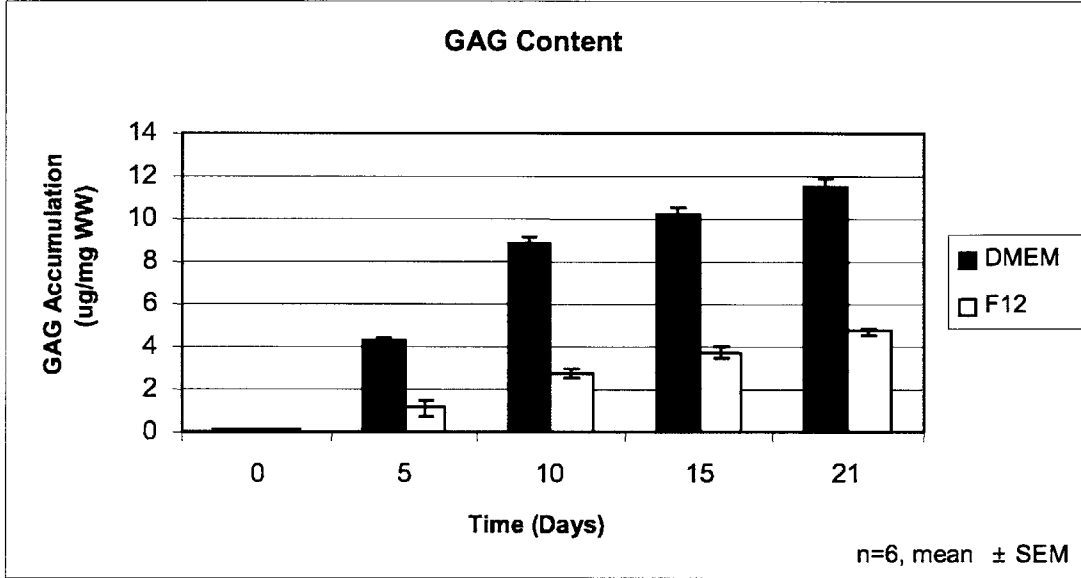
Figure A.2 GAG accumulation in chondrocyte-seeded agarose hydrogel. Marked increase in GAG content in DMEM-cultured chondrocyte-seeded agarose hydrogels than in F12-cultured chondrocyte-seeded hydrogels.
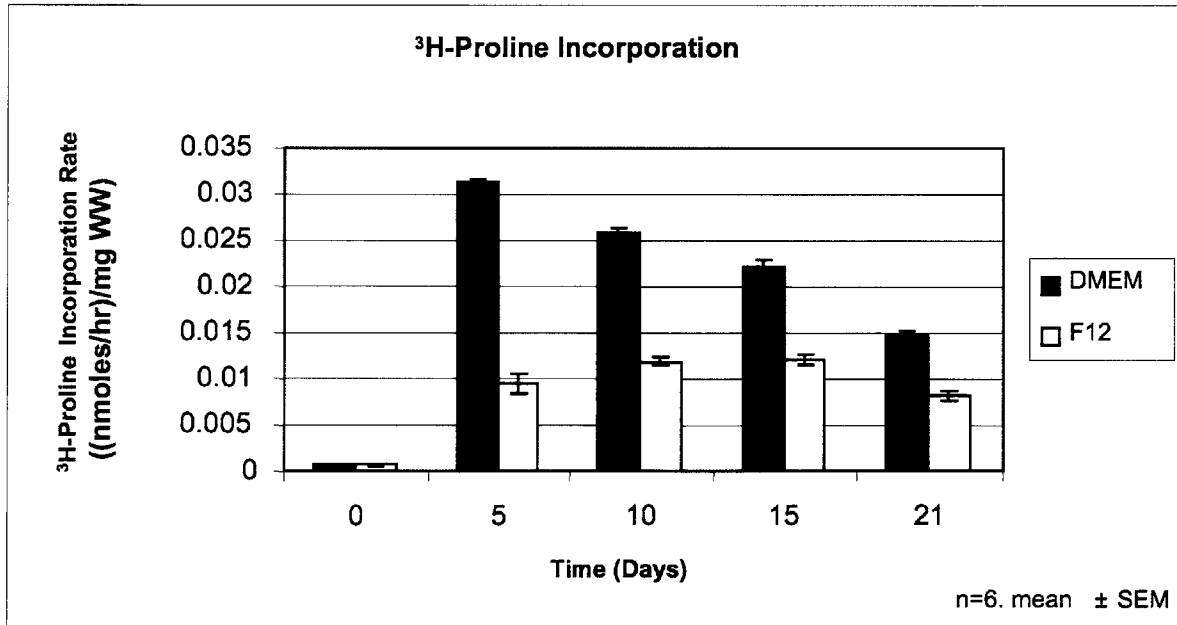

Figure A.3 Chondrocyte biosynthesis in agarose hydrogels. Discrepancies in ^{3}H-proline incorporation rates are indicative of differences in protein synthesis in chondrocyte-seeded agarose hydrogels based on the culture medium choice.

35S-Sulfate Incorporation
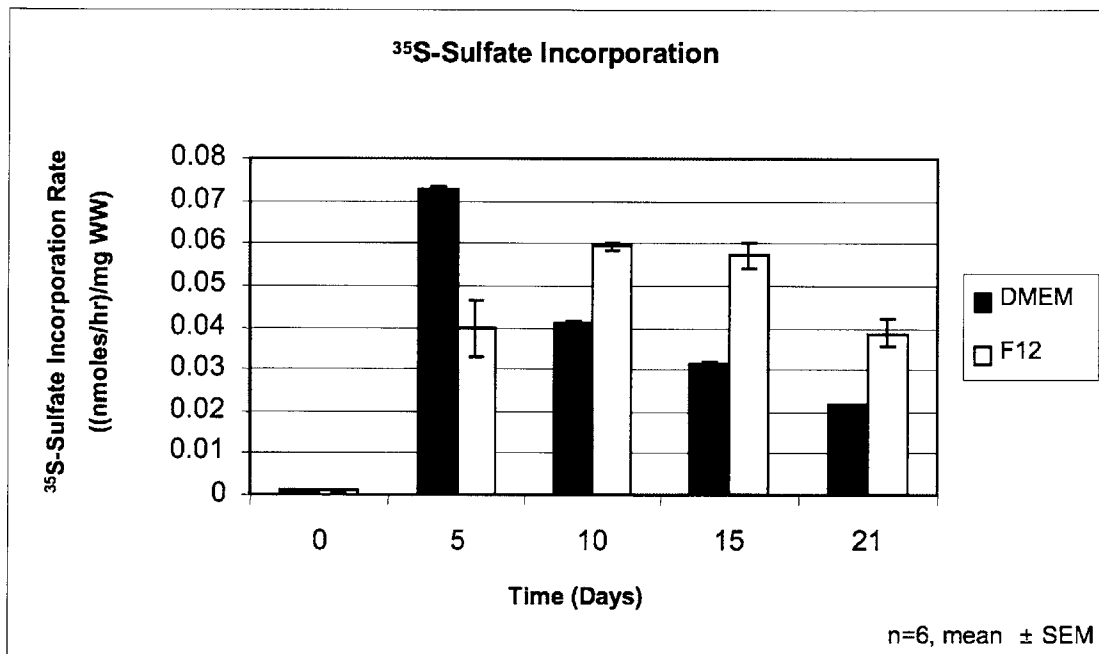
Figure A.4 Chondrocyte biosynthesis in agarose hydrogel. ^{35}S-sulfate incorporation rates, indicative of sulfated proteglycan synthesis, appear to be higher in F12-cultured chondrocyte-seeded agarose hydrogels than DMEM-cultured chondrocyte-seeded agarose hydrogels at later time points.

Equilibrium Modulus

Figure A.5 Mechanical properties of chondrocyte-seeded agarose hydrogel. Mechanical testing of 3mm plugs was performed in uniaxial confined compression. Equilibrium modulus was computed as the ratio of the relaxed equilibrium stress to the engineering strain for compressive strains of 5% to 18%. Despite lower ^{35}S-

sulfate incorporation rates in the DMEM-cultured agarose hydrogels, these samples possessed higher equilibrium moduli than the F12-cultured chondrocyte-seeded agarose hydrogels.
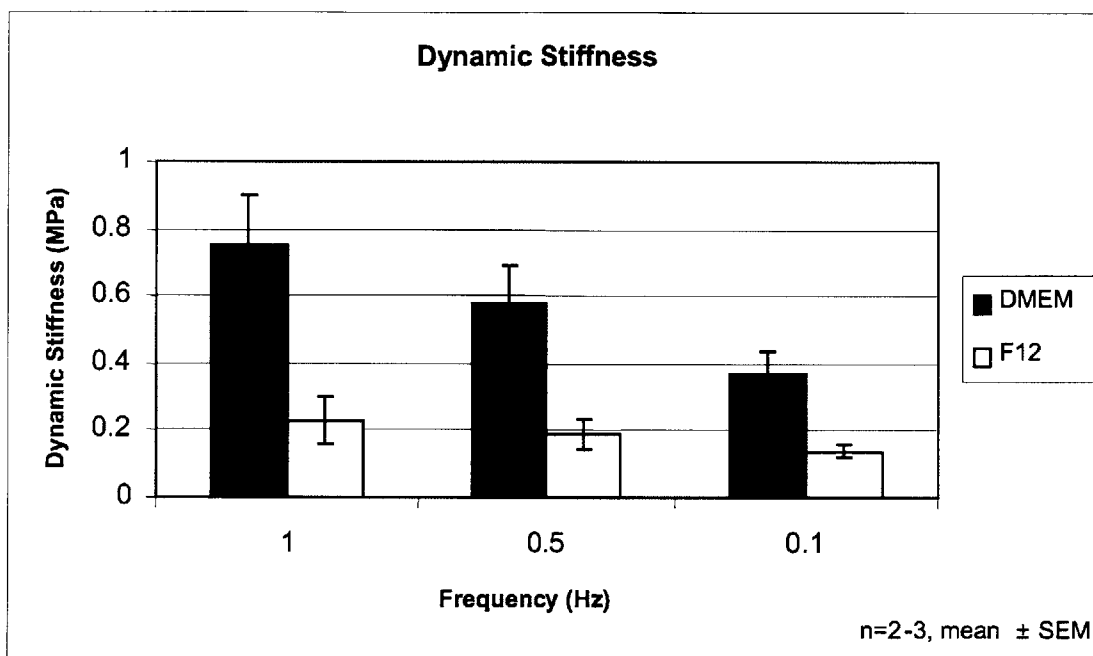
Figure A.6 Mechanical properties of dynamically compressed chondrocyte-seeded agarose hydrogel on day 21 of culture. Dynam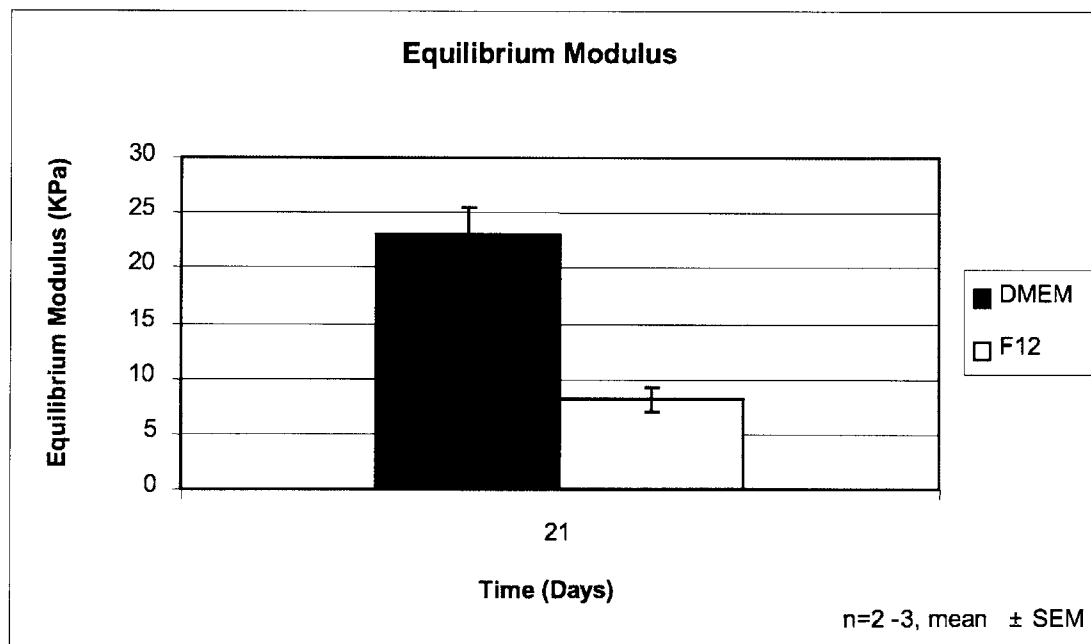ic compressive stiffness was computed as the ratio of the fundamental amplitudes of stress to strain with a dynamic strain amplitude of 1.0%.

Due to the significant discrepancy in the increase of GAG content over the first 10 days of culture based on selected culture medium, this study was repeated with a higher number of early time points to evaluate the kinetics of this process. The experimental design of this study was the same with the addition of days 2, 3, and 4 as time points.

Biochemical assays from this study provided similar results as those seen in the first study. In the DMEM cultured sample group, the maximum cell number, computed through Hoechst dye analysis, attained was 42,567 cells when normalized to the wet weight of 3mm plugs, however F12 samples displayed a maximum of only 31,761 cells. A 59% increase in cell number over the 21 days of culture was observed in the DMEM group, but there was only a 31% increase seen in the F12 group.

Figure A.7 Cell number in agarose hydrogel. Hoechst dye analysis utilized to quantify DNA content in chondrocyte-seeded agarose hydrogels.
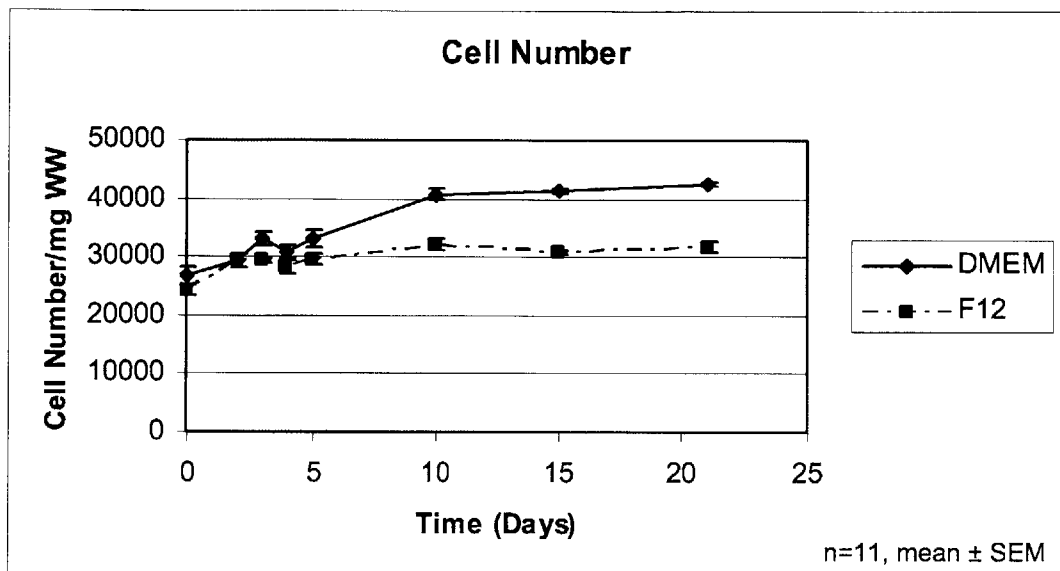
Measurements of GAG content in the second study were consistent in terms of magnitude and trends as those seen in the first study. Early time points provided insight into the kinetics of GAG synthesis and accumulation based on a distinction in culture medium choice. From day 0 to day 2 of culture, the DMEM-cultured samples displayed an increase of 256% in GAG content, while the F12-cultured samples increased by 181%. From day 2 to 3, GAG content in the DMEM samples increased by 74%, while GAG content in the F12 samples increased by 62%. From day 3 to day 4, however, there is a distinction in GAG accumulation between the sample groups. Over this time period, GAG content increases 62% in the DMEM samples, but decreases by 9% in the F12 samples. After this time point, increase in GAG content is higher in the F12 samples than in the DMEM samples from day 4 to 5, 5 to 10, and 15 to 21. Samples of medium were analyzed for GAG content via DMMB binding, as seen in Figure A.9. Drastic differences in GAG content lost to the medium are apparent on days 4 and 20, with the DMEM medium possessing higher GAG content. Because GAG content measured in the media are comparable at most time points, GAG loss to the medium may not be the primary and sole mechanism creating the apparent discrepancy in GAG content measured in the chondrocyte-seeded agarose hydrogel.

Again, proline incorporation rates in F12 samples were lower than DMEM samples throughout the time of culture. The F12 samples displayed the same leveling off behavior at

108

approximately 0.01nmoles/hr/mg WW as seen in study one, however proline incorporation rate in DMEM samples of this study did not drop off as dramatically from day 5 to day 21 as seen in study one. The maximum value was seen at day 5 in study one at approximately 0.03nmoles/hr/mg WW and decreased by 50% to 0.015nmoles/hr/mg WW. In the second study, the peak proline incorporation rate was observed on day 3 at 0.046nmoles/hr/mg WW and decreased to 0.034nmoles/hr/mg WW on day 21. Despite these differences in DMEM samples between studies, the consistency remains between studies with regard to higher proline incorporation rates in DMEM than in F12 throughout culture time. An interesting observation is noted when analyzing sulfate incorporation rates. In this study, the magnitudes and trends in sulfate incorporation rates between DMEM and F12 samples are extremely similar. As seen in the last study, this data is a contrast to that seen in the GAG content. Therefore, media samples were assessed to analyze GAG loss to the medium over the time course. As seen in Figure A.9, GAG loss to the medium is fairly comparable between the two groups, except at two distinct points. Considering this data, the higher accumulation of GAG content in the DMEM-cultured groups may be a reflection of the chemical composition of this medium. DMEM and F12 differ in sulfate content in their chemical compositions and the higher sulfate content in DMEM may be the cause of the higher measured GAG content when compared to the F12.
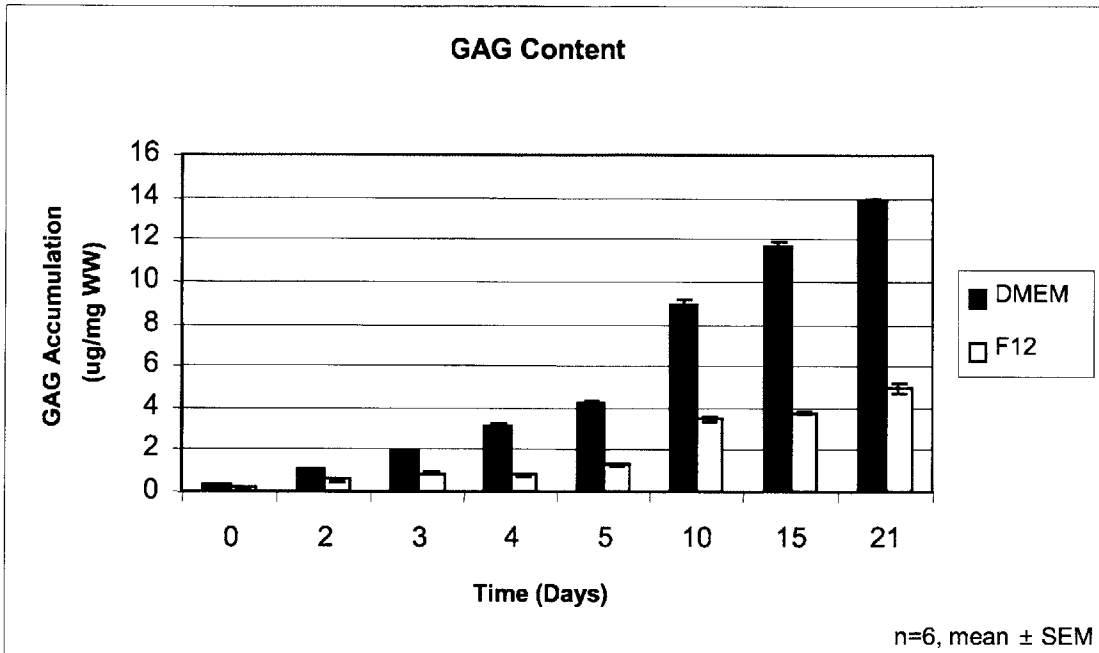
Figure A.8 GAG accumulation in chondrocyte-seeded agarose hydrogel. As seen in Figure A.2, a marked increase is evident in GAG content in DMEM-cultured chondrocyte-seeded agarose hydrogels than in F12-cultured chondrocyte-seeded hydrogels, even at earlier time points.
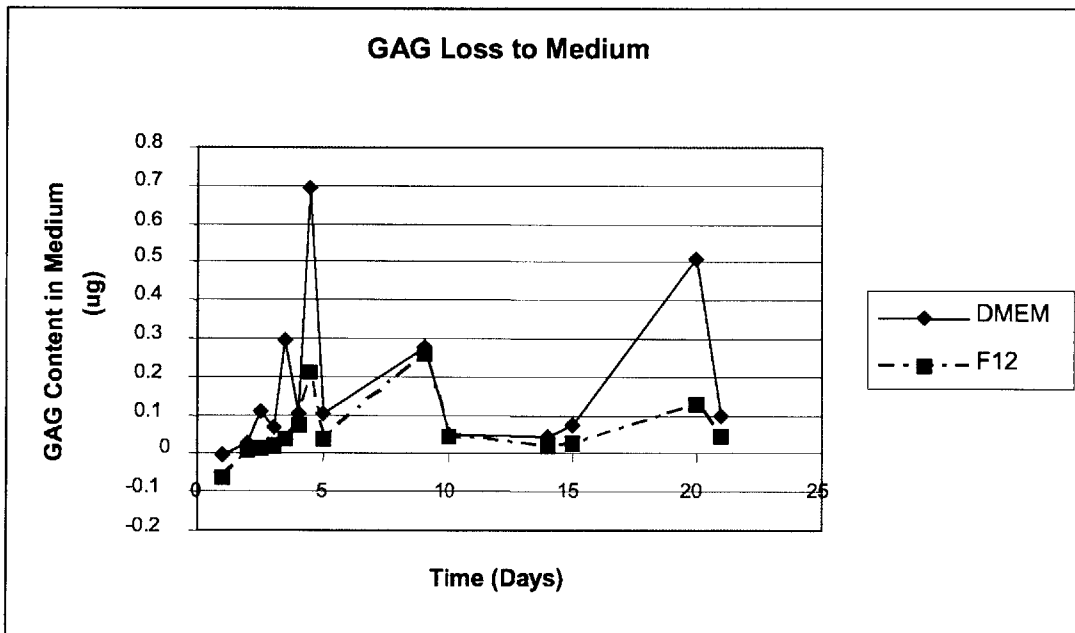
Figure A.9 GAG loss to culture medium.

110
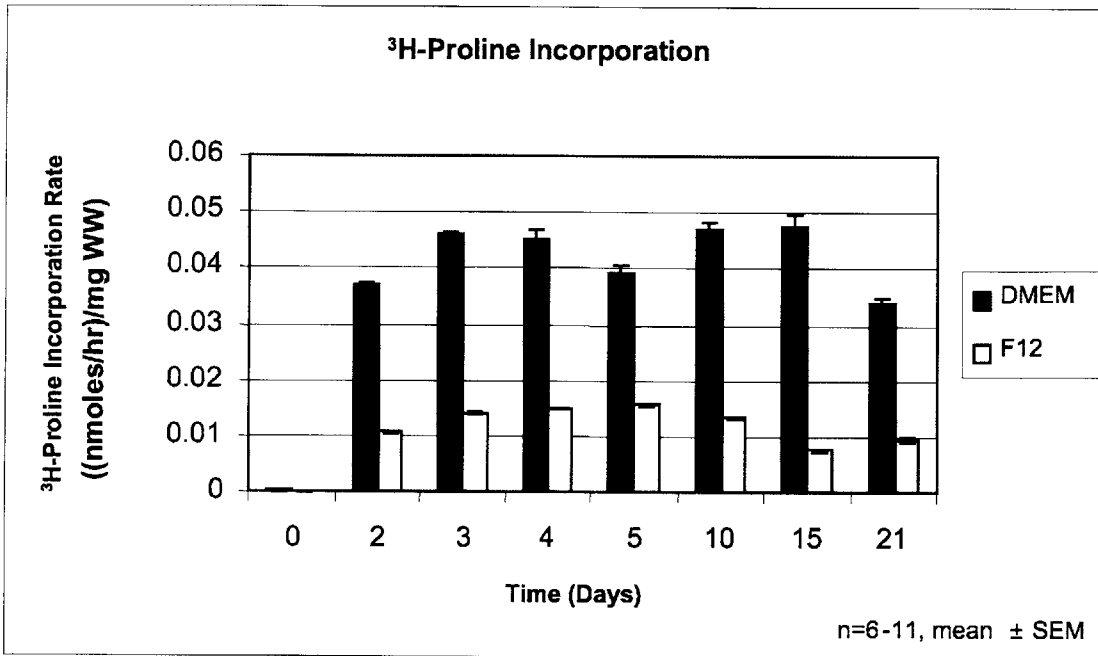
Figure A.10 Chondrocyte biosynthesis in agarose hydrogels. As seen in Figure A.3, DMEM-cultured chondrocyte-seeded agarose hydrogels display higher ^{3}H-proline incorporation rates, indicative of protein synthesis, than F12-cultured samples.

Figure A.11 Chondrocyte biosynthesis in agarose hydrogel. ^{35}S-sulfate incorporation rates appear to be comparable at all time points between DMEM-cultured chondrocyte-seeded agarose hydrogels and F12-cultured chondrocyte-seeded agarose hydrogels.

Appendix B: Material Testing

Mechanical properties of cell-seeded hydrogels have been measured in our group in radially confined uniaxial compression tests using a Dynastat mechanical spectrometer [23] (IMASS, Hingham, MA, Dynamic Acquisition System Software Version 9.9F) [44]. In the studies presented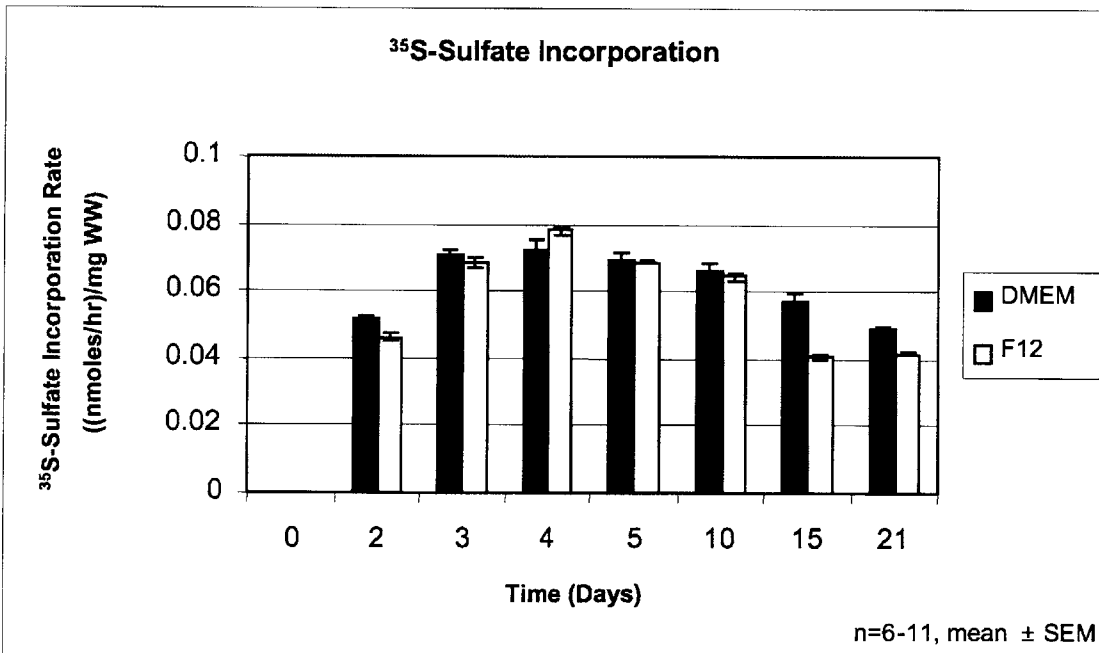 in this thesis, material testing was performed in radially confined uniaxial compression tests on a benchtop Incudyne (Industrial Devices Co. LLC, Petaluma, CA, Model Number RGC-06-180-E04-X23X, Dynamic Acquisition System Software Version 9.9F). In order to confirm the consistency between these instruments and, consequently, to be able to compare mechanical properties of materials across studies when accounting for any other experimental differences, a validation study was performed.

3mm diameter explants taken from the bovine femoropatellar groove within a few hours after slaughter were evaluated on the Incudyne, allowed to re-equilibrate in PBS for 7 hours at 4°C, and then tested on the Dynastat. Identical testing protocols were used on both instruments. A porous platen was used to apply 2 sequential ramp-and-hold compressive strains of 5%, followed by 4 sequential ramp-and-hold compressive strains of 2% to the sample. Each compressive strain was applied over 30seconds, followed by a holding period of 5 minutes to allow for stress relaxation. The ratio of the relaxed equilibrium stress to the engineering strain was used to compute the equilibrium modulus. At 18% compressive offset strain, a 1% amplitude sinusoidal strain was applied at 1, 0.5, and 0.1Hz. The dynamic compressive stiffness was calculated as the ratio of the fundamental amplitudes of stress to strain [44].

As shown in the data below, both instruments provide an accurate measurement of the mechanical properties of the samples. A 4.1% difference was observed in the equilibrium modulus measurements of explant 1 between the Incudyne and Dynastat. Differences in these values of explant 2 were negligible, less than 1%. Consistency between the Incudyne and Dynastat was also evident in dynamic stiffness measurements. Therefore, it is valid to conclude that either instrument is an acceptable means of obtaining mechanical properties of experimental samples. Furthermore, despite discrepancies in the choice of instrument between these studies and previous studies done in our group, experimental data can be compared across both the Incudyne and Dynastat.
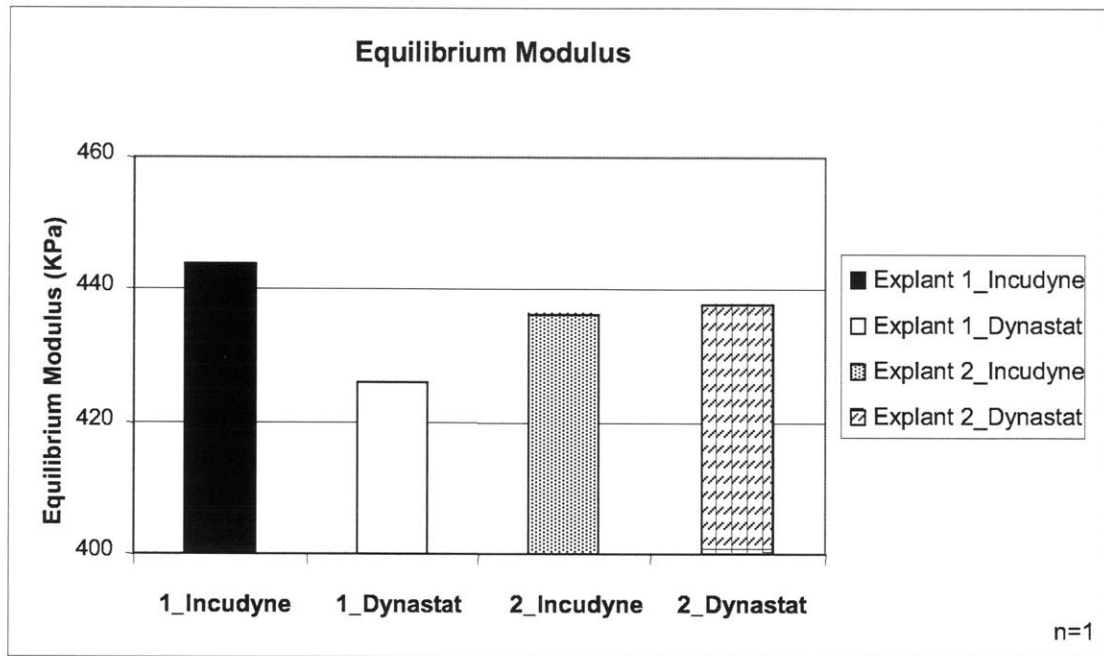
Figure B.1 Mechanical properties of bovine cartilage explants from femoropatellar groove. Mechanical testing of 3mm plugs was performed in uniaxial confined compression. Each sample was tested on the Incudyne, allowed to re-equilibrate, and subsequently tested on the Dynastat. Equilibrium modulus was computed as the ratio of the relaxed equilibrium stress to the engineering strain for compressive strains of 5% to 18%. Consistency between the mechanical testing instruments allowed for the selection of the Incudyne for future mechanical testing due to experimental ease and convenience.
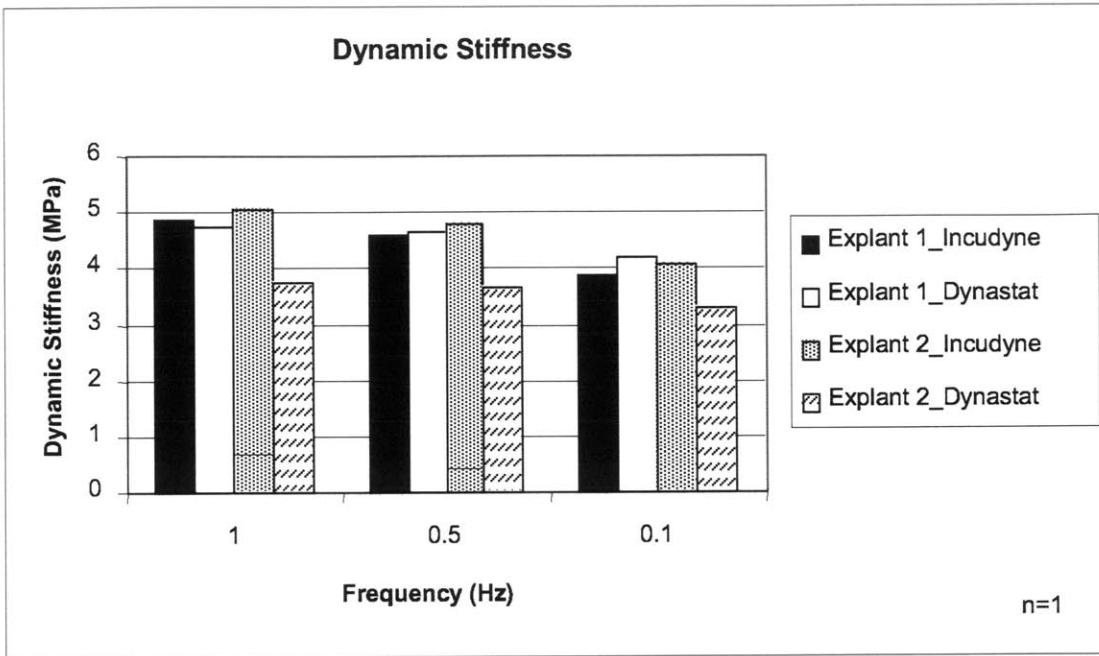
Figure B.2 Mechanical properties of dynamically compressed bovine cartilage explants from the femoropatellar groove. Dynamic compressive stiffness was computed as the ratio of the fundamental amplitudes of stress to strain with a dynamic strain amplitude of 1.0%.

Appendix C: Histology Challenges

A variety of processing techniques have been utilized to carry out histological analysis of tissue samples. Tissue samples are usually fixed, dehydrated, cleared, embedded in the medium of choice, sectioned, and then stained. Previous studies have embedded PCL samples in both paraffin and PMMA, while others have used cryosectioning techniques [45-47]. Performing histological analysis of the PCL samples proved to be challenging, as numerous obstacles were encountered with regard to the solubility of PCL.

Initially, standard processing techniques were invoked to prepare the PCL samples for sectioning. After being fixed in 4% paraformaldehyde overnight at 4°C, samples were stored in 70% ethanol at 4°C until histological assessment ensued. PCL samples were dehydrated by means of a graded ethanol series up to 100% ethanol, and cleared in xylene. Before the samples could be embedded in paraffin, they had completely dissolved. Investigations into the solubility of PCL indicated that it is soluble in xylene and insoluble in ethanol. Therefore, alternative clearing agents were suggested, such as toluene, benzene, or methyl salicylate. However, PCL was discovered to be soluble in both toluene and benzene. Consequently, the alternative clearing agent proved to be methyl salicylate, which is commonly used as a clearing agent for bone tissue specimens. Alternatively, the use of dehydrants and clearing agents could be eliminated by embedding the samples in a water-souble wax, such as polyethylene glycol (PEG). Stains can be applied to the tissue section after processing in PEG with little shrinkage of the sample or tissue distortion.

In the next attempt to process PCL samples, methyl salicylate and a citrus-based solvent were used as clearing agents after dehydration in a graded ethanol series up to 100%. The PCL samples did not dissolve in either of these agents. However, after 3 changes in liquid paraffin before embedding in paraffin blocks for sectioning, the samples had dissolved. These results led to the conclusion that the paraffin being used may be the culprit, as tissue samples may be sensitive to the type or molecular weight of paraffin used. The alternative to this obstacle appeared to be to eliminate the use of dehydration, clearing, and paraffin embedding by using PEG instead. Unfortunately, the PCL samples also dissolved when this approach was used. The remaining possibilities were to optimize the PEG embedding process by determining the appropriate conditions, such as molecular weight of PEG, that may prove effective, or to pursue cryosectioning.

An initial attempt at cryosectioning proved to be unsuccessful. OCT is a mixture of glycerol and polyvinyl alcohol that is viscous at room temperature and is routinely used to embed samples prior to freezing. Unlike paraffin, OCT does not infiltrate the tissue sample, but instead it surrounds the sample to position it for cryosectioning. This technique proved to be ineffective because the porous PCL samples, stored in 70% ethanol until histological processing, retained such a high volume of ethanol that the material was too soft to be sectioned in the cryostat. Dry unfixed PCL samples also proved to be problematic due to the high concentration of air trapped in the pores of the material. Sections prepared in the cryostat consisted only of the periphery of the PCL sample. An optimization to this processing technique that remained to be investigated was cryoprotecting the PCL samples in various concentrations of sucrose. Embedding the samples in sucrose solutions until the sucrose has infiltrated the samples would remove the residual water from the interior of the sample and prevent ice crystals from forming during the freezing process for cryosectioning.

A variety of protocols were employed to determine the optimal cryoprotecting process for the PCL samples. After being fixed in 4% paraformaldehyde overnight at 4°C, samples were rinsed in PBS, submerged in a gradient of sucrose solutions, embedded in 50% OCT in PBS overnight at 4°C, embedded in 100% OCT overnight at 4°C, embedded in OCT, frozen in isopentene and dry ice, and then sectioned in the cryostat. Only after the sucrose solution had completely saturated the sample, as is evident by the sinking of the sample to the bottom of the solution, was the concentration of the sucrose solution increased. The four distinct gradients of sucrose solution included: (1) 15% sucrose in PBS followed by 30% sucrose, (2) 20%, 30% sucrose, (3) 10%, 20%, 30% sucrose, and (4) 5%, 10%, 20%, 30% sucrose. The protocols involving the sucrose gradient schemes of methods (3) and (4) produced frozen samples that could be sectioned on the cryostat, without discrepancies in results between sucrose gradients. The PCL architecture was maintained and cells could be visualized via H&E staining and proteoglycan content was visualized via Toluidine Blue staining. Protocol (4) was chosen as the cryoprotection protocol of choice and applied to the samples histologically analyzed in Chapters 4 and 5.

Appendix D: Long Term Culture of Chondrocyte-Seeded Peptide Hydrogel

The objective of the following study was to investigate the long term efficacy of the KLD-12 peptide hydrogel as a scaffold material for primary bovine chondrocytes. Bovine chondrocytes were harvested from the femoral condyles and femoropatellar grooves of 1-2 week old calves within a few hours of slaughter, as previously described [40]. Chondrocytes were isolated by standard digestion procedures as utilized and described in previous chapters. Peptide hydrogel sheets, comprised of the KLD-12 peptide sequence, were cast using the stainless steel casting frame at a cell seeding density of 30million cells/mL. Culture medium consisted of high-glucose DMEM supplemented with 1% ITS, 0.2% FBS, 0.4% proline, 1.0% PenStrep, and 4µl/mL ascorbate added at the time of medium change every other day. 3mm plugs were taken from the peptide hydrogel sheet on day 64 of culture. The samples were characterized biochemically for chondrocyte viability via the MTS assay and GAG content through DMMB binding, mechanically for material properties, and histologically for a visual representation of matrix deposition and accumulation.

Chondrocyte viability at this time point was evaluated with the MTS assay using procedures previously described in earlier chapters. The absorbance readings at a 490nm wavelength can be interpreted as a relative understanding of viable cell number when compared to previous studies. The viability values for this long term peptide sheet ranged from 0.054 to 0.059absorbance/mg WW. These values are comparable to those seen in chapter 5, which describe chondrocyte viability with absorbance readings ranging from 0.040 to 0.052absorbance/mg WW in the peptide hydrogel and 70% or 90% porous PCL scaffold composites on day 19 of culture.
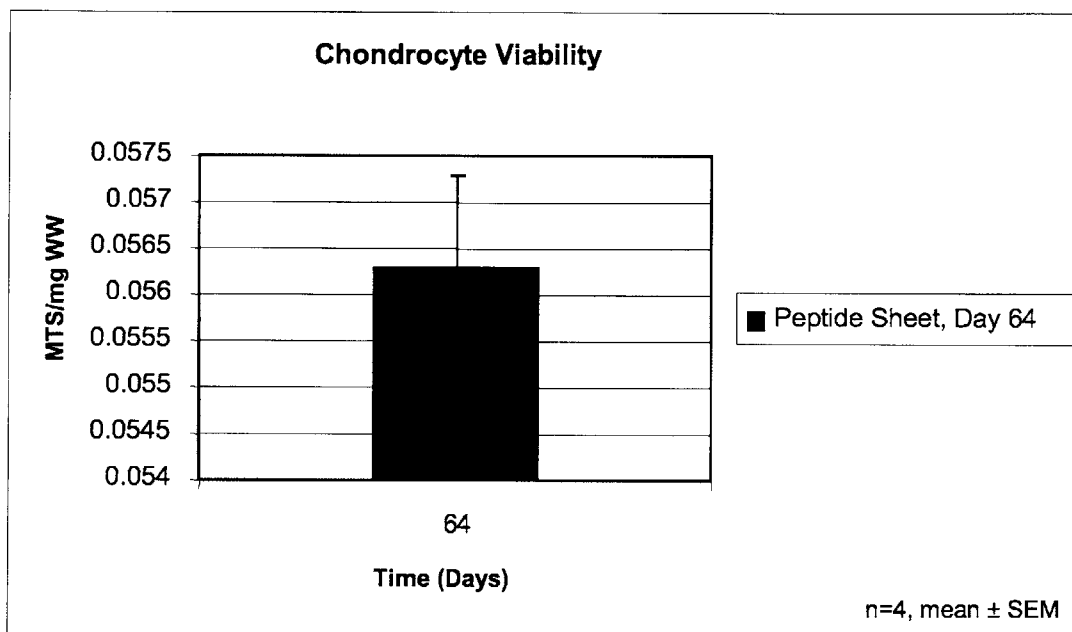
Figure D.1 Cell viability in chondrocyte-seeded peptide hydrogel cultured for 64 days. MTS absorbance at 490nm provides relative measurement of viable chondrocytes in peptide hydrogel.

Accumulated GAG content was measured biochemically via DMMB binding as previously described. On day 64 of culture, GAG content in 3mm plugs of the peptide hydrogel ranged from 11.05µg/mg WW to 24.23µg/mg WW. As seen in Figure D.2, average GAG content at this time point was measured as 19.26µg/mg WW. As a representative example of the study carried out in Chapter 4, GAG content in the peptide hydrogel region of the composite involving 90% porous PCL was 12.26µg/mg WW on day 21 of culture. In Chapter 5, GAG content in the peptide hydrogel region of composites involving the 70% porous PCL and 90% porous PCL samples was measured as 18.30µg/mg WW and 12.60µg/mg WW, respectively, on day 19.

120

GAG Content

Peptide Sheet, Day 64

n=13, mean ± SEM

Figure D.2 GAG accumulation in chondrocyte-seeded peptide hydrogel cultured for 64 days.

The confined compression equilibrium modulus of the peptide sheet was also characterized via mechanical testing of the ma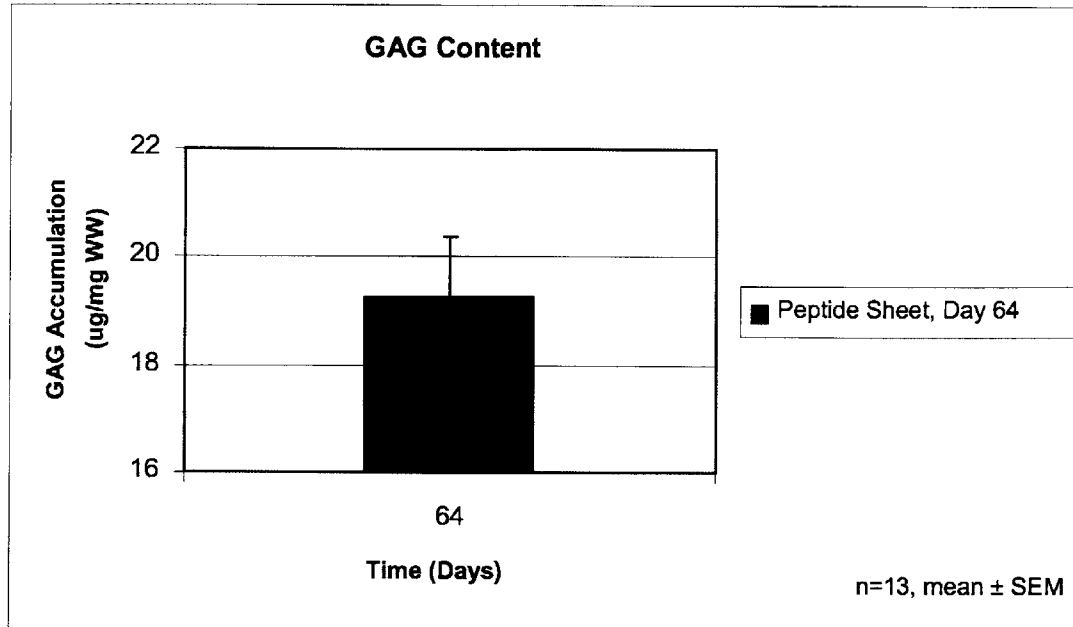terial. The equilibrium modulus was measured as 179.8kPa. The equilibrium modulus of a 3mm plug from the peptide hydrogel region of a representative sample in Chapter 4 involving a 90% porous PCL scaffold was 68kPa on day 21 of culture. From Chapter 5, it is evident that the equilibrium moduli of the peptide hydrogel region of composites consisting of either the 70% porous PCL scaffolds or 90% porous PCL scaffolds ranged from 30kPa to 81kPa or 36kPa to 38kPa, respectively, on day 19 of culture. Therefore, a marked increase in equilibrium modulus was evident in the long term culture of the peptide hydrogel when compared to these relatively short term studies. The dynamic stiffness values of the long term peptide hydrogel sheet were also distinctly higher than those of the representative example from Chapter 4, which utilized the identical dynamic sinusoidal strain amplitude of 1%. These dynamic stiffness values of the peptide hydrogel sheet were approximately two-fold higher than those measured in the peptide hydrogel regions of the composite samples.

Therefore, this study indicated that through the use of long term *in vitro* culture, the material properties of the peptide hydrogel increase significantly. Although the peptide hydrogel

has weak material properties initially, this potential to approach material properties that are approximately one-third that of native cartilage is indicative of its promise as a cartilage scaffold substitute material.

Stress vs Strain

- Peptide Sheet, Day 64

n=6, mean ± SEM

$y = -0.1798x - 0.0699$

$R^2 = 0.9959$

Equilibrium Modulus = 179.8KPa
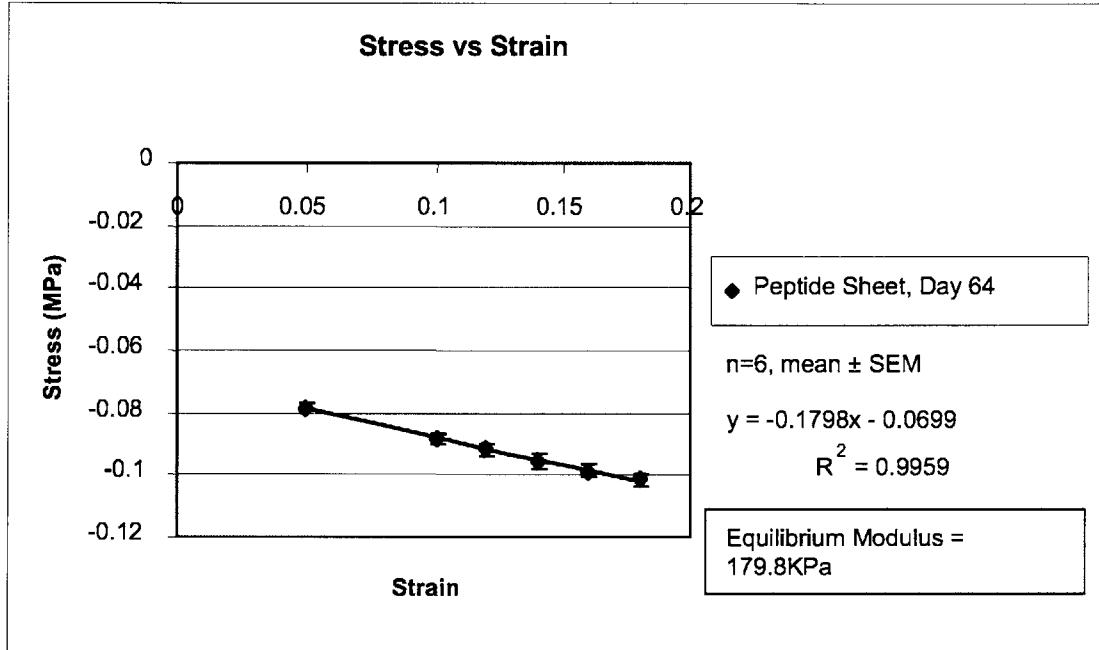
Figure D.3 Mechanical properties of chondrocyte-seeded peptide hydrogel cultured for 64 days. Mechanical testing of 3mm plugs was performed in uniaxial confined compression. Equilibrium modulus, 179.8kPa, was computed as the ratio of the relaxed equilibrium stress to engineering strain for compressive strains of 5% to 18%.

122
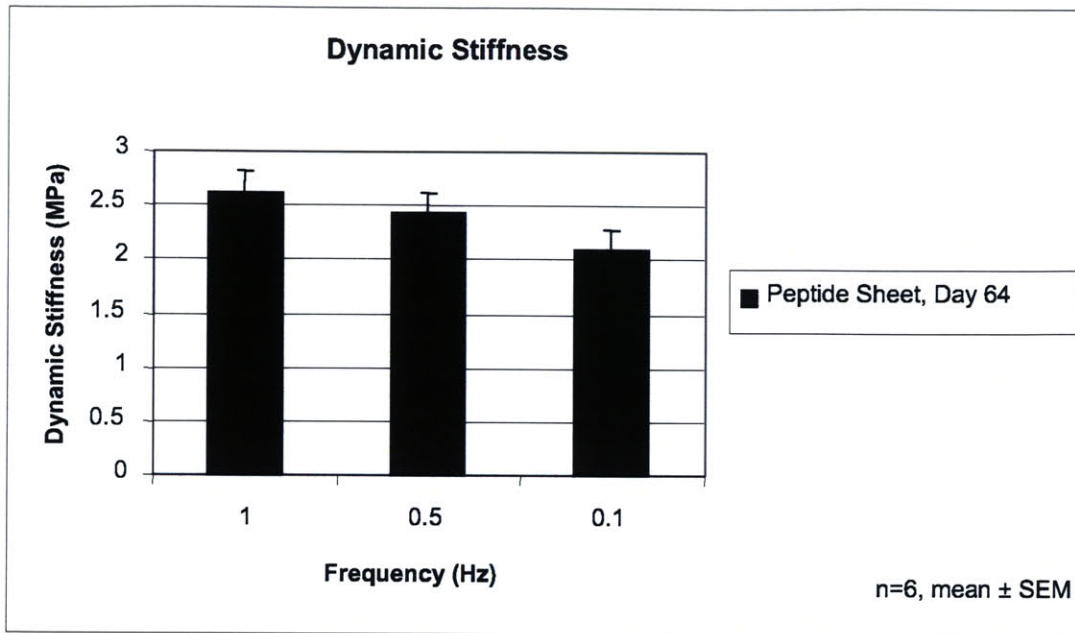
Figure D.4 Mechanical properties of dynamically compressed chondrocyte-seeded peptide hydrogel on day 64 of culture. Dynamic stiffness was computed as the ratio of the fundamental amplitudes of stress to stain with a dynamic strain amplitude of 1.0%.

Histological analysis provided a visual representation of the dense and continuous accumulation of ECM in the chondrocyte-seeded peptide hydrogel sheet on day 64 of culture.
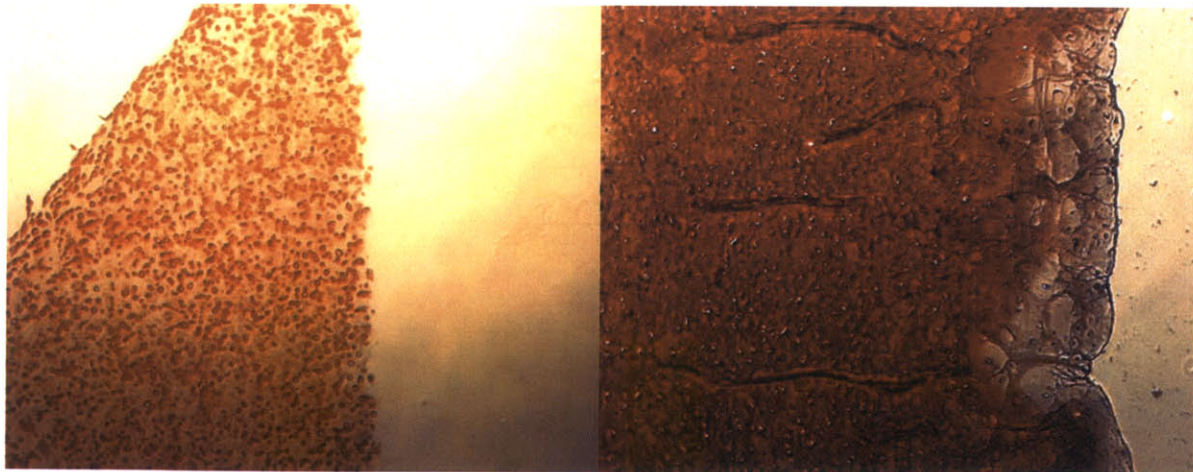
Figure D.5 5µm section of chondrocyte-seeded peptide hydrogel sheet at (a) 4X and (b) 10X. Safranin O staining on day 64 of culture indicates the dense and continuous accumulation of ECM in the hydrogel.

Appendix E: Alternative Bone Substitute Materials

E.1 Introduction

As part of the Cambridge-MIT Institute (CMI) collaborations with the University of Cambridge, a traditionally accepted bone substitute material, hydroxyapatite, was investigated as a potential scaffold material in an osteochondral composite. Hydroxyapatite (HA), $[Ca_{10}(PO_4)_6(OH)_2]$, mimics the chemical composition of the mineral component of bone, which is a multi-substituted calcium phosphate apatitite. Porous HA is a commonly used bone substitute material because of its similarity in microarchitecture and interconnectivity to that of native trabecular bone. This bone graft material is an advantageous selection because of its high biocompatibility and bioactivity.

The chemical composition of native bone mineral is one of a multi-substituted calcium phosphate apatite [48]. Carbonate ions are one of the most abundant ions present in bone mineral and silicon ions are commonly found in active growth areas of developing bone. Patel et al. performed *in vivo* characterization of HA, carbonate-substituted HA (C-HA) and silicate-substituted HA (Si-HA) granules to determine the effect of carbonate and silicate ion incorporation on the bioactivity of HA [48]. These studies indicated that both HA and 2 wt % C-HA granules were well accepted by the host tissue, and new bone formation was observed within and on the surface of the granules. *In vivo* studies comparing HA and 0.8 wt % Si-HA were also carried out. These studies delineated the increase in bone ingrowth and bioactivity of HA with silicate substitution. Therefore, an improvement in the bioactivity of HA was observed with the substitution of carbonate and silicate ions into its structure.

E.2 Methods

E.2.1 Hydroxyapatite, Carbonate-Substituted Hydroxyapatite, and Silicate-Substituted Hydroxyapatite Disc Fabrication Process

These materials were fabricated by Patel et al. at the University of Cambridge, UK [48]. Synthetic HA particles were synthesized by an aqueous precipitation reaction between calcium hydroxide, $Ca(OH)_2$, and orthophosphoric acid, H_3PO_4, solution at room temperature and pH 10. A molar ratio of 1.67 Ca/P was utilized to emulate the stoichiometric relationship between calcium and phosphate in natural HA. Precipitation occurred when H_3PO_4 was dripped continuously into the $Ca(OH)_2$ solution over a 2-3 hour period. pH was maintained during the

precipitation reaction. The suspension was aged at room temperature for a minimum of 16 hours, while the HA particles settled. At this time, the precipitate was filtered, rinsed, and dried.

1.72 C-HA (1.13 wt %) particles were also synthesized by a precipitation reaction. An aqueous solution of $Ca(OH)_2$, the calcium solution, was created. Carbon dioxide gas was bubbled into DI water for 30 minutes to create CO_2-treated water, with a corresponding decrease in pH from 7 to 4. H_3PO_4 was then added to the CO_2-treated water. This phosphate/carbonate solution was then added drop-wise to the calcium solution over 2-3 hours at room temperature. The mixture was allowed to age for 16 hours. The 1.72 C-HA particles were then filtered, rinsed, and dried.

0.8 wt % and 0.4 wt % Si-HA (0.8Si-HA and 0.4Si-HA, respectively) particles were created by means of a similar precipitation reaction with the incorporation of silicon tetra-acetate (SiAc), $Si(CH_3CO_2)_4$, in addition to calcium hydroxide and orthophosphoric acid solutions. An aqueous solution of $Ca(OH)_2$ and an aqueous solution of SiAc solution were synthesized. SiAc solution was added to the H_3PO_4 solution. This phosphate/silicate solution was then added drop-wise to the $Ca(OH)_2$ solution over 3 hours at room temperature with a constant pH maintained at 10.5. This solution was allowed to age for 16 hours. At this point, 0.8 wt % and 0.4 wt % Si-HA particles were filtered, washed, and dried. The dried HA was then crushed using a pestle and mortar and sieved to a particle size less than 75µm in diameter. The powder was then pressed into discs using an isostatic press and subsequently sintered. The HA, 0.8Si-HA, and 0.4Si-HA discs were sintered at 1200°C in air for 2 hrs, while the 1.72C-HA discs were sintered at 1000 °C in a moist CO_2 environment for 2 hours. The discs are 98% dense and 9mm in diameter with a thickness of 2mm – 2.5mm. HA discs were then sterilized at 200°C for 2 hours and subsequently autoclaved.

E.2.2 Cell Isolation

Bovine chondrocytes were harvested from the femoral condyles and femoropatellar grooves of 1-2 week old calves within a few hours of slaughter, as previously described [40]. The chondrocyte isolation process consisted of an incubated two hour digestion period in a pronase solution at a concentration of 20U/mL (Sigma-Aldrich, St. Louis, MO), followed by an overnight incubated digestion period in a collagenase solution at a concentration of 200U/mL (Worthington, Lakewood, NJ). At the completion of the digestion process, the chondrocyte suspension was then filtered through a 40µm cell strainer and centrifuged at 1900rpm for

8minutes. Cell pellets were resuspended and centrifuged in 1X PBS a total of three times. At this point, the chondrocytes were resuspended in high glucose DMEM (Gibco, Auckland, New Zealand). A sample of cell suspension was microscopically analyzed for cell viability using ethidium bromide/FDA and concentration using Trypan Blue Staining (Sigma Chemical Co., St. Louis, MO). The cell suspension was then stored at 4° C until use.

E.2.3 Casting

2.5% agarose molds were created by pipetting 5ml into 35mm Petri dishes. All molds were 4mm thick with an inner diameter (ID) of 9mm and an outer diameter (OD) of 20mm. The peptide KLD-12 was custom synthesized (SynPep Corp., Dublin, CA) and lyophilized to a powder. KLD-12 powder was dissolved in a 10% sucrose solution at a concentration of 3.6mg/mL. The peptide solution was then sonicated until further use to prevent aggregation. The volume of cell suspension targeted for a cell seeding density of 30million/mL was centrifuged at 1900rpm for 8 minutes. Isolated chondrocytes were then resuspended in a 10% sucrose plus 5mM HEPES buffer solution equal in volume to 10% of the final hydrogel casting volume. The peptide solution was then added to the cell suspension in volume equal to 90% of the final hydrogel casting volume. The casting solution was then lightly vortexed and injected directly on top of the HA, C-HA, and Si-HA scaffolds inside the cylindrical core of the agarose mold. After a waiting period of 10 minutes, the composite samples were then submerged in 1.5X PBS without agitation for 30 minutes to initiate self-assembly of the peptide hydrogel. At this point, PBS was aspirated and culture medium, high-glucose DMEM with 0.2% FBS and 1% ITS, was added. Each sample received 5mL of culture medium that was changed every other day.

E.2.4 Chondrocyte Viability

On days 5 and 14 of culture, chondrocyte viability was assessed qualitatively through ethidium bromide/FDA analysis.

E.2.5 Biochemical Analysis

On days 5 and 14 of culture, the peptide hydrogel layer was separated from each scaffold and four 3mm plugs were taken from this region of the composite using a disposable punch. Samples designated for mechanical testing were tested at this point on day 14. Each plug was then digested in 1mL of proteinase K-TRIS HCL solution at 60°C overnight. Accumulated

127

sulfated glycosaminoglycan (GAG) content, determined by means of DMMB dye binding, was measured as described previously [34].

E.2.6 Mechanical Testing

On day 14 of culture, 3mm plugs of the peptide hydrogel were tested in radially confined uniaxial compression using a benchtop Incudyne to determine the equilibrium modulus and dynamic stiffness of the materials, as previously described [44]. (Industrial Devices Co. LLC, Petaluma, CA, Model Number RGC-06-180-E04-X23X, Dynamic Acquisition System Software Version 9.9F). After measuring the thickness of each sample, the plug was placed into a confining cylindrical chamber clamped into the platform of the Incudyne. A porous platen was used to apply 2 sequential ramp-and-hold compressive strains of 5%, followed by 4 sequential ramp-and-hold compressive strains of 2% to the sample. Each compressive strain was applied over 30 seconds, followed by a holding period of 3 minutes to allow for stress relaxation. The ratio of the relaxed equilibrium stress to the engineering strain was used to compute the equilibrium modulus. At 18% compressive offset strain, a 0.2% amplitude sinusoidal strain was applied at 1, 0.5, and 0.1Hz. The dynamic compressive stiffness was calculated as the ratio of the fundamental amplitudes of stress to strain [44].

E.3 Results

E.3.1 Chondrocyte Viability

Qualitative analysis of chondrocyte viability on days 5 and 14 via ethidium bromide/FDA displayed 65-80% viability. Casting of the chondrocyte-seeded peptide hydrogel onto the HA discs used in this study did not appear to aversely affect chondrocyte viability.

E.3.2 GAG Accumulation

GAG accumulation in the peptide hydrogel region of each of these composites increased from a range of 7.8μg/mg WW - 9.4μg/mg WW on day 5 of culture to 12.6μg/mg WW – 15.9μg/mg WW on day 14 of culture. The peptide hydrogel and HA composites displayed a 41.7% increase in GAG content in the peptide hydrogel region from day 5 to day 14, while GAG content in the corresponding region of the 1.72 C-HA, 0.8 wt % Si-HA, and 0.4 wt % Si-HA composites increased by 87.9%, 34.0%, and 65.3%, respectively. On day 5, there was no significant difference in GAG content measured in the peptide hydrogel region based on the

128

choice of bone scaffold material ($p > 0.05$). On day 14 of culture, GAG content in the peptide hydrogel region of the 1.72 C-HA composite was significantly higher than that in the HA and 0.8 Si-HA composite ($p < 0.05$). However, there was no significant difference in GAG content of the peptide hydrogel region of the 1.72 C-HA composite when compared to the 0.4 Si-HA composite.
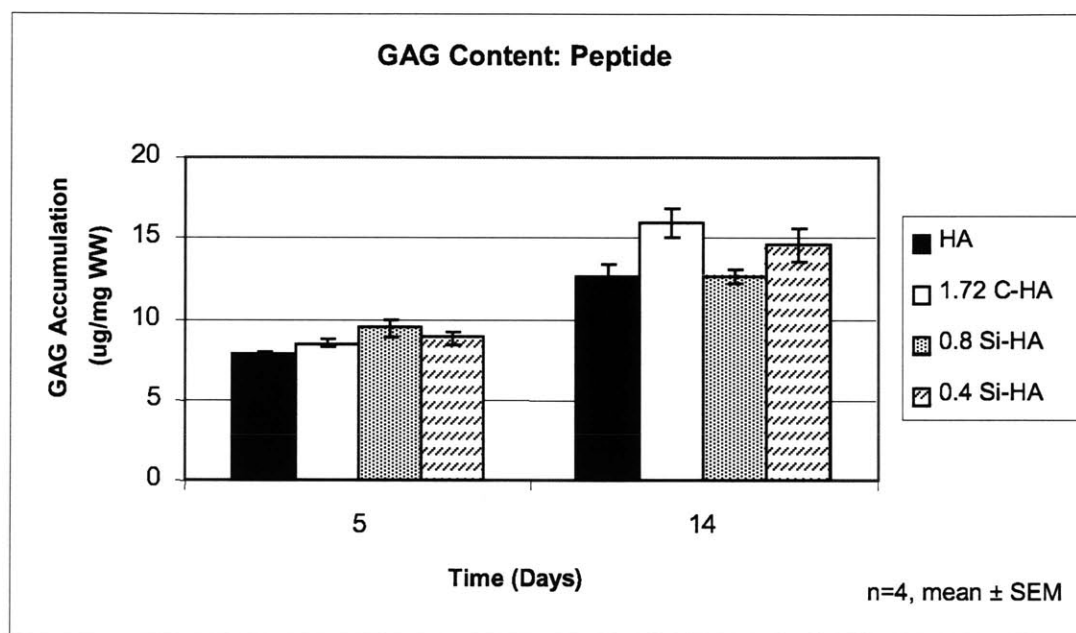

Figure E.1 GAG accumulation in peptide hydrogel. 3mm plugs punched from peptide hydrogel layer of each composite at each time point, digested in Proteinase K, and analyzed for GAG content via DMMB binding. GAG accumulation in the chondrocyte-seeded peptide hydrogel appears to be independent of bone substitute scaffold material upon which it is cast and cultured.

E.3.3 Mechanical Properties

The equilibrium moduli of 3mm plugs removed from the peptide hydrogel region of the composites involving HA, 1.72 C-HA, 0.8 wt % Si-HA, and 0.4 wt % Si-HA ranged from 15kPa to 24kPa on day 14 of culture. With a dynamic sinusoidal strain amplitude of 0.2%, the dynamic stiffness values of these samples ranged from 0.9MPa to 2.4MPa at a frequency of 1.0Hz, and decreased correspondingly with decreasing frequency.
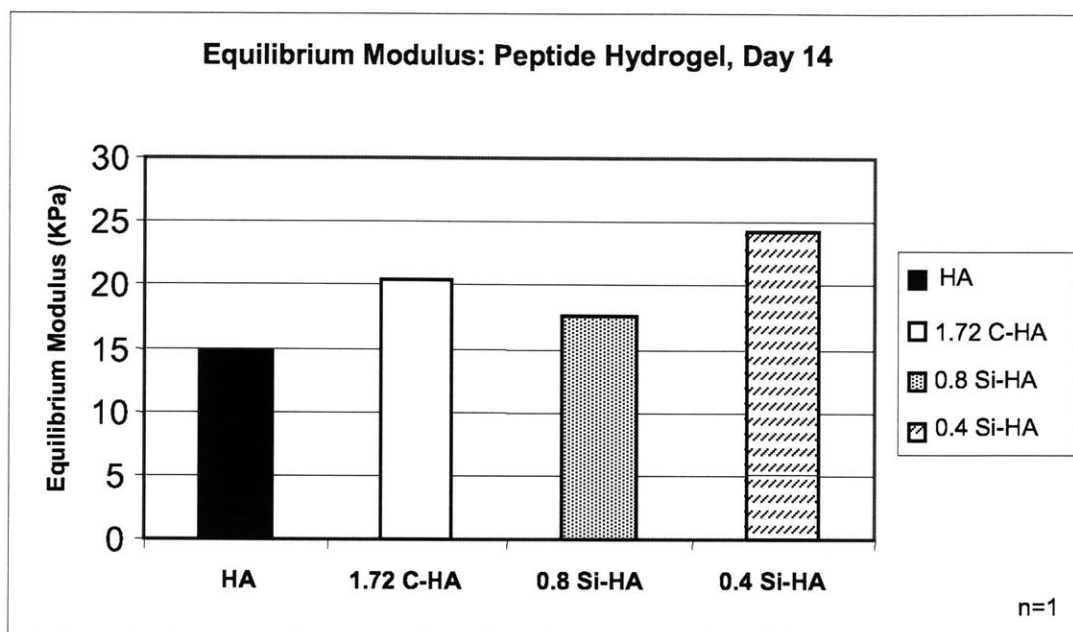
Figure E.2 Mechanical properties of chondrocyte-seeded peptide hydrogel. Mechanical testing of 3mm plugs of the chondrocyte-seeded peptide hydrogel retrieved from each type of composite was performed in uniaxial confined compression on day 14 of culture.
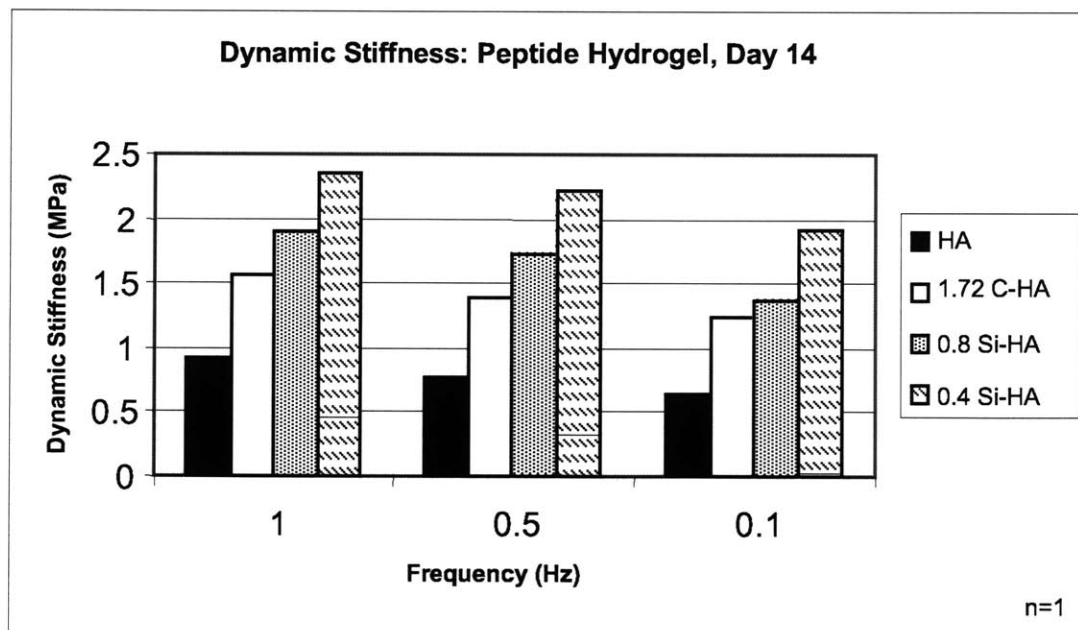
Figure E.3 Mechanical properties of dynamically compressed chondrocyte-seeded peptide hydrogel on day 14 of culture. Dynamic compressive stiffness was computed as the ratio of the fundamental amplitudes of stress to strain with a dynamic strain amplitude of 0.2%.

E.4 Discussion

These results can be compared to those presented in Chapters 4 and 5 to understand the impact of HA, C-HA, and Si-HA, as potential bone scaffold materials with regard to GAG accumulation and material properties in the peptide hydrogel region of the osteochondral composite. As a representative example of the study carried out in Chapter 4, GAG content in the peptide hydrogel region of the composite involving 90% porous PCL increased by 72.1% from 6.19μg/mg WW on day 6 to 10.7μg/mg WW on day 15 of culture. With the exception of the HA composite on day 15 of the study presented in this section ($p > 0.05$), GAG content in the peptide hydrogel region of each of the other composites, 1.72 C-HA, 0.8 wt % Si-HA, and 0.4 wt % Si-HA, was significantly higher than that measured in the peptide hydrogel and 90% porous PCL composite at both time points ($p < 0.05$).

The effect of HA, C-HA, and Si-HA on GAG accumulation in the peptide hydrogel region of an osteochondral composite can be further elucidated by comparison to the study carried out in Chapter 5. In Chapter 5, GAG content in the peptide hydrogel region of composites involving the 70% porous PCL and 90% porous PCL samples increased from 3.96μg/mg WW and 4.32μg/mg WW, respectively, on day 6 to 13.83μg/mg WW and 13.57μg/mg WW, respectively, on day 14. GAG content in these composites increased by over 200% from day 6 to 14. However, these marked larger percent increases in GAG content of the peptide hydrogel and porous PCL composite samples from day 6 to 14 are a result of the fact that overall GAG content in these samples is significantly lower than that observed in the peptide and HA, C-HA, Si-HA composites on day 6 ($p < 0.05$). The studies involving the porous PCL and HA composites proved to be more synonymous in terms of accumulated GAG content on day 14 of culture. With the exception of the HA and 0.4 wt % Si-HA composites compared to the peptide hydrogel and 70% porous PCL on this time point, there is no significant difference in GAG content between the composites involved in these two studies ($p > 0.05$).

Mechanical properties of the peptide hydrogel in these HA, C-HA, and Si-HA samples can also be compared to previous studies to verify the potential use of these materials as an osteochondral composite material. In the studies presented in Chapter 4, the confined compression equilibrium modulus of the 3mm peptide hydrogel samples integrated with the 70% porous PCL scaffold was 25KPa on day 15, while that of the peptide hydrogel samples cultured on the 90% porous PCL scaffolds was 41kPa. Similarly, the studies presented in Chapter 5

depicted peptide hydrogel samples with an equilibrium modulus of 61kPa when cultured on the 70% porous PCL scaffolds for 14 days, and 79kPa when cultured on the 90% porous PCL scaffolds for the identical period of time. Although the range of equilibrium moduli from 15kPa to 24kPa in the peptide and HA, C-HA, and Si-HA composites is lower than those observed in previous peptide hydrogel and porous PCL samples, the potential use of HA, C-HA, and Si-HA in such osteochondral composites should not be disregarded.

The focus of this preliminary study was to investigate the potential use of HA, C-HA, and Si-HA scaffolds as bone substitute materials in osteochondral constructs, while simultaneously probing any discrepancies in potential based on distinct ionic substitutions into HA. Using the same casting techniques involved in the fabrication of peptide hydrogel and porous PCL scaffolds, this study verified that an osteochondral construct can be created using these HA, C-HA, and Si-HA materials with regard to the successful self-assembly of the peptide hydrogel. Although the peptide hydrogel is capable of self-assembling when cast directly on top of the HA, C-HA, and Si-HA scaffolds, integration of the two materials is not evident due to the 98% density level of the HA scaffolds. Based on the measured magnitudes and trends in GAG accumulation in the peptide hydrogel region of these composites, the HA, C-HA, and Si-HA scaffolds do not appear to have any adverse effects on chondrocyte viability or behavior. However, the MTS viability assay and radiolabel incorporation rates would have to be investigated to further confirm this observation. GAG accumulation in the peptide hydrogel region of these composites appears to be comparable, if not higher, than those seen in the composites involving porous PCL. Although the mechanical properties of the peptide hydrogel samples removed from these composites are lower than those observed in the composites consisting of the porous PCL scaffolds, the main concern that could potentially hinder the use of the HA materials in an osteochondral construct is the lack of integration between the two materials. If porous HA samples can be fabricated, or if a layer of surface roughness can be introduced on the top surface of the HA discs, then the issue of integration can be addressed and these materials would prove to be viable options for osteochondral composite materials.

132

References

1. http://healthlink.mcw.edu/article/926049711.html
2. http://www.kneeindia.com/view_links1.asp?lid=25
3. Glowacki, J, *In vitro engineering of cartilage*. J Rehabil Res Dev, 2000. **37**(2): p. 171-7.
4. Hunziker, EB, *Articular cartilage repair: are the intrinsic biological constraints undermining this process insuperable?* Osteoarthritis Cartilage, 1999. **7**(1): p. 15-28.
5. Hunziker, EB, *Articular cartilage repair: basic science and clinical progress. A review of the current status and prospects*. Osteoarthritis Cartilage, 2002. **10**(6): p. 432-63.
6. Godbey, WT and Atala, A, *In vitro systems for tissue engineering*. Ann N Y Acad Sci, 2002. **961**: p. 10-26.
7. Chaikof, EL, Matthew, H, Kohn, J, Mikos, AG, Prestwich, GD, and Yip, CM, *Biomaterials and scaffolds in reparative medicine*. Ann N Y Acad Sci, 2002. **961**: p. 96-105.
8. Zeltinger, J, Sherwood, JK, Graham, DA, Mueller, R, and Griffith, LG, *Effect of pore size and void fraction on cellular adhesion, proliferation, and matrix deposition*. Tissue Eng, 2001. **7**(5): p. 557-72.
9. Kreklau, B, Sittinger, M, Mensing, MB, Voigt, C, Berger, G, Burmester, GR, Rahmanzadeh, R, and Gross, U, *Tissue engineering of biphasic joint cartilage transplants*. Biomaterials, 1999. **20**(18): p. 1743-9.
10. Wang, X, Grogan, SP, Rieser, F, Winkelmann, V, Maquet, V, Berge, ML, and Mainil-Varlet, P, *Tissue engineering of biphasic cartilage constructs using various biodegradable scaffolds: an in vitro study*. Biomaterials, 2004. **25**(17): p. 3681-8.
11. Ratner, B, Hoffman, A, ed. *Biomaterials Science*. 1996.
12. Chang, B, et al., *Osteoconduction at porous hydroxyapatite with various pore configurations*. Biomaterials, 2000. **21**: p. 1291-1298.
13. van Susante, JL, Buma, P, Homminga, GN, van den Berg, WB, and Veth, RP, *Chondrocyte-seeded hydroxyapatite for repair of large articular cartilage defects. A pilot study in the goat*. Biomaterials, 1998. **19**(24): p. 2367-74.
14. Schaefer, D, Martin, I, Jundt, G, Seidel, J, Heberer, M, Grodzinsky, A, Bergin, I, Vunjak-Novakovic, G, and Freed, LE, *Tissue-engineered composites for the repair of large osteochondral defects*. Arthritis Rheum, 2002. **46**(9): p. 2524-34.
15. Gao, J, Dennis, JE, Solchaga, LA, Goldberg, VM, and Caplan, AI, *Repair of osteochondral defect with tissue-engineered two-phase composite material of injectable calcium phosphate and hyaluronan sponge*. Tissue Eng, 2002. **8**(5): p. 827-37.
16. Schaefer, D, Martin, I, Shastri, P, Padera, RF, Langer, R, Freed, LE, and Vunjak-Novakovic, G, *In vitro generation of osteochondral composites*. Biomaterials, 2000. **21**(24): p. 2599-606.
17. Cao, T, Ho, KH, and Teoh, SH, *Scaffold design and in vitro study of osteochondral coculture in a three-dimensional porous polycaprolactone scaffold fabricated by fused deposition modeling*. Tissue Eng, 2003. **9 Suppl 1**: p. S103-12.
18. Quinn, TM, Schmid, P, Hunziker, EB, and Grodzinsky, AJ, *Proteoglycan deposition around chondrocytes in agarose culture: construction of a physical and biological interface for mechanotransduction in cartilage*. Biorheology, 2002. **39**(1-2): p. 27-37.

19. Buschmann, MD, Gluzband, YA, Grodzinsky, AJ, Kimura, JH, and Hunziker, EB, *Chondrocytes in agarose culture synthesize a mechanically functional extracellular matrix.* J Orthop Res, 1992. **10**(6): p. 745-58.

20. Hung, CT, Lima, EG, Mauck, RL, Taki, E, LeRoux, MA, Lu, HH, Stark, RG, Guo, XE, and Ateshian, GA, *Anatomically shaped osteochondral constructs for articular cartilage repair.* J Biomech, 2003. **36**(12): p. 1853-64.

21. Oka, M, *Biomechanics and repair of articular cartilage.* J Orthop Sci, 2001. **6**(5): p. 448-56.

22. Kisiday, J, Jin, M, Kurz, B, Hung, H, Semino, C, Zhang, S, and Grodzinsky, AJ, *Self-assembling peptide hydrogel fosters chondrocyte extracellular matrix production and cell division: implications for cartilage tissue repair.* Proc Natl Acad Sci U S A, 2002. **99**(15): p. 9996-10001.

23. Kisiday, J, *In Vitro Culture of a Chondrocyte-Seeded Peptide Hydrogel and the Effects of Dynamic Compression.* PhD Thesis, MIT, 2003.

24. Hutmacher, DW, *Scaffolds in tissue engineering bone and cartilage.* Biomaterials, 2000. **21**(24): p. 2529-43.

25. Park, A, Wu, B, and Griffith, LG, *Integration of surface modification and 3D fabrication techniques to prepare patterned poly(L-lactide) substrates allowing regionally selective cell adhesion.* J Biomater Sci Polym Ed, 1998. **9**(2): p. 89-110.

26. Rohner, D, Hutmacher, DW, Cheng, TK, Oberholzer, M, and Hammer, B, *In vivo efficacy of bone-marrow-coated polycaprolactone scaffolds for the reconstruction of orbital defects in the pig.* J Biomed Mater Res, 2003. **66B**(2): p. 574-80.

27. Zhang, S, Marini, DM, Hwang, W, and Santoso, S, *Design of nanostructured biological materials through self-assembly of peptides and proteins.* Curr Opin Chem Biol, 2002. **6**(6): p. 865-71.

28. Zhang, S, Holmes, T, Lockshin, C, and Rich, A, *Spontaneous assembly of a self-complementary oligopeptide to form a stable macroscopic membrane.* Proc Natl Acad Sci U S A, 1993. **90**(8): p. 3334-8.

29. Zhang, S, Holmes, TC, DiPersio, CM, Hynes, RO, Su, X, and Rich, A, *Self-complementary oligopeptide matrices support mammalian cell attachment.* Biomaterials, 1995. **16**(18): p. 1385-93.

30. Schneider, JP, Pochan, DJ, Ozbas, B, Rajagopal, K, Pakstis, L, and Kretsinger, J, *Responsive hydrogels from the intramolecular folding and self-assembly of a designed peptide.* J Am Chem Soc, 2002. **124**(50): p. 15030-7.

31. Holmes, TC, *Novel peptide-based biomaterial scaffolds for tissue engineering.* Trends Biotechnol, 2002. **20**(1): p. 16-21.

32. Xiong, H, Buckwalter, BL, Shieh, HM, and Hecht, MH, *Periodicity of polar and nonpolar amino acids is the major determinant of secondary structure in self-assembling oligomeric peptides.* Proc Natl Acad Sci U S A, 1995. **92**(14): p. 6349-53.

33. Buschmann, MD, Gluzband, YA, Grodzinsky, AJ, and Hunziker, EB, *Mechanical compression modulates matrix biosynthesis in chondrocyte/agarose culture.* J Cell Sci, 1995. **108** (**Pt 4**): p. 1497-508.

34. Sah, RL, Kim, YJ, Doong, JY, Grodzinsky, AJ, Plaas, AH, and Sandy, JD, *Biosynthetic response of cartilage explants to dynamic compression.* J Orthop Res, 1989. **7**(5): p. 619-36.

35.   Kisiday, JD, Jin, M, DiMicco, MA, Kurz, B, and Grodzinsky, AJ, *Effects of dynamic compressive loading on chondrocyte biosynthesis in self-assembling peptide scaffolds*. J Biomech, 2004. **37**(5): p. 595-604.

36.   Hutmacher, DW, Schantz, T, Zein, I, Ng, KW, Teoh, SH, and Tan, KC, *Mechanical properties and cell cultural response of polycaprolactone scaffolds designed and fabricated via fused deposition modeling*. J Biomed Mater Res, 2001. **55**(2): p. 203-16.

37.   Li, WJ, Danielson, KG, Alexander, PG, and Tuan, RS, *Biological response of chondrocytes cultured in three-dimensional nanofibrous poly(epsilon-caprolactone) scaffolds*. J Biomed Mater Res, 2003. **67A**(4): p. 1105-14.

38.   Zein, I, Hutmacher, DW, Tan, KC, and Teoh, SH, *Fused deposition modeling of novel scaffold architectures for tissue engineering applications*. Biomaterials, 2002. **23**(4): p. 1169-85.

39.   Sherwood, JK, Riley, SL, Palazzolo, R, Brown, SC, Monkhouse, DC, Coates, M, Griffith, LG, Landeen, LK, and Ratcliffe, A, *A three-dimensional osteochondral composite scaffold for articular cartilage repair*. Biomaterials, 2002. **23**(24): p. 4739-51.

40.   Ragan, PM, Chin, VI, Hung, HH, Masuda, K, Thonar, EJ, Arner, EC, Grodzinsky, AJ, and Sandy, JD, *Chondrocyte extracellular matrix synthesis and turnover are influenced by static compression in a new alginate disk culture system*. Arch Biochem Biophys, 2000. **383**(2): p. 256-64.

41.   Jackson, JK, Springate, CM, Hunter, WL, and Burt, HM, *Neutrophil activation by plasma opsonized polymeric microspheres: inhibitory effect of pluronic F127*. Biomaterials, 2000. **21**(14): p. 1483-91.

42.   Lin, W, et al., *A novel fabrication of poly(caprolactone) microspheres from blends of poly(caprolactone) and poly(ethylene glycol)s*. Polymer, 1999. **40**: p. 1731-1735.

43.   Woessner, JF, Jr., *The determination of hydroxyproline in tissue and protein samples containing small proportions of this imino acid*. Arch Biochem Biophys, 1961. **93**: p. 440-7.

44.   Frank, EH and Grodzinsky, AJ, *Cartilage electromechanics--I. Electrokinetic transduction and the effects of electrolyte pH and ionic strength*. J Biomech, 1987. **20**(6): p. 615-27.

45.   Yoshimoto, H, Shin, YM, Terai, H, and Vacanti, JP, *A biodegradable nanofiber scaffold by electrospinning and its potential for bone tissue engineering*. Biomaterials, 2003. **24**(12): p. 2077-82.

46.   Schantz, JT, Hutmacher, DW, Ng, KW, Khor, HL, Lim, MT, and Teoh, SH, *Evaluation of a tissue-engineered membrane-cell construct for guided bone regeneration*. Int J Oral Maxillofac Implants, 2002. **17**(2): p. 161-74.

47.   Schantz, JT, Hutmacher, DW, Chim, H, Ng, KW, Lim, TC, and Teoh, SH, *Induction of ectopic bone formation by using human periosteal cells in combination with a novel scaffold technology*. Cell Transplant, 2002. **11**(2): p. 125-38.

48.   Patel, N, *In vivo assessment of hydroxyapatite and substituted apatites for bone grafting*. PhD Thesis, University of Cambridge, 2003.